Robust Design Optimization of Structures under Uncertainties

Von der Fakultät Luft- und Raumfahrttechnik und Geodäsie
der Universität Stuttgart
zur Erlangung der Würde eines Doktor-Ingenieurs (Dr. -Ing.)
genehmigte Abhandlung

vorgelegt von

Zhan Kang

aus Liaoning, V.R. China

Hauptberichter:	Priv.Doz. Dr. -Ing. Ioannis Doltsinis
Mitberichter:	Prof. Dr. -Ing. habil. Bernd Kröplin
Mitberichter:	em. Prof. Dr. -Ing. Werner Schiehlen

Tag der mündlichen Prüfung: 27. Juni 2005

Institut für Statik und Dynamik der Luft- und Raumfahrkonstruktionen
Universität Stuttgart
2005

Sich zu ändern und sich zu verbessern sind zwei verschiedene Dinge.
-Deutsches Sprichwort

To change and to change for the better are two different things.
- a German proverb

Acknowledgements

This thesis has been accomplished during my three years' stay at the Faculty of Aerospace Engineering and Geodesy of the University of Stuttgart. This work was financially supported by the Deutscher Akademischer Austausch Dienst (DAAD) in the framework of the scholarship for doctoral study and by the Faculty of Aerospace Engineering and Geodesy, University of Stuttgart.

First and foremost, I wish to express my deepest gratitude to my advisor PD. Dr. -Ing. Ioannis Doltsinis for giving me the opportunity to do my doctoral study at the Institute of Statics and Dynamics of Aerospace Structures (ISD) and for his invaluable guidance and support throughout this research. I have benefited greatly from frequent and stimulating discussions with him. Moreover, his critical review also contributes significantly to this thesis. I feel extremely fortunate to have had an excellent supervision from him during the past years.

I would like to express my sincerest appreciation to my co-advisor Prof. Dr. Cheng Gengdong from Dalian University of Technology (China), who has encouraged me to do my doctoral research at the University of Stuttgart and has given me valuable advice on defining the subject of this thesis. I have also benefited a lot from his constructive suggestions regarding the research work throughout the years.

It is my great pleasure to thank Prof. Dr. -Ing. Bernd Kröplin and em Prof. Dr. -Ing. Werner Schiehlen for taking the responsibility to read and to evaluate my dissertation. I am also very grateful to them for their interests and valuable comments on my work.

My special gratitude goes to Prof. Dr. Gu Yuanxian from Dalian University of Technology (China). Without his constant encouragement and continual support in every aspects of my research work, the fulfilment of my doctoral study would be impossible.

I am indebted to my colleagues at the Faculty of Aerospace Engineering and Geodesy, in particular Dr. -Ing. Kurt A. Braun, Gerhard Frik, Helmut Schmid, Peter Gelpke, Sibylle Fuhrmann, Marion Hackenberg, Inge Biberger, Vlasta Reber-Hangi, for their excellent work and kindly help during my stay at the faculty.

Moreover, I would like to express my thanks to all the friends that made my stay in Stuttgart a memorable part of my life, specially Dr. -Ing. Haupo Mok, Friedlich Rau, Dr. -Ing. Yan Shuiping, Chen Zhidong, Xiao Li and the DAAD Coordinator Ursula Habel.

Last but not the least, I would like to thank my wife, Sui Changhong and my parents for their patience and encouragement throughout my doctoral study.

Contents

Zusammenfassung

Die vorliegende Arbeit befaßt sich mit der Formulierung und den numerischen Methoden für das robuste Design von Strukturen mit stochastischen Parametern. Die Theorie und die numerischen Methoden der Strukturoptimierung haben sich in den letzten zwei Jahrzehnten stark entwickelt. Ausserdem ermöglichen die schnell wachsenden Berechnungsmöglichkeiten die Berücksichtigung der Ungewissheiten im optimalen Strukturdesign. Die vorliegende Arbeit soll zu einem besseren Verständnis der Strukturoptimierung beitragen, indem man den Einfluß der stochastischen Streuung auf die Designrobustheit unter realistischen Bedingungen betrachted.

Robustes Strukturdesign bietet zuverlässige, quantitativ bestimmbare und leistungsfähige Methoden an, Produkte und Prozesse zu entwerfen, die gegenüber Systemschwankungen unempfindlich sind. Robustes Design kann in verschiedenen Phasen des Strukturdesigns, wie im Konzeptdesign, Parameterdesign und Toleranzdesign, erreicht werden. In dieser Arbeit wird das robuste Parameterdesign mit der Technik der Strukturoptimierung durchgeführt.

In der vorliegenden Arbeit wird das robuste Design der Struktur als ein multiobjektives Optimierungsproblem formuliert, in dem nicht nur der Mittelwert, sonder auch die Standardabweichung des strukturellen Verhaltens zu minimieren sind. Die Robustheit der Nebenbedingungen wird behandet, indem man die Standardabweichung der ursprünglichen Beschränkungsfunktionen miteinbezieht. Das Problem der Multikriterienoptimierung wird dann in ein skalares Optimierungsproblem durch eine gewichtete Summe der beiden Designkriterien umgewandelt. Das Optimierungsproblem des robusten Designs lässt sich mit den Algorithmen für das mathematische Programmieren lösen.

Die auf Perturbation zweiterordnung basierende stochastische Finite-Elemente-Analyse wird für das Auswerten des Mittelwertes und der standardabweichung der Strukturantwort im Problem des robusten Designs verwendet. Die auf Perturbation basierte Methode wird auch auf die stochastische Analyse der wegabhängigen Strukturen erweitert. Dabei wird eine entsprechende inkrementalle Lösung verwendet. Ausserdem werden die Sensitivitäten der statistischen Momente bezüglich der En-

twurfsvariablen im Rahmen der auf Perturbation basierten stochastischen Analyse bestimmt. Diese Sensitivitäten werden in den gradientenbasierten Optimierungsalgorithmen zur Lösung des Optimierungsproblems des robuste Designs eingesetzt.

Die Anwendbarkeit der vorgestellten Methode wird durch numerische Beispiele bestätigt. Die Ergebnisse zeigen, daß die Methode auf Pareto Optima des robusten Designproblems führen. Die numerischen Unterzuchungen zeigen auch, dass das Vermindern der Güteschwankungen des Strukturverhaltens häufig durch eine Verschlechterung entsprechender Mittelwerte erreicht wird.

Im letzten Teil dieser Abhandlung, wird das Problem des robusten Designs für inelastische Prozesse behandelt. Die auf Perturbation basierte stochastische Finite-Elemente Methode wird für die Analyse der inelastischen Prozesse erweitert, indem ein iterativer Algorithmus für das Lösen der Perturbationsgleichungen eingesetzt wird. Die numerischen Beispiele, einschliesslich der Auslegung des Werkzeugs für einen Extrusionsprozess und eines Metallvorformprozesses, zeigen die Eigung der vorgeschlagenen Methode für das robuste Design industrieller Umformungsprozesse.

Abstract

In this thesis, the formulation and the numerical method for the structural robust design are addressed. The theory and numerical techniques of structural optimization have seen a significant progress in the last two decades. Moreover, the rapidly increasing computational capabilities allows the structural optimal design to incorporate system uncertainty. The present study is intended to contribute to a better understanding of the structural optimization by putting emphasis on the design robustness in the presence of random noise under realistic conditions.

Robust structural design offers reliable, quantifiable and efficient means to make products and processes insensitive to sources of variability. Robust design may be attained in various stages of structural design, such as concept design, parameter design and tolerance design. In this study, the robust parameter design is accomplished using structural optimization techniques.

In the present study, the structural robust design problem is formulated as a multi-criteria optimization problem, in which not only the mean structural performance function but also its standard deviation is to be minimized. The robustness of the constraints are accounted for by involving the standard deviation of the original constraint function. The multi-criteria optimization problem is then converted into a scalar optimization problem by a performance function containing the weighted sum of the two design criteria. The robust design optimization problem can be then solved with mathematical programming algorithms.

The second-order perturbation based stochastic finite element analysis is used for evaluating the mean value and the variance of the structural response in the robust design problem. The perturbation based approach is also extended to the stochastic analysis of path-dependent structures, in accordance with the incremental integration scheme employed for the corresponding deterministic analysis. Furthermore, the moments sensitivity analysis for structural performance functions are developed based on the perturbation based stochastic finite element analysis. This sensitivity information is used in the gradient based optimization algorithms for solving the robust design optimization problem.

The feasibility of the presented method is demonstrated by truss benchmarks. As shown by the obtained results, the Pareto optima of the robust design problem can be obtained using the this method. The results also reveal that the diminishing of the structural performance variability is often attained at the penalty of worsening its expected mean value.

In the last part of the thesis, the robust design problems of inelastic deformation processes are addressed, with applications to the design of an extrusion die and of a metal preform. The perturbation technique is used for the stochastic analysis of the inelastic process, where an iterative algorithm is employed for solving the perturbation equations. The numerical examples show the potential applicability of the proposed method for the robust design of industrial forming process, too.

Nomenclature

$\mathbf{a}$	- Vector of acceleration
$\mathbf{b}$	- Vector of random variables
$\mathbf{c}$	- Vector of transformed random variables
C	- Coefficient of Coulomb friction
$\mathrm{Cov}(x, y)$	- Covariance
$\mathbf{C}$	- Damping matrix
$\mathbf{d}$	- Vector of design variables
$\mathbf{d}_\mathrm{L}$	- Lower bound of the design variables
$\mathbf{d}_\mathrm{U}$	- Upper bound of the design variables
$\mathbf{D}$	- Viscosity matrix
$\mathbf{D}_\mathrm{T}$	- Tangential viscosity matrix
e_{ij}	- Strain rate
$\bar{e}$	- Effective strain rate
E	- Young's modulus
$\mathrm{E}(\,)$	- Mean (expected) value
f	- Objective function
$\tilde{f}$	- Desirability function
g	- Constraint function
$\mathbf{K}$	- Stiffness matrix
$\mathbf{K}_\mathrm{T}$	- Tangential stiffness matrix
$\mathbf{K}_\mathrm{G}$	- Geometrical stiffness matrix
$\mathbf{M}$	- Mass matrix
n	- Number of degrees of freedom
p	- Hydrostatic pressure
$\mathbf{p}$	- Vector of external force
q	- Number of random variables
$\hat{q}$	- Number of reduced random variables

$\mathbf{r}$	- Vector of residual force
s( )	- Standard deviation of the samples
$\mathbf{s}$	- Vector of internal force
T	- Temperature
$\mathbf{u}$	- Vector of displacement
$\mathbf{v}$	- Vector of velocity
Var( )	- Variance
$\mathbf{x}$	- Geometry
α	- Weighting factor
β	- Feasibility index
λ_V	- Penalty factor for incompressibility
μ	- Coefficient of viscosity
ν	- Coefficient of Coulomb friction
$\boldsymbol{\sigma}$	- Stress
$\boldsymbol{\sigma}'$	- Deviatoric stress
σ_{f}	- Flow stress
σ_{H}	- Hydrostatic stress
$\sigma(\,)$	- Standard deviation
$\mathbf{\Sigma}$	- Covariance matrix
τ	- Time increment
τ_{c}	- Friction shear stress
ζ	- Time integration parameter
$\bar{[\,]}$	- Mean value of the samples

List of Figures

List of Tables

Chapter 1

Introduction

1.1 Motivation and background

Structural optimization is seeking the best set of design parameters defining a structural system. This technique provides a powerful tool to improve the engineering structural design in a rational manner and has been proved to be much more efficient than the conventional trial-and-error design process. Due to the developments of faster digital computers, more sophisticated computing techniques and more frequent use of finite element methods, structural optimization techniques have found their way into many facets of engineering practice for the sake of design improvement during the past decades. To some extent, design optimization has become a standard tool in many industrial fields and covers applications in civil engineering, mechanical engineering, vehicle engineering and more.

Particularly, structural optimization techniques have been intensively employed in the design practice of aerospace and aeronautical engineering. Typical space structures are often characterized by large structural scales, light weight designs, high flexibility and extreme environment conditions. Consequently, the structural behaviour under static and transient loads are usually important concerns in the design process. Numerical optimization methods have been applied to the optimal structural design of satellites, spacecrafts, aircraft fuselages and similar for the purpose of reducing the structural weight and satisfying the design requirements on structural properties such as improving the structural stiffness and strength, reducing the vibration levels, adjusting the natural frequencies and increasing the buckling loads[1][2][3][4].

In real engineering, the structural design problem may be subject to uncertainties. As an inherent characteristic of the nature, uncertainties appear everywhere and can not be avoided. Uncertainties may enter every aspects of engineering problems, such as model validation, model verification, design improvement, and so on. Particularly, in the problems of engineering structural design, uncertainties may arise from fluctuation and scatter of external loads, environmental conditions, boundary conditions, geometrical parameters and material properties. Some of these uncertainties are rather uncontrollable in practice. Nevertheless, incomplete knowledge about the parameters that enters the design process as well as the model errors are usually also considered as uncertainties.

For a structural system, uncertainties may be involved in four stages of its life-cycle, namely in system design, in manufacturing process, in service time and in the aging process (Fig. 1.1). In the stage of structural design, uncertainties may be introduced due to model errors as well as vague or incomplete knowledge about the system. In the manufacturing process, process non-uniformity, manufacturing tolerance and material scatter usually result in unit-to-unit variations. The external load fluctuation, temperature changes, boundary condition changes and the human error factor are major sources of variability in the service time of a structural system. As a structural system ages, the deterioration of material properties may become crucial to performance variability. These uncertainties will give rise to structural performance variations during its whole life-cycle.

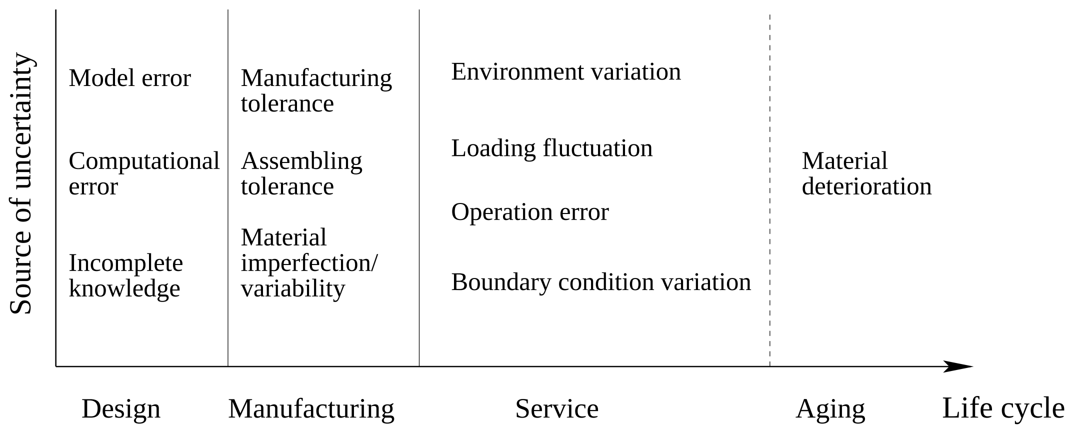

Figure 1.1: Sources of uncertainty

In conventional design procedures, it is a common practice to neglect the uncertainty when setting up the analysis model of a structural system. Then a deterministic model of the structural system is established, where only ideal / nominal values of parameter are considered. The structural performance is calculated based on deterministic structural analysis. To compensate for performance variability caused by system variations, a so-called safety factor defined as the ratio of capacity to demand is introduced. Larger safety factors are correlated with higher levels of uncertainty. Typical safety factors can range between two to five, or even exceed ten for some important structural components. In practical engineering designs, the value of the safety factor is mainly determined by corresponding design codes or by relative importance of the structural components of structural systems, rather than by a scientific consideration of the nature behind the design problem. It is well recognized that the safety factors specified in current design practice may be either too conservative or too dangerous due to lack of knowledge about the scatter of structural performance. Under an ever increasing demand on efficiency and reliability of the design process, the shortcomings of conventional design procedures need to be overcome by the computer aided structural optimization techniques.

Conventional structural optimization problems are formulated under deterministic assumptions and the uncertainties involved in the problem are not addressed in a rational way. In such a formulation, the objective function and the constraints are calculated with nominal values of the parameters. Based on results of the deterministic analysis of the idealised numerical model, the so-called optimal design can be attained with optimization tools. Although the deterministic optimum signifies the best performance in theory, practical implementation exactly in accordance with such a design is not feasible, due to manufacturing tolerances, for example. Moreover, the parameters of the structural system might be subject to changes during the service stage, due to, for instance, thermal action or material deterioration. Such variations about the nominal value of the parameters will result in the scatter of the actual system performance, so that the real system may behaviour far worse than predicted by the ideal mathematical model. Therefore, a design candidate having the best performance under nominal conditions may yield less than optimum performance in the presence of system uncertainties, whereas another design candidate with less optimal performance under nominal conditions may be less sensitive (more robust) to parameter variations and thus would be a more rational choice in the decision making process of structural design. For this reason, one is not sure to arrive at the most cost effective solutions by using the deterministic optimization techniques.

On the other hand, it is also meaningful to reduce the variations of structural performance in many engineering applications. From an engineering perspective, a higher performance variation not only increases the probability of failure, but also increases significantly the structural life-cycle costs, including inspection costs, repair costs and other maintenance costs. Well-designed structures minimize these costs by performing consistently.

With an increasing demand for more rational designs which are optimized under the aspect of costs and performance, there arises the need to account for design robustness in the optimal design problems. Compared with conventional design methods which completely neglect uncertainties, design methods based on the knowledge of the system behaviour under uncertainties are more advantageous in reducing maintenance costs, extending component life and improving the system performance. Therefore, it becomes highly important to acquire an understanding of the system performance under uncertain conditions in the structural optimization problems.

Design improvements for performance robustness by conventional trial-and-error approaches are rather difficult if the system has multiple design parameters and restrictions. Therefore, various systematic methods of robust structural design have been developed for the past decade. Engineering robust design has traditionally been implemented experimentally following Taguchi's methodology of using orthogonal experimental arrays [5]. Such techniques have found a wide range of applications especially where laboratory experiments are used for evaluation of a product/ process design. However, a combination of the finite element analysis techniques and the structural optimization techniques, which have been widely adopted in the structural design disciplines, makes it possible to accomplish robust design on the basis of numerical simulations. We call such an approach analytical robust design optimization. Compared with traditional robust design methods, analytical robust design optimization is much faster, more cost effective, more accurate and more insightful. However, this subject is still less frequently considered in structural design optimization studies.

This study attempts to consider the structural optimization under uncertainty from a broader perspective and to develop mathematical formulations as well as computational algorithms for robust design optimization of products and process. Unlike some other formulations usually considered in non-deterministic structural design problems such as Reliability Based Design Optimization, the robust structural design aims to reduce the variability of structural performance caused by regular fluctuations rather than to avoid occurrence of catastrophe in extreme events. Mathematically formulated, the structural robust design optimization proposed in the present study is to find a set of design variable values which fulfill the requirement of both improving structural performance and minimizing its variability under observance of constraint conditions. In the framework of the perturbation based stochastic finite element method, numerical algorithms for sensitivity analysis are developed and then the structural robust design problems are solved by optimization techniques. The perturbation based finite element analysis is also extended to problems with path-dependent nonlinearities for applications of robust design of materially nonlinear structures. Finally, the proposed methods are further extended to the robust design optimization of industrial forming process characterized by inelastic deformation.

It should be noted here, that although the robust design of deformation processes is also a subject of this study, its focus is confined to the size and shape design, similarly as in the structural optimal design problems. Therefore, the term *structural optimization* is used throughout the thesis.

1.2 Outline of the thesis

This thesis is divided into nine chapters and structured as follows:

- In chapter 2, an overview of the foundations of structural optimization is provided, with the focus on the conventional deterministic optimization problems. Particularly, the issues closely related to this study are addressed, including the multi-criteria optimization and the sensitivity analysis

- Chapter 3 deals with the review of structural optimization problems under consideration of system uncertainty. Several relevant formulations are presented. The fundamental differences between the frequently used Reliability Based Design Optimization (RBDO) and the robust design are discussed and the practical advantages of structural robust design is underlined. The last part of this chapter presents a review on the current state of the research on structural robust design.

- Chapter 4 exposes the existing perturbation based stochastic finite element methods (SFEM) for linear and path-independent nonlinear problems. A comparison between the perturbation based approaches and the Monte Carlo simulation is made.

- In Chapter 5, the structural robust design is mathematically formulated as a multi-criteria optimization problem. The proposed formulation is then compared with those based on Taguchi's orthogonal array concept.

- In Chapter 6, a response moment sensitivity analysis algorithm based on direct differentiation is developed and the robust design problem of linear structures is solved with a gradient-based optimization method. Several numerical examples are presented.

- Chapter 7 extends the perturbation based stochastic finite element analysis to the path-dependent nonlinear problems, where an incremental scheme consistent with the primary (background) deterministic analysis is proposed. The method has been applied to the robust design problems with material and geometrical nonlinearities.

- In Chapter 8, the first-order perturbation based stochastic finite element analysis for inelastic deformation process is developed based on an iterative scheme. The proposed method is applied to the robust design of an extrusion die and to a metal preform design problem. Numerical results show the potentials of the present method for applications regarding the robust design of industrial forming process.

- Chapter 9 contains a summary of the performed research, and proposals for future research work.

Chapter 2

Fundamentals of structural optimization

In this chapter, the conventional structural optimization methods are reviewed. The focus is put on the topics closely associated with the present study on structural robust design, including the theoretical and computational aspects of multi-criteria optimization and sensitivity analysis.

2.1 Conventional structural optimization

Methods of structural optimization are widely used in the design of engineering structures for the purpose of improving the structural performance and reducing their costs. The use of structural optimization has rapidly increased during the past decades, mainly due to the developments of sophisticated computing techniques and the extensive applications of the finite element method. Considerable progress has been made in the field of structural optimization.

In a structural optimization problem, the free parameters that need to be determined to obtain the desired structural performance are referred to as the *design parameters*. The function for evaluating the merits of a design is called the *objective function*. Generally, a number of restrictions must be satisfied in a structural design problem. These restrictions define the feasible domain in the design variable space and are referred to as the *design constraints*. Additionally, bound limits may be imposed to the design variables and they are known as *side constraints*. In a design optimization problem, the objective function and the constraints are often expressed as implicit functions of the design variables and the evaluation of these functions generally involve numerical simulation such as by the finite element method.

The classical statement of structural optimization problem is mathematically expressed as

$$\begin{array}{ll} \text{find} & \mathbf{d} \\ \text{minimizing} & f(\mathbf{d}) \\ \text{subject to} & g_i(\mathbf{d}) \leq 0 \; (i = 1, 2, ..., k), \\ & \mathbf{d}_\mathrm{L} \leq \mathbf{d} \leq \mathbf{d}_\mathrm{U} \end{array} \tag{2.1}$$

where $\mathbf{d} \in \mathrm{R}^{n+1}$ is the vector of design variables, f the objective function, $g_i \, (i = 1, 2, ..., k)$ the inequality constraint functions, $\mathbf{d}_\mathrm{L}$ and $\mathbf{d}_\mathrm{U}$ denote the lower and upper bound limits of the design variables, respectively. The design variables can be structural design parameters such as the parameters defining the geometrical dimensions, the shape or the topology of the structure. In practical applications, it is usual to make use of the design variable linking technique to reduce the number of the independent design variables by imposing a relationship between coupled design parameters. The objective function and the constraint functions can be the structural cost, the material volume/structural weight, structural performances such as structural compliance, nodal displacements, stresses, natural frequencies, buckling loads and similar. Since they are typically implicit functions of the design variables, we need to perform structural analysis (e.g. finite element analysis) whenever their values are required.

In the deterministic formulation of the structural optimization problems, the design variables and other structural parameters are assumed deterministic and the objective function as well as the constraints are referred to their nominal values.

According to the types of design parameters to be considered, the structural optimization problems can be broadly classified into three categories:

- **Sizing optimization**: design variables are geometrical dimensions such as cross sectional areas of truss members, beam section parameters and plate thickness.
- **Shape optimization**: design variables are the geometry parameters describ-

ing the shape of the designed parts [6].

– **Topology and layout optimization**: the number and locations of voids in a continuous structure or the number and connectivity of members in a discrete structure (e.g. truss and frame structure) are to be determined [7].

The research on the methods and applications of structural optimization has increased rapidly during the past decades. A variety of numerical techniques have also been developed and applied to both linear and nonlinear problems (e.g. [8][9]).

Basically, the solution methods for structural optimization problems can be classified into Optimality Criteria (OC) methods and mathematical programming methods.

In the Optimality Criteria methods [10][11], the optimality conditions for a given type of problems are derived based on Karush-Kuhn-Tucker condition or by heuristic assumptions and then the optimal design satisfying these conditions are to be sought using different forms of resizing rules. Such methods are recognized to be especially efficient for problems involving a large number of design variables. The most frequently used traditional OC approach is the Stressed Ratio (SR) method for the fully stressed design. It uses the intuitive optimality condition that all the member in the optimal design should reach the permissible stress. Examples of more recently developed OC methods are the Continuum-based Optimality Criteria method (COC) and the Discretized Optimality Criteria methods (DOC). Since some intuitive optimality conditions turn out to be misleading and closed-form expressions of optimality conditions are not always available, the applications of this approach are restricted to only a small number of specialized problems.

The dominating methods for the optimal design of structures are the mathematical programming methods, where the problem is treated as linear or nonlinear Mathematical Programming (MP). Different standard optimization algorithms can be used to seek the optimum, often in a iterative manner. Examples of such methods include the steepest descend method, conjugate gradient, trust domain method, SLP (Sequential Linear Programming) method and SQP (Sequential Quadratic Programming) method. In the context of structural optimization problems, a variety of programming methods can be employed, including gradient based algorithms and some direct search methods based on functional evaluations. Particularly, the SLP and SQP are two of the most frequently used methods.

SLP and SQP methods are both standard general purpose mathematical programming algorithms for solving Non-Linear Programming (NLP) optimization problems.

They are also considered to be the most suitable optimization algorithms in the structural optimization discipline. These approaches make use of derivatives of the function with respect to the design variables to construct an approximate programming model of the initial problem. A searching direction is then determined based on this model. By performing a line search along this direction, a new design point which produces a decrease of the merit function can be found. The procedures are repeated, until a local optimum is obtained. These methods present a satisfactory local convergence rate, but can not assure that the global optimum can be found. However, this shortcoming can be to some extend remedied by starting from multiple initial designs.

Some special techniques are needed for the discrete structural optimization problem when the mathematical programming optimization methods are employed. Such algorithms rely on the sensitivity calculation of the objective function and the constraints with respect to the design variables. Therefore, continuous functions representing the objective and constraints defining the optimization problem are required. For some engineering design problems, the design parameters are discrete variables by nature, if their values can only be chosen from a limited set. In these circumstances, an approximate continuous representation of the relationships between the discrete allowable values of design parameter and the desired structural properties must be set up and a round-off procedure is usually needed to present a allowable design using the optima obtained with gradient based methods.

Apart from the aforementioned methods, experimental designs are also used to set up approximate design performance models, for instance by the Response Surface methodology. Therein, the optimization problem is formulated based on these approximate performance models instead of the computationally expensive finite element model of the real structure. As results, the original structural optimization problems are transformed into more manageable problems.

In addition to these conventional methods, some innovative approaches using analogies of physics and biology, such as simulated annealing, genetic algorithms and evolutionary algorithms (Papadrakakis et al. [12], Deb [13]), are also employed for the solution of global optimization problems. These approaches are characterized by gradient-free methods and utilize only function values. Generally, they require a large number of function evaluations to achieve convergence and thus have limited use in applications involving complicated structures.

2.2 Multi-criteria optimization and Pareto optimum

The principles of multi-criteria optimization (also known as multi-objective optimization or vector optimization) are different from that of a single-objective one. The main goal in a single-objective optimization is to find a solution that minimizes the objective function. However, a multi-criteria optimization problem has more than one objectives and it is often characterized by conflicting objectives. Therefore, a multi-criteria optimization gives rise to a set of optimal solutions, instead of one optimal solution. In this solution set, no one solution can be considered to be better than any other with respect to all objective functions. These optimal solutions are known as *Pareto Optima* (also known as *non-inferior solutions* or *non-dominated solutions*) [14].

A common practice in solving multi-criteria optimization problems is to convert the multiple objectives into one objective function and thus a substitute scalar optimization problem is constructed, which can be handled using standard optimization routines. There exist a number of methods [14] addressed in the literature for accomplishing this task: weighted sum approach, ε- perturbation method, min-max method, goal programming method, and others. Multiple Pareto-optimal solutions can be obtained by setting different parameters when using these optimization algorithms.

The basic ideas for some multi-criteria optimization algorithms are given here:

- In the ε - perturbation (ε - constraints) method, one of the objectives is selected at a time and that objective is minimized while the other objectives are treated as constraints. By optimizing all the objectives one at a time, the Pareto set can be generated.
- In the Min-max method, the Pareto optima are obtained by minimizing a generalized distance between objective function values and their maximum possible values or target values set by the designer.
- In the goal programming method, the goals for each objective are set by the designer as constraints. The optimization is performed on the objective with highest priority first with other objectives considered as constraints. Then the procedure is applied to the objective with lower priority with an additional requirement that the solution must meet the optimum value of the objective

with higher priority. This procedure is repeated for all the objectives and thus a Pareto optimum can be obtained.

- The weighted sum approach is a familiar method for solving multi-criteria optimization problems. Thereby each objective is given a weighting factor and a scalar merit function is formulated as a sum of all the weighted objectives. The weights are normalized, so that the sum of all the weighting factors is equal to 1.0. The values of the weighting factors for each objective are determined based on the priorities of the designer. By changing the weighting factors in a systematic manner, the Pareto optima can be generated.

- Besides the conventional approaches mentioned above, a relatively new method known as Parameter Space Investigation (PSI) has been proposed by Statnikov and Matusov [15]. In this method, a set of trial designs covering the entire design space are generated. The objective function values for these designs are analyzed and suitable constraints on the objective functions are then determined. As a last step, a feasible region under these constraints is set up so that a set of Pareto optima can be selected. Then the task of the structural optimization becomes seeking the best design from a family of feasible designs.

2.3 Approximation concepts and sensitivity analysis

Typically, much computational effort is required for the prediction of the structural response for successive modifications in the design. In general, the computer implementation effort involved in the structural optimization can be substantially reduced when approximation techniques are used. Hence, researchers often use numerical methods to develop approximate relationships between the functional value of the objective/ constraints and the design variables. Subsequently, several most common approximation methods are addressed, while special emphasis is put on the sensitivity analysis.

Response surface model

Response Surface Methodology (RSM), introduced by Box and Wilson [16], is a technique to construct a global or midrange approximate mathematical model (surrogate model) by systematically sampling in parameter space. Such a model is used for the prediction of the performance function of an input-output system, where the function values are determined either experimentally or by numerical analysis. In structural optimization problems, the response surface model is specially useful in applications where the direct analysis is computationally expensive, or the design sensitivity information is difficult or impossible to compute.

The response surface method has been used in some studies to replace the original finite element model and it works well when the number of input variables is small. However, it has been criticised for its inaccuracy and inefficiency in real scale applications with a large number of input variables.

Approximate structural re-analysis

Structural re-analysis is a frequent task in the optimal design. Approximate re-analysis methods are intended to predict the response of a structure after modification using the result of a single exact analysis. The computational effort involved in a re-analysis is typically much less than a complete analysis [17]. Reviews of existing structural reanalysis methods can be found in the literature [18].

Sensitivity analysis

Sensitivity analysis is employed to evaluate the gradient of the structural performance with respect to the design variables. These derivatives are used to construct approximate explicit expressions and to solve the optimization problems when gradient based methods are employed. Therefore, cost efficient sensitivity analysis of the structural response is always of concern.

We denote the vector of the structural displacements by $\mathbf{u}$, the vector of the design variables by $\mathbf{d}$. Then, the design sensitivity of a structural performance functional $f(\mathbf{u}(\mathbf{d}), \mathbf{d})$ with respect to the ith design variable is defined as

$$\frac{\mathrm{d}f}{\mathrm{d}d_i} = \frac{\mathrm{d}f(\mathbf{u}(\mathbf{d}), \mathbf{d})}{\mathrm{d}d_i}. \tag{2.2}$$

There exist a variety of methods for structural sensitivity analysis in the literatures. The simplest approach for response sensitivity analysis is the finite difference method, in which the derivative of the function with respect to the design variable is approximated by a differential quotient obtained for a small perturbation to the design variable. For instance, the sensitivity can be approximated with the forward finite difference

$$\frac{\mathrm{d}f}{\mathrm{d}d_i} \approx \frac{f(\mathbf{u}(\mathbf{d}+\delta d_i\mathbf{e}_i), \mathbf{d}+\delta d_i\mathbf{e}_i) - f(\mathbf{u}(\mathbf{d}), \mathbf{d})}{\delta d_i}. \tag{2.3}$$

where $\mathbf{e}_i = \{0...1...0\}$ is an unit vector with the rth component being 1 and the other components zero.

This method is actually applicable to both linear and nonlinear problems. However, the method suffers from the drawback of inefficiency due to lengthy structural re-analysis for each design variable. Moreover, the results of the method depend strongly on the perturbation values and the accuracy can not be ensured.

Recently, the techniques of automatic differentiation (AD) has also been used as a tool for structural response sensitivity analysis [19]. In this approach, a new source code for calculating the derivatives explicitly is produced by an AD package from the function evaluation source code using the chain rule of differentiation. The implementation of this approach requires considerable memory usage and computational effort.

A considerable amount of research work on more sophisticated design sensitivity analysis methods has been done for the past decades. The existing numerical methods for sensitivity analysis fall into two categories: *discrete sensitivity analysis* and *variational sensitivity analysis*. In the former methods, the sensitivity equations are derived based on the discrete formulation (finite elements) of the primary problem, whereas in the latter methods, the response gradient is set up from the variational principle and then discretized with the finite element method. Theoretically, both methods should yield the same numerical results. It is also pointed out that the computational effort required for the implementation of both methods is comparable [20].

From the computational point of view, numerical methods for linear structural problems have been successfully developed, cf. the review papers [21][22]. The prevailing methods for linear structures are the aforementioned discrete sensitivity analysis methods, among which *semi-analytical methods* [23][24] are most frequently used and well known in the literature. In these methods, the sensitivity equation is derived by the analytical differentiation of the discrete governing equation, and the derivatives of the coefficients are calculated on the basis of finite differences, often at the element level. According to the type of the variables appearing in the sensitivity equations, the semi-analytical methods can be further classified as the *direct method* and the *adjoint method.*

– Direct method

The direct method is derived by differentiating the governing equations of the finite element analysis with respect to the design variables. Taking the linear static structural problem

$$\mathbf{K}\mathbf{u} = \mathbf{p} \tag{2.4}$$

as an example, the sensitivity equations are expressed as

$$\mathbf{K}\frac{\mathrm{d}\mathbf{u}}{\mathrm{d}d_i} = \frac{\mathrm{d}\mathbf{p}}{\mathrm{d}d_i} - \frac{\mathrm{d}\mathbf{K}}{\mathrm{d}d_i}\mathbf{u}, \tag{2.5}$$

and

$$\frac{\mathrm{d}f}{\mathrm{d}d_i} = \frac{\partial f}{\partial \mathbf{u}}\frac{\mathrm{d}\mathbf{u}}{\mathrm{d}d_i} + \frac{\partial f}{\partial d_i}. \tag{2.6}$$

where the differentiation of the stiffness matrix $\mathbf{K}$ and the external load $\mathbf{p}$ with respect to the design variable are evaluated either analytically or by finite differences (as in the semi-analytical method).

– Adjoint method

When the number of the design variables is much greater than the number of functions to be differentiated, the adjoint method can lead to substantial reduction of computational effort.

For a problem governed by Eq. (2.4), the procedures are described as follows:

$$\mathbf{K}\lambda = \left(\frac{\partial f}{\partial \mathbf{u}}\right)^{\mathrm{t}}, \tag{2.7}$$

$$\frac{\mathrm{d}f}{\mathrm{d}d_i} = \lambda^{\mathrm{t}} \left(\frac{\mathrm{d}\mathbf{p}}{\mathrm{d}d_i} - \frac{\mathrm{d}\mathbf{K}}{\mathrm{d}d_i}\mathbf{u} \right), \tag{2.8}$$

where λ is the vector of adjoint variables.

As can be seen from Eqs. (2.5) and (2.8), the sensitivity analysis does not require re-factorization of the stiffness matrix, and this is beneficial for both the direct and the adjoint methods.

In contrast to the sensitivity analysis of linear problems, the methods for structures with material and/or geometrical nonlinearities become more complicated and are much less well developed. The difficulties arise from the fact that the methods for linear problems can not directly be applied to the nonlinear ones due to the essential difference of the problems [25]. Particularly, for problems involving elastoplastic material, the sensitivity analysis must be formulated in consistency with the incremental scheme used in the primary analysis so as to account for the path-dependent nature of the problem. This issue has been addressed in a number of previous works, some of which are listed below.

Lee and Arora [26] studied the design sensitivity analysis of structural systems having elastoplastic material behavior using the continuum formulation. A computational procedure based on the response obtained by the load incrementation approach is developed by considering design variations in the equilibrium equation. In this procedure, iterations are required at each load step to obtain the sensitivity results but the stiffness matrix is kept unchanged. Schwarz [27] presented a variational and direct formulation for the analytical sensitivity analysis of structures involving elastoplastic material behavior as well as geometrical nonlinearities. The study reported underlines the importance of the incremental formulation in the problem of concern. Kim et al. [28] presented a continuum-based shape design sensitivity formulation for elastoplasticity with a frictional contact condition. The direct differentiation method (DDM) is used to compute the displacement sensitivity. The path-dependence of the sensitivity equations due to the constitutive relation and friction is discussed. It should be noted that the sensitivity analysis for path-dependent problems can be also performed using adjoint method. Nevertheless, it is revealed that such a method appears less attractive due to its inefficiency [26].

Recently, the sensitivity analysis of inelastic deformation process has also gained a considerable attention. The computations are usually performed by direct differentiation techniques, where either the equations of the continuum problem are design-differentiated and then discretized, or the discrete equations of the problem are design-differentiated. The first approach is termed as Continuum Sensitivity Method (CSM) and has been used by Zabaras and colleagues [29] for the sensitivity analysis of metal forming problems. Doltsinis and Rodic [30] addressed the discrete method of sensitivity evaluation for isothermal and non-isothermal deformation with respect to time-dependent parameters using. The numerical procedures of the direct method and the adjoint method were described.

Chapter 3

Structural optimization under uncertainty

This chapter presents an overview of structural optimization considering uncertainty and an insight into the structural robust design problem. First, several mathematical models of uncertainty in engineering are introduced. Then, we present an overview on existing formulations of non-deterministic structural optimization problems. In section 3.3, we discuss in detail the concept of structural robust design, as well as the fundamental differences between the structural robust design and another commonly used non-deterministic formulation - the Reliability-based Design Optimization (RBDO). In the last part of this chapter, we present a review on the current research state of the structural robust design.

3.1 Mathematical models of uncertainty

The formulation of a structural optimization problem under uncertainty is closely related to the modeling of the uncertainty. There exist various mathematical models of uncertainty when dealing with structural design problems. The existing models can be classified into probabilistic model e.g. stochastic randomness and non-probabilistic models including interval set, convex modeling, fuzzy set and leveled noise factors. A short introduction to these uncertainty models is given below.

Randomness

The prevailing model for uncertainties in structural engineering is *stochastic randomness* [31][32]. The Probability Density Function (PDF) and Cumulative Distribution Function (CDF) are used to define the occurrence properties of uncertain quantities which are random in nature. Randomness accounts for most of the uncertainties in engineering problems. In computational engineering problems, the model errors and the uncertainties that arise from incomplete knowledge about the system are often regarded as random uncertainties as well.

In the practical structural engineering problems, randomness of the uncertain parameters are often modeled as a set of discretized random variables. The statistical description of a random variable X can be completely described by a cumulative density function $F(x)$ or probability density function (PDF) $f(x)$ defined as

$$F_X(x) = P(X \leq x) \equiv \int_{-\infty}^{x} f_X(x)\mathrm{d}x, \tag{3.1}$$

where $P(\,)$ is the probability that an event will occur.

The probability distribution of the random variable X can be also be characterized by its statistical moments. The most important statistical moments are the first and second moment known as mean value $\mu(X)$, also referred to as expected value and denoted by $\mathrm{E}(X)$, and variance denoted by $\mathrm{Var}(X)$ or $\sigma^2(X)$, respectively, as given by

$$\mu(X) = \mathrm{E}(X) = \int_{-\infty}^{\infty} x\mathrm{d}F_X(x) = \int_{-\infty}^{\infty} x f_X(x)\mathrm{d}x, \tag{3.2}$$

and

$$\sigma^2(X) = \int_{-\infty}^{\infty} (x-\mu(X))^2\mathrm{d}F_X(x) = \int_{-\infty}^{\infty} (x-\mu(X))^2 f_X(x)\mathrm{d}x. \tag{3.3}$$

In structural engineering, distributions types such as lognormal, Weibull and uniform are the most commonly used ones [33].

Nevertheless, precise information on the probabilistic distribution of the uncertainties are sometimes scarce or even absent. Moreover, some uncertainties are not random in nature and can not be defined in a probability framework. For these reasons, non-probabilistic methods for modeling of uncertainties have been developed in recent years. These methods do not require apriori assumptions on PDFs for the description of uncertain variables.

Interval set

Interval set is used to model uncertain but non-random parameters. These uncertainties are assumed to be bounded within a specified interval and the small variation of the interval parameter is treated as a perturbation around the midpoint of this interval, allowing to use the interval perturbation method for the analysis of the structural performance variation (e.g. [34][35]). Using the so-called anti-optimization techniques, the least favourable response can be determined under assumption of small variations. The term anti-optimization is referred to the task of finding the worst-scenario of a given problem. The methods based on interval set do not allow for distinction on more or less probable occurrence of the variables. Moreover, it is difficult to consistently define bounded intervals for the uncertainties without a confidence level.

Convex modeling

To overcome the difficulties when data are insufficient to permit a reliability analysis using conventional probabilistic approaches, the worst-case scenario analysis based on Convex Modeling can be formulated [36][37]. The Convex Modeling is connected to uncertain-but-bounded quantities. In this method, the uncertainty which has bounded values is assumed to fall into a multi-dimensional ellipsoid or hypercube. In some sense, the convex model can be regarded as a natural extension of the interval set model. In virtue of the Convex Model theory, the worst-case performance of the structure is determined using the anti-optimization technique. This method has been proved to be advantageous to the traditional worst-case approach, where all the possible combinations of extreme values of the uncertain parameters need to be examined so that the worst case scenario can be determined [38].

Fuzzy set

Fuzzy set theory has been developed as a mathematical tool for quantitative modeling of uncertainty associated with vagueness in describing subjective judgements using linguistic information. In the fuzzy set method for engineering design problems, the uncertainty is modelled as fuzzy numbers rather than random values with certain distribution [39]. In other words, the fuzzy set theory presents a possibility rather than probability description of the uncertainty. The fuzzy analysis method has been used to deal with certain problems such as structural analysis under uncertain loading conditions [40].

Leveled noise factors

In Taguchi's robust design methodology [41], the system uncertainties are modeled as leveled noise factors. Here no *a priori* assumptions on the statistics of the uncertainties are required. Following the method of experimental design, the system outputs are examined at planed combinations of the discrete levels of these noise factors. Thus the interactions between system performance and noise factors can be explored.

3.2 Overview of problem formulations

Conventional structural design procedures accounting for system uncertainties are based on safety factors. This method has been criticised as lacking systematical background and often furnishing to too conservative designs. Moreover, in the design of novel structures or products, little prior knowledge for determining an appropriate safety factor is available.

In the past decades, more sophisticated formulations incorporating system uncertainty into design optimization have been proposed on the basis of various mathematical models of uncertainty [42], as given below.

3.2.1 Reliability based design optimization (RBDO)

In the present treatise, the term *reliability-based design optimization* (RBDO) is referred, in a narrow sense, exclusively to the optimal design where the cost function of the problem is to be minimized under observance of probabilistic constraints instead of conventional deterministic constraints [43][44]. Until recently, the RBDO has been the only way of taking account of uncertainty in structural optimization problems.

When the occurrence of catastrophic failure of the system or component is crucial in a structural system, the design optimization problem is usually characterized as a problem of reliability-based design optimization. In this framework, the probability of structural failure is involved in the constraint conditions of the design optimization problems. The failure of a structural system or a structural component is defined with limit state functions.

From the theoretical point of view, reliability-based design optimization has been a well-established concept. Mathematically, RBDO [45] can be stated as

$$\begin{aligned}
&\text{find} && \mathbf{d} \\
&\text{minimizing} && f(\mathbf{d}) \\
&\text{subject to} && P(g_i(\mathbf{d}) \leq 0) - \Phi(-\beta_i) \leq 0 \; (i = 1, 2, ..., k). \\
& && \mathbf{d}_L \leq \mathbf{d} \leq \mathbf{d}_U
\end{aligned} \tag{3.4}$$

where $P(g_i(\mathbf{d}) \leq 0)$ is the failure probability, Φ is the integral of the (0,1) standardized normal distribution and β_i is the so-called safety-index.

The statistical description of the failure of the performance functions $g_i(\mathbf{d})\,(i = 1, 2, ..., k)$ requires a reliability analysis. Prior to the reliability analysis, the statistical characteristics of the random quantities are first defined by suitable probability distributions. Then the probability of failure is evaluated by numerically stable and affordable procedures.

For the purpose of the probability integration in the structural reliability analysis, various methods have been developed [46]. In the direct Monte Carlo simulation or Importance Sampling method, the probability of failure is derived from the test data of a large amount of samples. In the First Order Reliability Method (FORM), the Second Order Reliability Method (SORM) or the Advanced Mean Value method, an additional nonlinear constrained optimization procedure is required for locating the Design Point or Most Probable Point of failure (MPP) and thus the reliability-based design optimization becomes a two-level optimization process with lengthy calculations of sensitivity analysis in the inner loop for locating the MPP.

Generally, the reliability based design is computationally expensive, typically requiring much more function evaluations than a corresponding deterministic design optimization problem. Therefore various numerical techniques have been proposed for reducing the computational cost in the reliability design optimization [47]. For example, Kaymaz et al. [48] used the response surface as a substitution of the real finite element model and combined the response surface method with Monte Carlo simulation to overcome the difficulty of the reliability calculation in terms of computational cost for the optimization problems, especially when highly non-linear performance functions are involved. Kleiber et al. [49] discussed problems of the interactive reliability-based design optimization of geometrically nonlinear truss structures, in order to overcome the convergence difficulties of the fully automated approach for large nonlinear structures. The techniques used by the authors are interactive control over the parameters of the finite element iterative algorithm and the convergence parameters of the optimizer, post-buckling response approximation, interactive adding/removing constraints, interactive modifying status of variables, and so on.

It is worth remarking, besides the construction costs or the loss directly caused by catastrophic failure, some metrics related to the overall costs of the structural system have been taken into considerations in the reliability based design optimization. Wen [50] has studied the design optimization of structures against multiple hazards based on considerations of minimization of expected life-cycle cost, including those incurred in construction, maintenance and operation, repair, damage and failure consequence, etc.. A close form solution of the expected total life-cycle cost is obtained for use in the optimization process.

Reliability-based design optimization exhibits severe limitations related mostly to low computational efficiency or convergence problems. Moreover, only in a small number of specialized cases, the complete statistical information about structural parameters and loads is available. As pointed out in [37], inadequate assumptions on the probabilistic distribution may lead to substantial errors in the reliability analysis. In this sense, RBDO might be of less practical value if information about the random uncertainty is not available or not sufficient to permit a reliability analysis.

3.2.2 Worst case scenario-based design optimization

In some non-deterministic structural optimization problems, the design against structural failure is based on the worst case analysis. In practical applications of this approach, the convex model or interval set can be used to model the system uncertainties. In these approaches, the anti-optimization strategy is adopted to determine the least favourable combination of the parameter variations [51] and the problem is then converted into a deterministic Min-max optimization. Here no probability density function of the input variables are required. Elishakoff et al.[52] applied this method to the structural optimal design problem considering bounded uncertainty. Yoshikawa et al. [36] presented a formulation to evaluate the worst case scenario for homology design caused by uncertain fluctuation of loading conditions using the convex model of uncertainty. The validity of the proposed method is demonstrated by applications to the design of simple truss structures. Lombardi and Haftka [53] combined the worst case scenario technique of anti-optimization and the structural optimization techniques to the structural design under uncertainty. The proposed method is suitable in particular for uncertain loading conditions.

Since a complete optimization routine needs to be nested for the worst case analysis at each structural optimization cycle, this approach may become prohibitively expensive when many uncertain parameters are present in the problem. Additionally, this design technique often results in too conservative designs.

3.2.3 Fuzzy set based design optimization

In the fuzzy set based structural optimization [54], the vague quantities which can not be clearly defined in a structural system are characterized by membership functions. In this context the possibility of structural failure is restricted in the optimal design. Since this method is featured as a non-probabilistic description of system reliability, it can be regarded as a possibility based approach. In a similar way as in RBDO, this approach focuses exclusively on the issue of the structural safety with the purpose of avoiding system catastrophe in the presence of parameter uncertainties.

Fuzzy set theory has been initially used by Rao [55][40] to handle structural optimization under uncertainties. A random set approach has been proposed by Tonon and Bernardini [42] as an extension of the fuzzy set method for structural optimization problem which is characterized by imprecise or incomplete observations on the uncertain design parameters. Gerhard and Haftka [56] used the fuzzy set theory for modeling the uncertainty associated with the design with future materials in the aircraft industry. The design problem involves maximizing the safety level of a structure. Response surface methodology is also used throughout the design process to reduce the computational effort.

3.2.4 Robust design

Apart from the aforementioned formulations, robust design, in which the structural performance is required to be less sensitive to the random variations induced in different stages of the structural service life cycle, has gained an ever increasing importance in recent years. In the next section, the structural robust design will be further addressed.

3.3 Structural robust design

3.3.1 Concept of structural robust design

Robust design is *an engineering methodology for optimal design of products and process conditions that are less sensitive to system variations.* It has been recognized as an effective design method to improve the quality of the product/process. Three stages of engineering design are identified in the literatures: conceptual design, parameter design and tolerance design. Robust design may be involved in the stages of parameter design and tolerance design.

For design optimization problems, the structural performance defined by design objectives or constraints may be subject to large scatter at different stages of the service life-cycle. It can be expected that this might be more crucial for structures with nonlinearities. Such scatters may not only significantly worsen the structural quality and cause deviations from the desired performance, but may also add to the structural life-cycle costs, including inspection, repair and other maintenance costs. From an engineering perspective, well-designed structures minimize these costs by performing consistently in presence of uncontrollable variations during the whole life-cycle. In other words, excessive variations of the structural performance indicate a poor *quality* of the product. This raises the need of structural robust design. To decrease the scatter of the structural performance, one possible way is to reduce or even to eliminate the scatter of the input parameters, which may either be practically impossible or add much to the total costs of the structure; another way is to find a design in which the structural performance is less sensitive to the variation of parameters without eliminating the cause of parameter variations, as in robust design.

The concept of robustness is schematically illustrated in Fig. 3.1. The horizontal axis represents the value of a structural performance function f, which is required to be minimized. The two curves show the distributions of the occurrence frequency of the value of f corresponding to two individual designs, when the system parameters are randomly perturbed from the nominal values. In the figure, μ_1 and μ_2 represents the mean values of the performance function f for the two designs, respectively. Though the first design exhibits a smaller mean value of the performance function, the second design is preferable from the robustness point of view, since it is much less sensitive to variations in the uncertain system parameters.

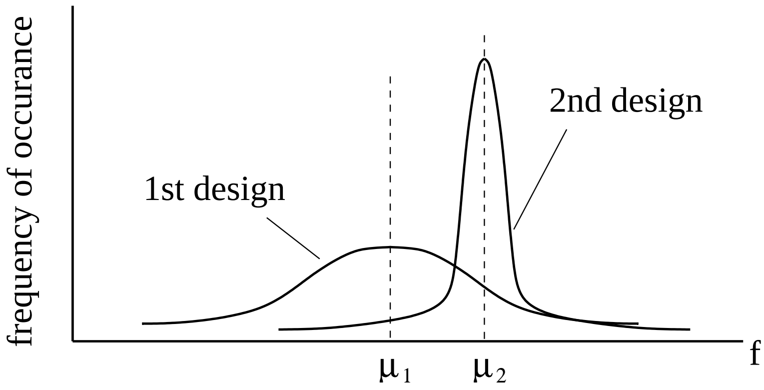

Figure 3.1: Concept of robust design

The principle behind the structural robust design is that, the merit or quality of a design is justified not only by the mean value but also by the variability of the structural performance. For the optimal design of structures with stochastic parameters, one straightforward way is to define the optimality conditions of the problems on the basis of expected function values resp. mean performance. However, the design which minimizes the expected value of the objective function as a measure of structural performance may be still sensitive to the fluctuation of the stochastic parameters and this raises the task of robustness of the design.

For illustration purposes, we study here the simple displacement minimization problem of a four-bar truss structure shown in Fig. 3.2. The fourth node of the truss is subjected to a horizontal static load with value $P = 1$. The Young's modulus for the first and the third bar, E_1 and for the second and the fourth bar, E_2, are assumed as uncorrelated random variables with mean or expected values $\mathrm{E}(E_1) = 210$, $\mathrm{E}(E_2) = 100$, standard deviation $\sigma(E_1) = 21$ and $\sigma(E_2) = 5$. The cross sectional areas of the first and the third bar A_1 and of the second and the fourth bar A_2 are considered as design variables. The mass density of the materials is $\rho = 1.0$.

The nodal displacement u is to be minimized under constraint of structural weight expectationE$(w) \leq 5.0$.

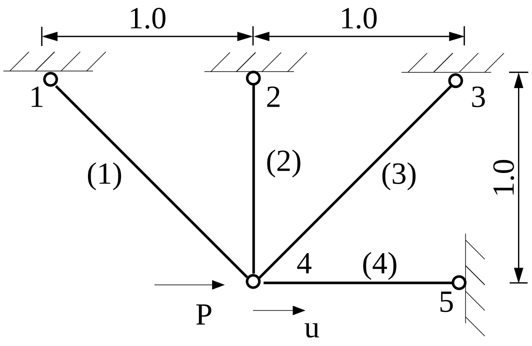

Figure 3.2: The four-bar truss

In this problem, the structural weight constraint must be active in the optimal design, which implies that $A_2 = 5/2 - \sqrt{2}A_1$ and therefore only one independent design variable A_1 needs to be determined. The variation of mean and the standard deviation of the concerned displacement u versus the design variable A_1 are presented in Fig. 3.3. It is seen from the figure that the optimal design minimizing the expected value of the objective u is $A_1' = 1.7678$, associated with $A_2' = 0$. To examine the scatter of u at this design point, a Monte Carlo simulation with $n = 10^6$ realizations is performed, where the stochastic input parameters are assumed to be normal distributed. The result is depicted in Fig. 3.4-a.

For comparison, the Monte Carlo result for an alternative design with $A_1^* = 0.3531$, $A_2^* = 2.0006$, which minimizes the standard deviation of u (cf. Fig.3.3), is also shown. The mean values of u for the two designs are 3.848×10^{-3} and 3.969×10^{-3}, respectively, whereas the standard deviations 3.97×10^{-4} and 1.78×10^{-4}. As can be seen from the simulation results in Fig. 3.4-b, the latter design leads to a higher expected value but a much smaller range of variation of the concerned displacement. This implies that the latter design is superior in terms of robustness, since the corresponding structural performance is less sensitive to the parameter variation and has a smaller scatter.

In fact, as a robust optimum design as pursued in the following chapters, the latter design aforementioned suggests a different topology than the familiar deterministic

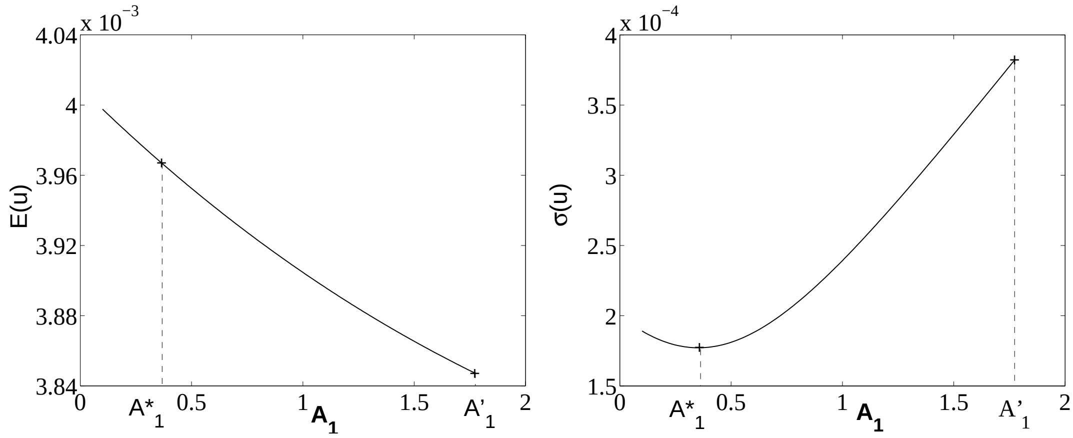

(a) Mean value (b) Standard deviation

Figure 3.3: Mean value and standard deviation of u vs. A_1

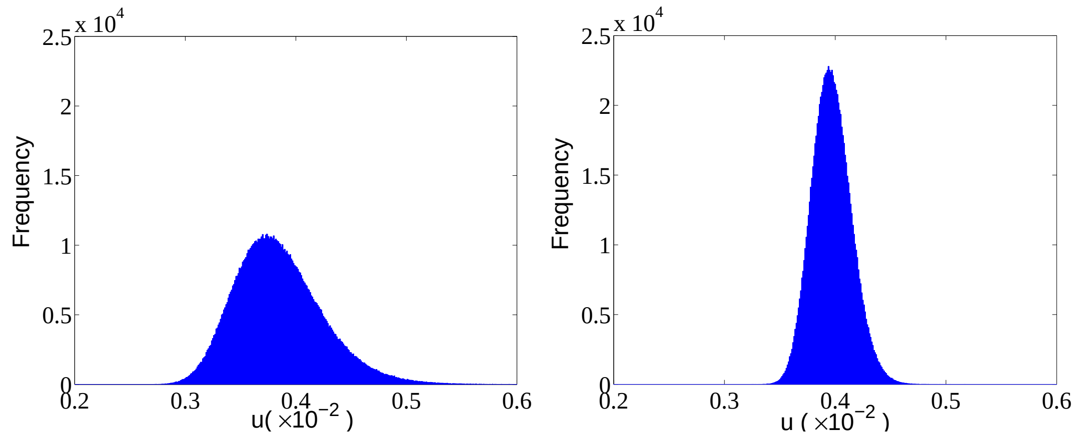

(a) First design (b) Second, robust design

Figure 3.4: Occurrence frequency distribution of u (by Monte Carlo simulation)

design (Fig. 3.5). With this illustrative example, we also show that the robustness of a structural performance against random variations of the system can be substantially improved both by adjusting the member sizes and by changing the structural topology.

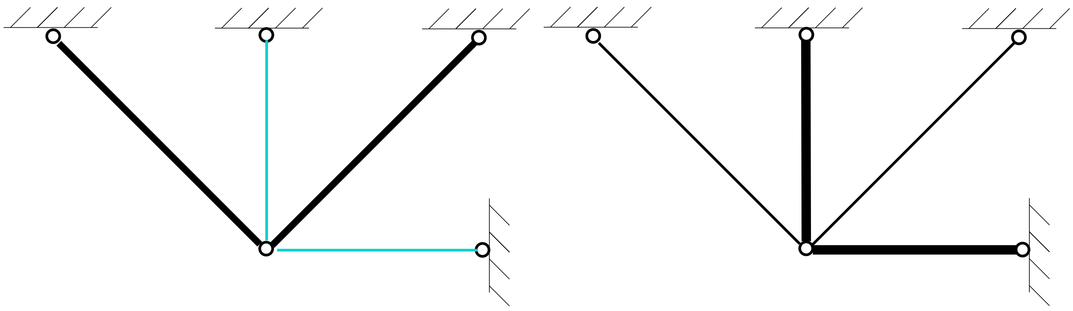

(a) Deterministic optimal design (b) Robust optimal design

Figure 3.5: Robust optimum vs. deterministic optimum for the four-bar truss

3.3.2 Differences between structural robust design and RBDO

Compared with RBDO, robust design is a relatively new issue in structural engineering. As representative non-deterministic structural optimization formulations, both of them aim at incorporating random performance variations into the optimal design process, and therefore they are sometimes not clearly distinguished in the literature. However, the two approaches differ in some fundamental aspects, despite the fact that the optimal solution of the robust design often exhibits an increased reliability.

First of all, the structural robustness is assessed by the measure of the performance variability around the mean value, most often by its standard deviation, whereas reliability is connected to the probability of failure occurrence (Fig.3.6). In general, RBDO is concerned more with satisfying reliability requirements under known probabilistic distributions of the input, and less concerned with minimizing the variation of the performance function, while the robust design aims to reduce the system variability to unexpected variations. In RBDO, the objective function is to be minimized under observance of probabilistic constraints. However, in robust design optimization, the objective function usually involves the performance variations, and the design constraints may be simply defined by the variance. Actually, RBDO is usually accomplished by moving the mean of the performance as depicted in Fig. 3.7, whereas the robust design is often implemented by diminishing the performance variability, as shown in Fig. 3.8.

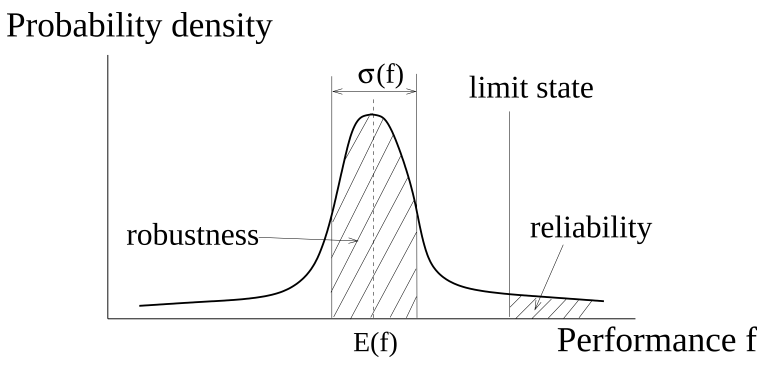

Figure 3.6: Difference between structural robustness and reliability

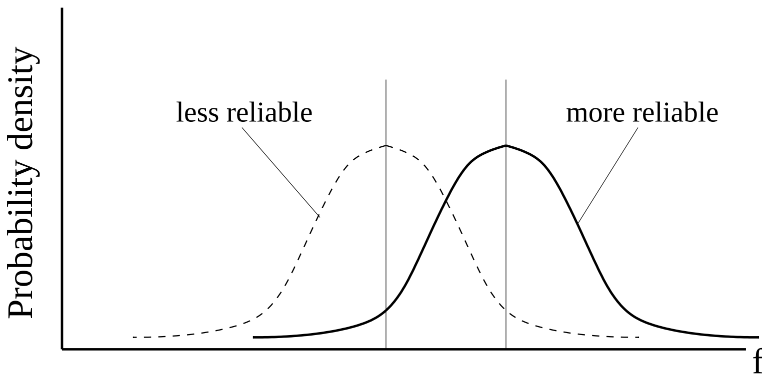

Figure 3.7: RBDO strategy

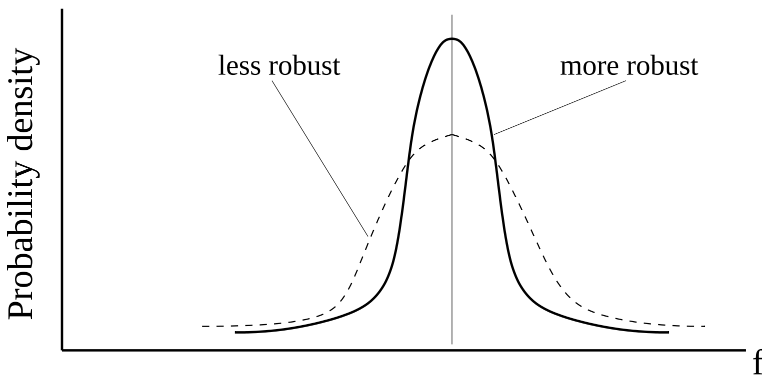

Figure 3.8: Robust design strategy

Secondly, in RBDO particular care is paid on the issue of structural safety in the extreme events, while in robust design more emphasis is put on the structural behavior under everyday fluctuations of the system during the whole service life. Zang et al. [57] presented the different scenarios concerned in the two types of problems as shown in Fig. 3.9.

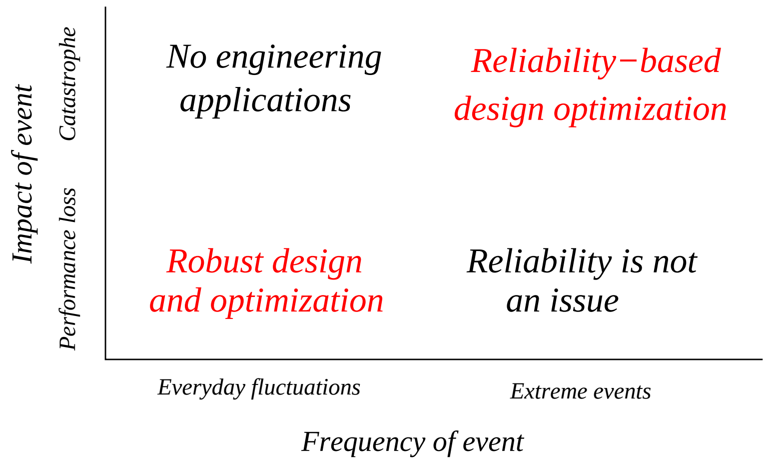

Figure 3.9: Different scenarios concerned in robust design and RBDO

For the same reason, the expected loss considered in RBDO problems is typically associated with the damages directly or indirectly induced by the catastrophic failure of the structural system, whereas the expected loss in robust design problems usually consists of the expense caused by poor quality of the structural performance, such as costs occurring in the maintenance and monitoring, or loss due to quality defects of the product.

Moreover, the applicability of RBDO relies on the availability of the precise description on the distributions of the stochastic parameters, which makes RBDO strongly depending upon the assumptions on the probabilistic distribution of the random variables [37]. However, a precise description of the overall statistics of the structural performance is not of concern in the formulation of robust design problem, as it is in the reliability based design problems. Additionally, the computer implementation of RBDO is known for the tedious reliability analysis, whereas robust design usually involves only prediction of basic characteristics of the performance variability, such as its standard deviation.

Finally, in the RBDO problems, a limit state function is required to define the failure of the structural system. However, an adequate limit state function can not always be given explicitly in practical engineering problems. In such circumstances, it might be more realistic to seek a design reducing the performance scatters, as by robust design.

To summarize, we list the differences between typical formulations of the structural robust design and RBDO in Table 3.1.

Table 3.1: A comparison between robust design and RBDO

	Robust design	RBDO
Description of input	Mean and variability	PDF / CDF
Design objective	Variability reduction	Minimization under Probabilistic constraints
Analysis type	Variation analysis	Reliability analysis
Strategy	Reducing variation	(more often) Moving the mean

3.3.3 Current state of research on structural robust design

Before the review of the structural robust design, it is useful to present a short introduction to the Taguchi's methodology.

Taguchi's robust design methodology

The conventional method of engineering robust design was proposed by Dr. Genichi Taguchi with the motive of improving the quality of a product or process by not only achieving performance target but also minimizing the performance variation without eliminating the cause of variations [5]. In the last two decades, Taguchi's methods have been applied to a wide variety of engineering design problems and have been proved effective in reducing the number of physical experiments for design improvement. A review of Taguchi's robust design methodology was given by Tsui [41].

Taguchi's methodology for robust design is based on orthogonal array experiments. Therein, two types of input that may affect the system performance are defined:

- **Control factors:** control factors are those parameters whose nominal settings can be specified during the design process. Control factors can be adjusted to meet the target performance and to diminish the performance variability. The combination of different levels of the control factors forms an orthogonal array termed as the *Inner Array.*

- **Noise factors:** noise factors represent the parameters that are impossible or to expensive to control. Noise factors cause the performance to deviate from the target and thus result in quality loss. The level combination of the noise factors is represented by the orthogonal array called the *Outer Array.*

- **Loss function:** the loss induced by the performance deviation of a product from its target performance. In Taguchi's methodology, the loss is defined as a quadratic function of the performance deviation.

Another essential concept in the Taguchi's methodology is the Signal/Noise (S/N) ratio. The S/N ratio, defined as a summary statistic calculated across the outer array for each row of the inner array, is a metric of product/process robustness and serves as an objective for optimization. Three types of S/N ratios can be defined: Larger the Best (LTB), Smaller the Best (STB) and Nominal the Best (NTB). By maximizing the S/N ratio, the loss function can be minimized.

In Taguchi's robust design, the noise factors are varied in designed experiments along with the control factors. The levels of the control factors are then chosen to attain a mean response that is not only close to the desired target but also robust to changes of the noise factors, thus reducing the variability of the response. Taguchi's robust design consists of the following procedures:

1. Stating the problem and the objective;
2. Identifying the control factors and the noise factors as well as their levels;
3. Planing the orthogonal array matrix experiment;
4. Conducting the planned experiment, predict the optimal levels and performance;
5. Performing the verification of the obtained design;
6. If the design objective is not achieved, return to step 2; otherwise, the design is accepted.

Though Taguchi's robust design methodology has been very popular in practical engineering, there is still critique on it. For example, as pointed out by Schmidt and Launsby [58], Taguchi's robust design methodology has the drawback that it does not provide any information on what direction to take for improving the design beyond the range of the control factor levels considered. As a consequence, the results are confined to the factor ranges tested in the experiments. Thus this approach relies greatly on the selection of the factor levels. Moreover, it has been recognized that the Taguchi's method is weak in handling interactions between control factors (Lucas [59]).

Structural robust design

In recent years, robust design has also attracted attention in structural design studies. However, a direct application of Taguchi's method to the structural design problem is rarely found in the literature. The reason may be due to the following facts: (1) the Taguchi method is based on experimental design techniques and thus not favorable for the structural design problem where usually a finite element model is employed; (2) generally, the relations between the structural behaviour and the design variable or the random variables are highly nonlinear. Thus more rational methods other than the Taguchi's orthogonal arrays are needed to explore the interactions between the performance functions and these variables; (3) conventional robust design treats design parameters with leveled control factors and therefore does not offer adequate flexibility in the sense that design parameters in a structural design problem can be usually selected from a continuous range.

In what follows, a brief review on the computational methods of the structural robust design optimization is presented.

In general, the existing methods for structural robust design fall into two categories: the methods using Taguchi's concept based on Design of Experiments (DOE) and the methods based on minimization of performance function variation measures such as the sensitivity.

In the former approaches, the uncontrollabe uncertainties are considered as leveled noise factors. Systematically selected numerical experiments are conducted with reference to different levels of the noise factors and then the design variables are adjusted with the purpose of maximizing the Signal/Noise ratio defined by Taguchi. Some approximate models such as the neural network and the response surface have been adopted to replace the expensive computer analysis for improving the computational efficiency.

Makkapati [60] has developed a technique based on the Artificial Neural Network (ANN). The technique involves evaluation of the response at selected design points, and then training a neural network using this data as examples. Once the network is properly trained, it can be used as a replacement of the finite element model for response prediction. An exhaustive research is then carried out for a global optimum that maximizing the S/N ratio. In this study, only influence of variations of the design parameters is accounted for. The sample size for training the neural network is expected to increase dramatically as the number of the design variables increases.

Chen et al. [61] have incorporated the concept of Taguchi's robust design into a multi-level optimization procedure for the robust design of thick laminated composite structures. The response surface model has been used for improving the efficiency. The study shows that the computational time for optimization with approximations is much smaller than the time required for the optimization using the original finite element model.

In the work of Lautenschlager and Eschennauer [62], the randomness of the structural parameters is modeled as leveled noise factors. Using the experimental design method, a response surface model is built for approximation of the structural performance and its variance. Based on the response surface model, the robust structural design is obtained with an optimization algorithm. The results obtained show the necessity for considering robustness during structural optimization. In their work, the shortcomings the Taguchi's original crossed-array approach are also discussed.

Chi and Bloebaum [63] described applications using the Taguchi's orthogonal arrays to solve structural optimization problems with continuous and discrete variables.

Using the orthogonal arrays, Lee et al. [64] treated the unconstrained optimization problem with discrete design variables. Numerical results for robust design of simple truss structures were illustrated.

In another type of approach, the robustness is measured by the performance sensitivity or by some other measures of the performance variability and the optimal setting of the design variables are determined by minimizing these measures, or a combination of them and the nominal performance, using optimization techniques. In these methods, the structural performance variations are estimated using either local derivative information or Monte Carlo simulations.

In the work of Latalski [65], the fact that the sensitivity of some structural response to small variations of design variables increases rapidly for near-optimal structures are underlined. The author presented an approach accounting for the manufacturing tolerance of member cross sections and lengths in the optimal design of truss structures. In this approach, the possible worst-case condition is approximately evaluated by introducing the product of the tolerance value and the sensitivity of the structural response (displacement and member stress) with respect to it as a penalty to the nominal response value in the inequality constraints of the primary optimization problem.

Anthony and Elliott [66] use Genetic algorithms to seek the robust optimal design of a planar truss structure with the design objective of reducing the vibration transmission. The robustness of the designs are achieved by minimizing the spreads of the frequency response, which can be depicted in a histogram, with the purpose of reducing the variation of the objective function with respect to small changes in the structural geometry.

Lee and Park [67] defined the robust design problem as a revised deterministic optimization problem. In the problem, the objective function is defined by a weighted sum of the performance mean and the performance variation represented by the tolerance bands of the design parameters and the performance sensitivity with respect to the design variables. A penalty factor is introduced to accounts for the worst-case variation of the constraint functions within the tolerance bands. A robust optimum of the minimum weight design problem was obtained by mathematical programming. Hereby, the random parameters other than the design variables were not considered.

Monte Carlo simulation was applied by Sandgren and Cameron [68] in a genetic optimization algorithm to produce an output distribution for objective function and constraints in order to locate a design which was less sensitive to fluctuations.

Gumber et al. [69] presented reliability results for the robust design optimization of a flexible wing under geometric uncertainty. The robust design was conducted incorporating first order approximations based on automatic differentiation in previous work of the authors. The paper also discussed the conceptual difference between robust design and RBDO underlining the utility of structural robust design.

The current state of the art on the subject of structural robust design optimization problem is summarized as follows:

– Compared with the robust design in other engineering disciplines, such as the automobile production and the consumer electronics fabrication, the robust design of structures has been much less frequently addressed in the literature. Generally speaking, numerical analysis methods for structural robust design are less well developed, despite the widely adopted sophisticated optimization techniques in conjunction with finite elements in the discipline of engineering structural design.

– In contrast to the case of probabilistic definitions used in the well developed theory of Reliability Based Design Optimization, there has not been an unified mathematical definition of the metric for the structural robustness, though the concept of robust design has been widely recognized. Commonly used metrics of the structural robustness include the Taguchi's signal-to-noise ratio and the performance variation measure represented by sensitivities.

– There exist a variety of approaches based on Taguchi's robust design methodology or Design of Experiments (DOE). In concerned studies, the DOE techniques originally proposed for conducting cost effective laboratory experiments are directly transplanted into structural optimization problems based on numerical models. These approaches lack of a theoretical background and the interactions among design the parameters and the random parameters are not studied enough, however. Moreover, the constraints are not well treated in the methods using Taguchi's concept.

– Some approximate models such as Response Surface and Artificial Neural Network (ANN) are used as substitutes of the Finite Element model of the real system for prediction of the structural response characteristics. Robust design is implemented on the basis of such models in conjunction with optimization techniques. These approximate models are usually subject to either accuracy or efficiency shortcomings in most practical engineering applications. In particular, in cases where strong nonlinearities are present, the methods based on experimental designs or response surface might fail to reproduce the relations between the response and the design variables. Additionally, whether these models are capable of modeling the interactions among the design variables and other parameters is still an open question. Large discrepancies between the approximate performance model and the complete analysis will lead to sub-optimal results and constraint violations.

– Most of the currently known research using the sensitivity or variance measures take into account only variations of the design variables, while the variability of other parameters and loads are not accounted for in the problem statements. A unified approach which is capable of treating variations both in design parameters and in other parameters needs to be developed for the robust design problems of engineering practice.

– The reported methods based on the sensitivity or variance measures address the nominal performance instead of the statistical mean performance as a merit of the design. The latter might be of more practical value in the design of structures with stochastic parameters, however.

– From the computational point of view, existing methods require further refinements with respect to efficiency, accuracy and applicability. For example, the methods utilizing the DOE techniques or Monte Carlo simulations exhibit some disadvantages regarding efficiency or accuracy. The methods based on sensitivity measures need to be extended to applications with nonlinear structural behaviour.

– The random input variables may be statistically correlated in practical problems. However, the potential correlations have not been accounted for in available robust design methods.

To summarize, the state of the art reported in the literatures indicates a need for a more concise problem formulation and a systematic computational methodology for practical engineering applications.

Chapter 4

Perturbation based stochastic finite element method (SFEM)

The numerical analysis of the structural response to random input is a prerequisite for the robust design proposed in this study. The methodology of stochastic structural analysis is introduced in this chapter. First, an overview of the existing methods is given, including statistical methods and non-statistical methods, is given. Then the perturbation based stochastic finite element method exposed in the literature is briefly introduced.

4.1 Overview of stochastic structural analysis

As the computational stochastic structural analysis receives considerable attention, extensive research has been done on this subject. In general, the prevalent methods of stochastic structural analysis are classified into two major categories: statistical methods and non-statistical methods. In what follows, a brief introduction to both approaches is outlined. A more comprehensive review on recent developments of the structural stochastic analysis can be found in the work of Schueller [32].

4.1.1 Statistical methods

The statistical methods, e.g. the direct Monte Carlo simulation (MCS) [70] and its variants, employ repetitive tests over a sufficiently large amount of sampling.

In the Monte Carlo simulation, the information on the probabilistic distribution of the stochastic input variables is required. The statistical samples are generated according to the prescribed probabilistic characteristics. Each realization of these random input variables produces one realization of the problem itself through deterministic analysis. From the analysis of the simulation results, the overall statistics can be summarized, as schematically represented [71] in Fig. 4.1, and the accuracy of the estimation of population characteristics can be improved by increasing the sample size.

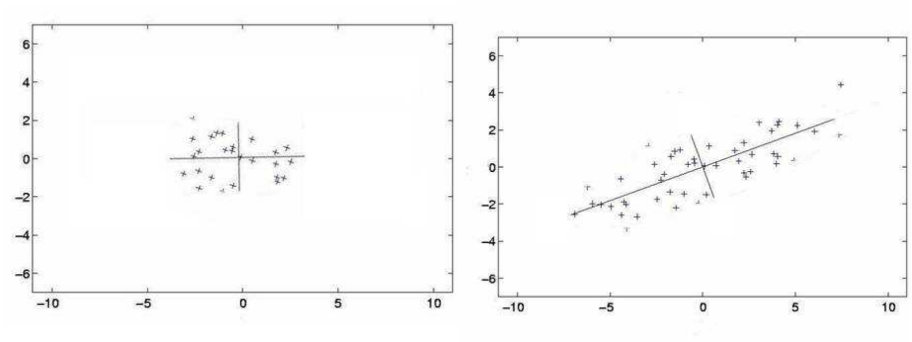

(a) Input sample (b) Output sample

Figure 4.1: Statistical Monte Carlo simulation

An alternative approach [72] to the conventional Monte Carlo simulation is to conduct the sampling on the basis of an approximate performance model, such as a response surface. The evaluations of the approximate response function are much less expensive, making the Monte Carlo simulation more efficient. The disadvantages are that the number of random variables are limited and the approximation may become highly inaccurate.

4.1.2 Non-statistical methods

Some other methods such as stochastic finite element methods (SFEM) based on second order perturbation techniques [73], method of Neumann series expansion [74][75] and mesh-less perturbation method [76] are based upon an analytical treatment of the uncertainty and known as non-statistical methods. These methods employ approximations for the prediction of the probabilistic response under system changes and the basic statistical characteristics, such as the mean and the variance of the response are obtained on the basis of the approximate models.

A well-known non-statistical approaches for stochastic structural analysis is the perturbation based stochastic finite element method, where the random quantities are expanded via Taylor series about their mean values. The perturbation based stochastic finite element method is regarded a powerful tool for the analysis of structures with moderate parameter variability. In the framework of this approach, the random or uncertain structural parameters are treated as random variables or random fields, which can be further discretized into a set of uncorrelated random variables [77][78]. These basic random variables are described with up to the second statistical moment, regardless of the type of the actual distribution. Typically, at most second order Taylor series expansion is employed for derivation of the perturbed equilibrium equations. By consecutively solving these equations, the zeroth, first or second-order solutions are obtained and then the mean value and the covariance matrix of structural response variables such as nodal displacement, elemental stress and structural natural frequencies can be approximated. The principle of this approach is illustrated in Fig. 4.2. As reported in the literature, the perturbation based approach has also been extended to the stochastic analysis of structures having path-independent nonlinear behaviors [73].

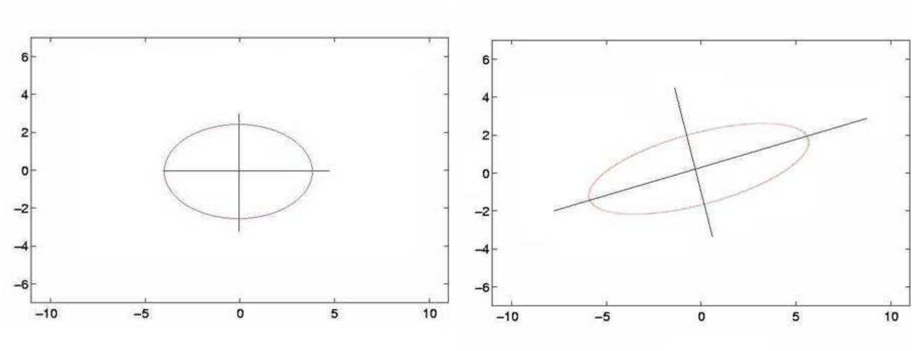

(a) Input (mean and variance) (b) Output (mean and variance)

Figure 4.2: Non-statistical perturbation based stochastic finite element

Due to its analytical nature, perturbation based stochastic finite element method generally attains a higher efficiency than the statistical methods. This approach provides an affordable algorithm for the analysis of problems with moderate parameter variability. It is now widely recognized that a satisfying accuracy can be achieved in cases where the coefficients of variation are up to COV=0.15-0.2.

4.1.3 A comparison between Monte Carlo simulation and Perturbation based method

Monte Carlo simulation and the perturbation based stochastic finite element analysis are both Representative approaches for structural analysis under random uncertainty. Here, the differences between the two approaches are discussed.

- **Monte Carlo simulation**
  Monte Carlo simulation relies on the statistical approximation of the probability distribution. The accuracy of the approximation depends on the sample size and the computational effort of the implementation is proportional to the sample size, regardless of the extent of the input scatter or the number of the random variables entering the problem.
  The advantage of Monte Carlo simulation is that accurate solutions can always be obtained with a sufficiently large number of realizations provided that the deterministic solution of the problem is available. As a rule, Monte Carlo simulation can be utilized as long as the deterministic solution is analytically or numerically available and it requires no modifications of an existing algorithm for structural analysis. Actually, Monte Carlo simulation is the only universal method that can provide accurate solutions of stochastic analysis problems. For this reason, the Monte Carlo simulations is often used to evaluate the accuracy of other more sophisticated stochastic analysis methods and to verify a new technique. Due to its intrinsic parallelism, Monte Carlo simulation can be implemented in parallel or distributed computing environment. In structural design problems, Monte Carlo simulation can be used to explore the design space of the problem and to assess the robustness of a certain design. However, despite the fact that the availability of High Performance Computing resources enables implementations of large scale Monte Carlo simulations, the high computational cost limits its applications in engineering practice, especially with regard to complicated structures.

- **Perturbation based stochastic finite element analysis**
  As an alternative approach to the Monte Carlo simulation, perturbation based finite element analysis provides an elegant tool for stochastic structural analysis. This approach relies on a functional approximation of the random response about the mean input whereby the smoothness and the derivability of the performance function are required. Unlike the Monte Carlo simulations, the computational cost involved in this approach is proportional to the number

of the random variables. Nevertheless, the perturbation based stochastic finite element analysis is generally much more efficient than Monte Carlo simulation. In case of small parameter variations, perturbation based stochastic finite element method may satisfy the needs of practical engineering. Moreover, the optimal numerical approaches have to be able to determine the impacts of each single random variables, since this information may serve as indicators for improving the structural performance effectively and will be of great importance in the process of structural design optimization under consideration of parameter randomness. In this connection we should point out that the perturbation based method is more capable of revealing the approximate contribution of each random variable to the system response variations.

4.2 Perturbation based SFEM for linear structures

As a prerequisite for response moment analysis in the structural robust design, the perturbation based stochastic finite element method for linear structures under static or transient loads is briefly outlined in this section.

4.2.1 Perturbation equations for static problems

The stochastic analysis referred to here is confined to the first two statistical moments (i.e. the mean and the variance) of the displacement response. As will be shown in following chapters, it is very easy to calculate the moments of other quantities such as stresses and the structural compliance given that the moments of the displacements are already known.

To begin with, we write the virtual work principle for the linear static deformation problem under random uncertainty in matrix form as

$$\int_{\Omega} \boldsymbol{\sigma}^{\mathrm{t}}(\mathbf{b})\delta\tilde{\boldsymbol{\varepsilon}}\mathrm{d}\Omega - \int_{\Omega} \mathbf{f}^{\mathrm{t}}(\mathbf{b})\delta\tilde{\mathbf{u}}\mathrm{d}\Omega - \int_{\Gamma_{\mathrm{t}}} \mathbf{t}^{\mathrm{t}}(\mathbf{b})\delta\tilde{\mathbf{u}}\mathrm{d}\Gamma_{\mathrm{t}} = 0, \tag{4.1}$$

where $\boldsymbol{\sigma} = \mathbf{E}(\mathbf{b})\boldsymbol{\varepsilon}$ is the stress tensor and $\tilde{\boldsymbol{\varepsilon}}$ is the strain tensor, $\mathbf{E}$ is the elasticity tensor, $\tilde{\mathbf{u}}$ represents the virtual displacement field, $\mathbf{f}$ is the body force and $\mathbf{t}$ the traction force acting on the surface Γ_t. The symbol $\mathbf{b} \in \mathbf{R}^{q\times 1}$ denotes the vector of random variables. In this formulation, the components of $\mathbf{b}$ can be random variables for material properties such as Young's modulus, for geometrical parameters such as member dimensions or spatial positions and for environmental conditions such as magnitude of applied loads.

In the context of the finite element method, after the spatial discretization using the shape function $\mathbf{N}$ we obtain the discrete equilibrium equations from the virtual work principle

$$\mathbf{K}(\mathbf{b})\mathbf{u} = \mathbf{p}(\mathbf{b}), \tag{4.2}$$

where $\mathbf{u} \in \mathbf{R}^{n\times 1}$ is the vector of nodal displacement, $\mathbf{p} \in \mathbf{R}^{n\times 1}$ is the vector of external load

$$\mathbf{p}(\mathbf{b}) = \int_{\Gamma_t} \mathbf{N}^{\mathrm{t}}(\mathbf{b})\mathbf{f}(\mathbf{b}) + \int_{\Omega} \mathbf{N}^{\mathrm{t}}(\mathbf{b})\mathbf{t}(\mathbf{b})\mathrm{d}\Gamma_t, \tag{4.3}$$

and $\mathbf{K} \in \mathbf{R}^{n\times n}$ is the global stiffness matrix

$$\mathbf{K}(\mathbf{b}) = \int_{\Omega} \mathbf{B}^{\mathrm{t}}(\mathbf{b})\mathbf{E}(\mathbf{b})\mathbf{B}(\mathbf{b})\mathrm{d}\Omega, \tag{4.4}$$

where $\mathbf{B}$ is the matrix relating the strain field with the nodal displacements.

Since structural responses such as nodal displacements and member stresses are complex functions of the random variables, an analysis of their complete probability distributions is practically impossible. However, if the functions of the responses are smooth and the fluctuations of the random variables are moderate, the perturbation method that utilizes a second-order expansion of the response can be applied for an approximation of the first two moments [73].

The basic idea of the perturbation-based finite element analysis method as exposed in [73] is to expand the stiffness matrix $\mathbf{K}$, the nodal displacement vector $\mathbf{u}$ and the external load vector $\mathbf{p}$ in Eq. (4.2) about the mean of the random input variables via second-order Taylor series:

$$\mathbf{K} = \overline{\mathbf{K}} + \sum_{i=1}^{q} \overline{\mathbf{K}}_{b_i}\mathrm{d}b_i + \frac{1}{2}\sum_{i,j=1}^{q} \overline{\mathbf{K}}_{b_i b_j}\mathrm{d}b_i\mathrm{d}b_j + ..., \tag{4.5}$$

$$\mathbf{u} = \overline{\mathbf{u}} + \sum_{i=1}^{q} \overline{\mathbf{u}}_{b_i} \mathrm{d}b_i + \frac{1}{2} \sum_{i,j=1}^{q} \overline{\mathbf{u}}_{b_i b_j} \mathrm{d}b_i \mathrm{d}b_j + ..., \tag{4.6}$$

and

$$\mathbf{p} = \overline{\mathbf{p}} + \sum_{i=1}^{q} \overline{\mathbf{p}}_{b_i} \mathrm{d}b_i + \frac{1}{2} \sum_{i,j=1}^{q} \overline{\mathbf{p}}_{b_i b_j} \mathrm{d}b_i \mathrm{d}b_j + ..., \tag{4.7}$$

By substituting Eqs. (4.5), (4.6) and (4.7) into Eq. (4.2) and equating the terms of the same order, we have the following $(q+2)$ perturbation equations :

Zeroth-order equation:

$$\bar{\mathbf{K}}\bar{\mathbf{u}} = \bar{\mathbf{p}}\,, \tag{4.8}$$

First-order equations:

$$\bar{\mathbf{K}}\bar{\mathbf{u}}_{b_i} = \bar{\mathbf{p}}_{b_i} - \bar{\mathbf{K}}_{b_i}\bar{\mathbf{u}} \qquad (i = 1, 2, ..., q)\,, \tag{4.9}$$

Second-order equation:

$$\bar{\mathbf{K}}\bar{\mathbf{u}}_2 = \sum_{i,j=1}^{q} \left(\frac{1}{2}\bar{\mathbf{p}}_{b_i b_j} - \frac{1}{2}\bar{\mathbf{K}}_{b_i b_j}\bar{\mathbf{u}} - \bar{\mathbf{K}}_{b_i}\bar{\mathbf{u}}_{b_j} \right) \mathrm{Cov}(b_i, b_j)\,, \tag{4.10}$$

with

$$\bar{\mathbf{u}}_2 = \frac{1}{2} \sum_{i,j=1}^{q} \bar{\mathbf{u}}_{b_i b_j} \mathrm{Cov}(b_i, b_j)\,. \tag{4.11}$$

Here the terms with subscripts b_i and $b_i b_j$ denote first-order derivatives with respect to the i-th random variable and the mixed or second-order partial derivatives with respect to the i-th and the j-th random variables, respectively. The upper bars indicate that the corresponding quantities are evaluated at the mean or expected values of the stochastic parameters. For instance,

$$\overline{\mathbf{K}}_{b_r} = \left. \frac{\partial \mathbf{K}}{\partial b_r} \right|_{\overline{\mathbf{b}}} \tag{4.12}$$

Once Eqs. (4.8), (4.9) and (4.10) are solved, we have the second order approximate mean value and the first-order covariance of the nodal displacements

$$\mathrm{E}_2(\mathbf{u}) = \bar{\mathbf{u}} + \bar{\mathbf{u}}_2,$$

and

$$\mathrm{Cov}(u^r, u^s) = \sum_{i,j=1}^{q} \bar{u}^r_{b_i} \bar{u}^s_{b_j} \mathrm{Cov}(b_i, b_j)\,. \tag{4.13}$$

If the second order term in Eq. (4.6) is also neglected, we get the first order approximate mean displacement:

$$\mathrm{E}_1(\mathbf{u}) = \bar{\mathbf{u}}. \tag{4.14}$$

When describing the scatter of the structural parameters, especially when discretizing stochastic fields, correlated random variables may be involved. In order to reduce the computational efforts caused by the double summations in evaluating the terms on the right hand side of the second-order equation, the original random variables $\mathbf{b}$ can be transformed into a set of uncorrelated random variables $\mathbf{c}$ through principal component analysis [79] by the linear transformation:

$$\mathbf{c} = \mathbf{A}^{\mathrm{t}}\mathbf{b}\,. \tag{4.15}$$

The transformation matrix $\mathbf{A}$ is obtained by solving a standard eigenvalue problem defined as

$$\mathbf{\Sigma A} = \mathbf{A \Lambda} \tag{4.16}$$

where $\mathbf{\Sigma}$ is the covariance matrix of the original set of random variables, $\mathbf{A}$ is the matrix consisting of the q normalized eigenvectors, $\mathbf{\Lambda}$ comprises the eigenvalues and is the variance matrix of the transformed random variables:

$$\mathbf{\Lambda} = \begin{bmatrix} \mathrm{Var}(c_1) & 0 & \cdots & 0 \\ & \mathrm{Var}(c_2) & \cdots & 0 \\ & & \ddots & \vdots \\ \text{sym.} & & & \mathrm{Var}(c_q) \end{bmatrix}.$$

Usually, only the eigenvectors corresponding to a small number of the highest eigenvalues are needed to capture the major variability characteristics of a certain type of original random variables. Thus, a reduced set of uncorrelated random variables c_i can be defined as

$$c_i = \sum_{j}^{q} A_{ji} b_j \, , \ i = 1, 2, ..., \hat{q},$$

where $\hat{q}$ ($\hat{q} \ll q$) is the number of the eigenvectors involved in the transformation of the random variables.

In terms of the transformed uncorrelated random variables c_i, the perturbation equations are then expressed as

Zeroth-order equation:

$$\bar{\mathbf{K}}\bar{\mathbf{u}} = \bar{\mathbf{p}} \, , \tag{4.17}$$

First-order equations:

$$\bar{\mathbf{K}}\bar{\mathbf{u}}_{c_i} = \bar{\mathbf{p}}_{c_i} - \bar{\mathbf{K}}_{c_i}\bar{\mathbf{u}} \ \ (i = 1, 2, ..., \hat{q}) \, , \tag{4.18}$$

Second-order equation:

$$\bar{\mathbf{K}}\bar{\mathbf{u}}_2 = \sum_{i=1}^{\hat{q}} \left(\frac{1}{2}\bar{\mathbf{p}}_{c_i c_i} - \frac{1}{2}\bar{\mathbf{K}}_{c_i c_i}\bar{\mathbf{u}} - \bar{\mathbf{K}}_{c_i}\bar{\mathbf{u}}_{c_i} \right) \mathrm{Var}(c_i) \, , \tag{4.19}$$

where

$$\bar{\mathbf{u}}_2 = \frac{1}{2} \sum_{i=1}^{\hat{q}} \bar{\mathbf{u}}_{c_i c_i} \mathrm{Var}(c_i) \, . \tag{4.20}$$

Here the terms with subscripts c_i and $c_i c_i$ denote first-order and the second-order partial derivatives with respect to the ith random variables, respectively. The derivatives of the stiffness matrix $\mathbf{K}$ and load vector $\mathbf{p}$ can be determined analytically or by finite differences on the elemental level.

After solving the perturbation equations as in Eqs. (4.17), (4.18) and (4.19), the first-order and the second-order mean of nodal displacements are obtained using the solutions of these equations:

$$E_1(\mathbf{u}) = \bar{\mathbf{u}}\,, \tag{4.21}$$

and

$$E_2(\mathbf{u}) = \bar{\mathbf{u}} + \bar{\mathbf{u}}_2\,, \tag{4.22}$$

respectively, and the first-order approximate covariance of the nodal displacements is expressed as

$$\mathrm{Cov}(u^r, u^s) = \sum_{i=1}^{\hat{q}} \bar{u}^r_{c_i} \bar{u}^s_{c_i} \mathrm{Var}(c_i)\,. \tag{4.23}$$

Particularly, the approximate variance of the rth component of the nodal displacement vector is given by

$$\mathrm{Var}\,(u^r) = \sum_{i=1}^{\hat{q}} (\bar{u}^r_{c_i})^2 \mathrm{Var}(c_i)\,. \tag{4.24}$$

As can be seen from above, the perturbation equations required to be solved have the same coefficient matrix as the primary deterministic analysis, thus only forth- and backward substitutions are involved in the solution of these equations. For this reason, the perturbation based stochastic analysis has substantial advantages over the Monte Carlo simulations as regarding computational efficiency.

The above approach relies on a roughly quadratic resp. linear involvement of the fluctuations in the structural response, and the assumption that the scatter of the stochastic structural parameters is small, such that the use of the first-order covariance is considered adequate for engineering applications.

4.2.2 Perturbation based stochastic analysis for transient problems

The perturbation technique can be analogously applied to to stochastic analysis of the transient response problem as expressed by

$$\mathbf{M}(\mathbf{b})\mathbf{a} + \mathbf{C}(\mathbf{b})\mathbf{v} + \mathbf{K}(\mathbf{b})\mathbf{u} = \mathbf{p}(\mathbf{b}, t), \tag{4.25}$$

where $\mathbf{M} \in \mathbf{R}^{n\times n}$, $\mathbf{C} \in \mathbf{R}^{n\times n}$, $\mathbf{a} \in \mathbf{R}^{n\times 1}$ and $\mathbf{v} \in \mathbf{R}^{n\times 1}$ denote the mass matrix, the damping matrix, the nodal acceleration vector and the velocity vector, respectively. It is assumed here that the random input vector $\mathbf{b}$ is time invariant.

The derivation of the perturbation equations is straightforward and therefore omitted here in favour of conciseness of the presentation. We write here directly the zeroth, first and second order perturbation equations in terms of transformed random variable $\mathbf{c}$ [73][79]:

Zeroth-order equation:

$$\bar{\mathbf{M}}\bar{\mathbf{a}} + \bar{\mathbf{C}}\bar{\mathbf{v}} + \bar{\mathbf{K}}\bar{\mathbf{u}} = \bar{\mathbf{p}}\,, \tag{4.26}$$

First-order equations:

$$\bar{\mathbf{M}}\bar{\mathbf{a}}_{c_i} + \bar{\mathbf{C}}\bar{\mathbf{v}}_{c_i} + \bar{\mathbf{K}}\bar{\mathbf{u}}_{c_i} = \bar{\mathbf{p}}_{c_i} - \bar{\mathbf{K}}_{c_i}\bar{\mathbf{u}} - \bar{\mathbf{C}}_{c_i}\bar{\mathbf{v}} - \bar{\mathbf{M}}_{c_i}\bar{\mathbf{a}} \;\; (i = 1, 2, ..., \hat{q})\,, \tag{4.27}$$

Second-order equation:

$$\begin{aligned}\bar{\mathbf{M}}\bar{\mathbf{a}}_2 + \bar{\mathbf{C}}\bar{\mathbf{v}}_2 + \bar{\mathbf{K}}\bar{\mathbf{u}}_2 \;&=\; \sum_{i=1}^{\hat{q}} \left(\frac{1}{2}\bar{\mathbf{f}}_{c_ic_i} - \frac{1}{2}\bar{\mathbf{M}}_{c_ic_i}\bar{\mathbf{a}} - \frac{1}{2}\bar{\mathbf{C}}_{c_ic_i}\bar{\mathbf{v}} - \frac{1}{2}\bar{\mathbf{K}}_{c_ic_i}\bar{\mathbf{u}} \right.\\ &\qquad \left. - \bar{\mathbf{M}}_{c_i}\bar{\mathbf{a}}_{c_i} - \bar{\mathbf{C}}_{c_i}\bar{\mathbf{v}}_{c_i} - \bar{\mathbf{K}}_{c_i}\bar{\mathbf{u}}_{c_i} \right) \mathrm{Var}(c_i)\,. \end{aligned} \tag{4.28}$$

The first two moments of the probability distribution of the transient structural response can be calculated after the perturbation equations (4.26), (4.27) and (4.28) are solved. For example, the mean value and the covariance of the nodal acceleration are given by

$$\mathrm{E}(\mathbf{a}(t)) = \bar{\mathbf{a}}(t) + \bar{\mathbf{a}}_2(t), \tag{4.29}$$

and

$$\mathrm{Cov}(a^i(t), a^j(t)) = \sum_{r=1}^{\hat{q}} \bar{a}^i_{c_r}(t)\bar{a}^j_{c_r}(t)\mathrm{Var}(c_r). \tag{4.30}$$

It should be noted that the above perturbation equations can be solved by the same step-wise time integration scheme as in the corresponding deterministic transient analysis.

Chapter 5

Formulation of structural robust design

As stated in Chapter 3, the task to be performed in structural robust design is to reduce the variability of the structural performance while improving its mean level. In this chapter, the mathematical statement of the structural robust design problem is given. Several aspects related to the problem are first discussed. Then the robust design of structures is formulated as a multi-criteria optimization problem. In the last part of this chapter, a conceptual comparison between the present formulation and those based upon conventional Taguchi's methods is given. A comparative numerical study with reference to a simple truss design problem is also presented.

5.1 General considerations

Before setting up a framework for the structural robust design optimization problem, it is convenient to discuss first several aspects associated with the problem formulation.

5.1.1 Uncertainty and design variables in the problem

A main difficulty that restricts the application of structural robust design optimization is the expensive computation not only for the mean value and the variability of the performance function but also for their sensitivity information which allows for gradient based optimization algorithms. This issue is connected to the treatment of the uncertainty present in the structural system.

The basic idea behind the present statement of the robust design is that a stochastic representation of the uncertainty is used. However, it is practically not always possible to acquire the entire probabilistic distribution characteristics of the stochastic parameters and to obtain the whole insight into the scatter of the structural performance. Therefore, the uncertain input and the structural performance are quantified by the first two statistical moments, namely the mean values and the variances in the present study. In other words, the uncertainty of the random input and the objective function/ constraints are described in a probabilistic way, as by the perturbation based stochastic finite element method. This facilitates an efficient numerical analysis of the stochastic response characteristics as well as their sensitivity with respect to the design variables in the framework of perturbation based stochastic finite element method.

We now classify the variables entering the non-deterministic structural design problem. Typically, we have :

- Random variables

  In the present study, random variables are referred to the structural parameters or loads that vary about their nominal values. These variables include both discrete system parameters and variables which are introduced by discretion of random fields. The random variables may be independent or correlated. As we do in the previous chapters, we denote the random variables by

$$\mathbf{b} = [b_1, b_2, ..., b_q].$$

- Design variables

  Design variable are the controllable design parameters that need to be determined by the designer. Depending on the problem, design variables can be member sizes, geometrical shape parameters, nodal positions, composite material properties, and similar. The vector of the design variables is denoted by

$$\mathbf{d} = [d_1, d_2, ..., d_n].$$

  In the present formulation, we assume that the design variables themselves can be non-deterministic, which implies, the vector of design variables $\mathbf{d}$ may also contain components that correspond to the random parameters present in the vector **b**. If this is the case, the design variable can also be the mean or variance (or standard deviation) of the concerned parameters. The latter case bases on the fact that cost-effective designs are always associated with reasonable specifications on the manufacturing or assembling tolerances of the product. Such tolerances are suitably represented by the standard deviations of the geometrical dimensions.

5.1.2 Numerical representation of structural robustness

Robust design addresses both the design objective robustness, where the variability of the objective function is to be minimized, and the design feasibility robustness, where the constraint conditions are required to be satisfied as possible in presence of parameter variations.

As mentioned in Chapter 3, there has not been an unified numerical representation of structural robustness in the literature. In general, when the robustness of the design is considered in structural optimization problems, the scatter of the structural performance defined by the objective function and the constraints are of primary concern. Basically, the variability of the structural performance can be roughly described by its standard deviation. Hence, in this study, we use the standard deviation of the performance as a measure of the structural robustness.

Unlike some other approaches, such as those based on Taguchi's methodology, we use here a continuous description of the robustness. By virtue of this, we are able to employ analytical tools, such as perturbation techniques and sensitivity analysis, in the computer implementation of the robust design.

5.1.3 Employment of the perturbation based stochastic finite element analysis

In the present study, the objective function and the constraint contain not only the mean values but also the standard deviations of the performance functions by definition. Several aspects favor the employment of perturbation based stochastic finite element method for the analysis of those response moments required by the proposed robust design. These are:

1. Compared with Monte Carlo simulation approaches, the perturbation based stochastic structural analysis is substantially more efficient for computation of the response mean and variance required by the proposed formulation.

2. In structural-, mechanical-, and aerospace engineering the deviations of the random parameters from their nominal values can be controlled in a number of cases within coefficients of variation less than 0.2. In such circumstances, the perturbation based finite element method is considered sufficiently accurate for stochastic structural analysis in the robust design problem.

3. Most important, the analytical nature of the perturbation based approach allows for a cost effective sensitivity analysis of the response moments and thus facilitates the employment of gradient based optimization algorithms in the structural robust design problem, as can be seen in the subsequent chapters.

Based on these considerations, we propose the formulation for structural robust design optimization problems.

5.2 Problem formulation

The task of robust structural design optimization is to improve the design by minimizing the variance of the structural performance while meeting the requirements of optimum performance. In this study, the structural robust design problem is stated as an optimization problem with the objective to diminish the performance variability and to improve the mean. With employment of structural optimization techniques, the optimal set of design variables is to be determined in a rational way.

5.2.1 Mathematical formulation

In the present statement, the mean value of the response functions, instead of their nominal values, as well as the standard deviations are used to define the objective functions and the constraints. Thus the mathematical model of the robust design problem is cast as a multi-criteria optimization problem

$$
\begin{aligned}
&\text{find} && \mathbf{d}, \\
&\text{minimizing} && \{\mathrm{E}\left(f(\mathbf{d})\right), \sigma\left(f(\mathbf{d})\right)\}, \\
&\text{subject to} && \mathrm{E}\left(g_i(\mathbf{d})\right) + \beta_i \sigma\left(g_i(\mathbf{d})\right) \leq 0 \qquad (i = 1, 2, ..., k), \\
& && \sigma\left(h_j(\mathbf{d})\right) \leq \sigma_j^+ \qquad (j = 1, 2, ..., l), \\
& && \mathbf{d}_{\mathrm{L}} \leq \mathbf{d} \leq \mathbf{d}_{\mathrm{U}},
\end{aligned} \tag{5.1}
$$

where $f(\mathbf{d})$ and $g_i(\mathbf{d})\,(i = 1, 2, ..., k)$ are the objective function and the constraint functions as in the corresponding deterministic optimization problem, $h_j(\mathbf{d})\,(j = 1, 2, ..., l)$ represent constraints on standard deviations of the response. The quantity $\beta_i > 0$ is a prescribed feasibility index for the ith original constraint and σ_j^+ denotes the upper limit for the standard deviation of structural performance.

In this formulation, the robust structural design optimization problem is shown to be a vector optimum problem, in which two criteria namely the statistical mean $\mathrm{E}(f)$ and the standard deviation $\sigma(f) = \sqrt{\mathrm{Var}(f)}$ of the goal performance are to be minimized.

In some special cases, the structural robust design can also be stated on the basis of cost/ loss function measures. If a function c that represents the loss induced by variation in goal performance, or the costs related to material volume and manufacturing tolerance is given explicitly, an alternative statement of structural robust design can be given by rewriting the optimization criterion in Eq. (5.1) as

$$
\begin{aligned}
&\text{find} && \mathbf{d}, \\
&\text{minimizing} && c = c\left(\mathrm{E}(f(\mathbf{d})), \sigma(f(\mathbf{d})), \mathbf{d}\right), \\
&\text{subject to} && \mathrm{E}(g_i(\mathbf{d})) + \beta_i \sigma(g_i(\mathbf{d})) \leq 0 \qquad (i = 1, 2, ..., k), \\
& && \sigma(h_j(\mathbf{d})) \leq \sigma_j^+ \qquad (j = 1, 2, ..., l), \\
& && \mathbf{d}_{\mathrm{L}} \leq \mathbf{d} \leq \mathbf{d}_{\mathrm{U}},
\end{aligned} \tag{5.2}
$$

Particularly, if variabilities of uncertain parameters such as manufacturing tolerances are also considered as design variables and the cost-versus-tolerance relations are taken into account, Eq. (5.2) represents the tolerance optimization problem for minimum cost under performance variability constraints.

A schematic representation of the first type of constraints defined in (5.1) and (5.2) is given in Fig. 5.1. Therein, g is the structural performance function and $p(g)$ is the probability density function of g. In Fig.5.1, we show a structural design ($\mathbf{d}_1$) satisfying the constraint and another one ($\mathbf{d}_2$) violating the constraint.

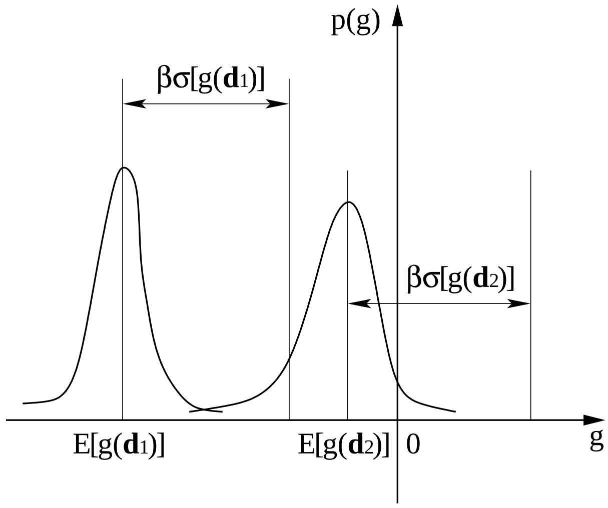

Figure 5.1: Constraint in robust design

In Eqs. (5.1) and (5.2), the first k constraints are equivalent to

$$\gamma_i \geq \beta_i \qquad (i = 1, 2, ..., k) \tag{5.3}$$

where $\gamma_i = -\mathrm{E}(g_i(\mathbf{d}))/\sigma(g_i(\mathbf{d}))$ can be interpreted as the *safety index* of the ith constraint condition. The constraint in Eq. (5.3) is expressed in a similar form as in RBDO employing the First Order Second Moment (FOSM) method for reliability analysis, whereas in the latter formulation the response moments are evaluated at the most probable failure point (MPP), by which a sub-optimization loop is required for locating such a point. As mentioned above, the exact probability of failure is not of concern in this context, however, a larger value of β_i generally requires the corresponding performance to be more robust to the system variability. It should be noted that the inequality (5.3) may still serve as a probabilistic constraint under the assumption that the probabilistic distribution of the function value $g_i(\mathbf{d})$ is normal. In such a case, if β is set to be 3.0, for instance, the probability that the original constraint condition will be satisfied is required to be higher than 0.9987. From the engineering point of view, the assumption of the structural performance to be normal is often reasonable. Thus the feasibility index is considered here an appropriate measure of the robustness related to the design restrictions.

In the robust design problem stated in Eq. (5.1), the two design criteria often conflict with each other. Pareto optimality is one possible way of defining optimal solutions for such a multi-criteria resp. vector optimization problem. As the definition of the Pareto optimum implies, a movement from a Pareto optimal point in the criteria space must increase the value of at least one criterion. Therefore, a rational trade-off between the two sub-objectives is necessary for robust design problems.

5.2.2 Computational aspects

Solution strategy for the multi-criteria optimization

In order to obtain a Pareto optimum of the multi-criteria optimization problem as in Eq. (5.1), it is a common practice to replace the vector of design objective by a scalarized objective function (see Chapter 2).

Though other methods can be employed for seeking of Pareto optimal solutions, a straightforward scalarization approach is the linear combination method, in which the minimum of a weighted linear combination of the individual objectives is regarded as Pareto optimal. In this approach, the relative weights to put on the different objective functions can be easily specified by a prescribed factor, which enables the designer to investigate the trade-offs between the individual objectives. Then the problem of structural robust design expressed in Eq. (5.1) is formulated in terms of a desirability function $\tilde{f}$ as follows:

$$\begin{aligned} &\text{find} && \mathbf{d}, \\ &\text{minimizing} && \tilde{f} = (1-\alpha)\mathrm{E}(f(\mathbf{d}))/\mu^* + \alpha\sigma(f(\mathbf{d}))/\sigma^*, \\ &\text{subject to} && \mathrm{E}(g_i(\mathbf{d})) + \beta_i\sigma(g_i(\mathbf{d})) \leq 0 \qquad (i = 1, 2, ..., k)\ , \\ & && \sigma(g_j(\mathbf{d})) \leq \sigma_j^+ \qquad (j = 1, 2, ..., l), \\ & && \mathbf{d}_{\mathrm{L}} \leq \mathbf{d} \leq \mathbf{d}_{\mathrm{U}}. \end{aligned} \tag{5.4}$$

Here $0 < \alpha < 1$ is the factor weighting the two objectives, μ^* and σ^* are normalization factors. The problem expressed by Eq. (5.4) can be converted to a pure mean value minimization problem for $\alpha = 0$ or a pure standard deviation minimization problem for $\alpha = 1$.

Since the weighted sum approach is used to solve the multi-criteria optimization problem in this study, the problem of choosing the weighting factors arises. Unfortunately, a systematic method for such a purpose is not yet available. However, this can be amended by setting different weighting factors at each optimization process. Thus the present method provides a possibility of generating a set of Pareto optima in a cost-effective manner, but the final decision should be made by the designer based on the subjective judgement on design priorities.

The linear combination that forms the desirability function performs well in this study, as will be shown by the numerical examples. But it may present some difficulties in tracing the Pareto curve when the feasible region in the objective function space is not convex. This appears seldom in actual applications, however. In such a particular case, other techniques (e.g. the physical programming method [80]) need to be employed for the purpose of locating all the Pareto optima in a robust design problem.

The robust design optimization problem defined by Eq. (5.4) (or Eq. (5.2)) can be efficiently solved with gradient-based mathematical programming methods iteratively. In the present study, the optimization package CFSQP [81], which is an implementation of two algorithms based on Sequential Quadratic Programming, is used to solve the optimization problem.

Flowchart of the computer implementation

The proposed numerical method for structural robust design has been implemented (see Chapter 6, 7 and 8), as shown in the flowchart of the computational procedure in Fig. 5.2. The Finite Element Programming System (FEPS [82][83]) developed by the Institute for Computer Application (ICA) at the University of Stuttgart provides a platform for this study, on which the stochastic finite element analysis and the sensitivity evaluation are further implemented.

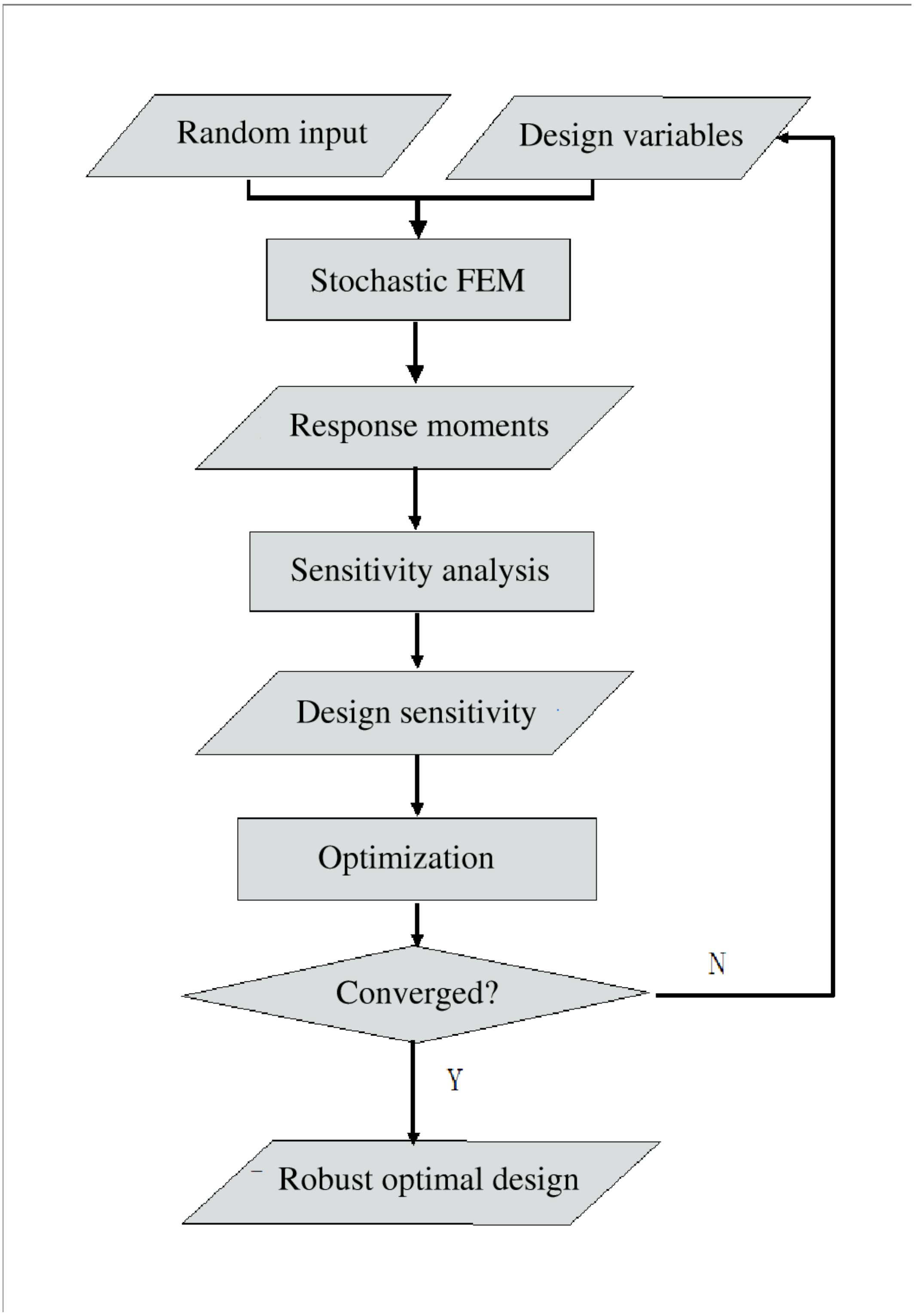

Figure 5.2: Flowchart of the developed robust design method

5.2.3 Comparison with formulations based on Taguchi's methodology

The basic ideas of Taguchi's methodology for robust design have also been adopted in some studies on the structural robust design. Here, a brief comparison between the present formulation and the formulations based on Taguchi's methodology is summarized in Table 5.1.

Table 5.1: A comparison between the present formulation and those based on Taguchi's methodology

	Present	Based on Taguchi's method
Description of input	Mean, variance	Leveled noise factors
Description of output	Mean, variance	Leveled control factors
Design objective	Minimizing objective/ desirability function	Maximizing S/N ratio
Design constraints	Including performance variance	Difficult to consider
Objective/constraints evaluation	Perturbation SFEM	Experimental design

A comparative numerical study on robust design using Taguchi's method

For the sake of comparison, a case study with reference to the four-bar truss problem considered in Section 3.3 is performed using both the Taguchi's robust design method and the present formulation. In the problem there is only one independent design parameter A_1 serving as a control factor and nine candidate levels for it are selected, which are $A_1 = 0.0, 0.2, 0.4, 0.6, 0.8, 1.0, 1.2, 1.4, 1.6$. These control factor levels are tested for seeking the best one furnishing the robust design for minimization of the nodal displacement u. The noise factors (Young's moduli E_1 and E_2) are divided into 3 levels. The levels of the noise factors are determined by the mean values and the standard deviations of the corresponding random parameters, as

$$\begin{aligned}
\mathrm{L}_{\mathrm{low}}(E_1) &= \mathrm{E}(E_1) - 3\sigma(E_1) = 147,\\
\mathrm{L}_{\mathrm{medium}}(E_1) &= \mathrm{E}(E_1) = 210,\\
\mathrm{L}_{\mathrm{high}}(E_1) &= \mathrm{E}(E_1) + 3\sigma(E_1) = 273.
\end{aligned}$$

The levels for E_2 are defined analogously and amount to: $\mathrm{L}_{\mathrm{low}}(E_2) = 85$, $\mathrm{L}_{\mathrm{medium}}(E_2) = 100$, $\mathrm{L}_{\mathrm{high}}(E_2) = 115$.

Since the objective of the design is to minimize the nodal displacement u, the S/N ratio for the Smaller-the-best problem is used for evaluating the robustness of the designs. A full factorial design, with $n = 3^2$ numerical experiments for each level of the control factor, is conducted and the performance function value (u) for all the experiments are listed in Table 5.2.

Table 5.2: Experimental design results ($\times 10^{-3}$)

		$E_1 = 147$	147	147	210	210	210	273	273	273
		$E_2 = 85$	100	115	85	100	115	85	100	115
Run	A_1									
1	0	4.706	4.000	3.478	4.706	4.000	3.478	4.706	4.000	3.478
2	0.2	4.779	4.124	3.626	4.584	3.977	3.513	4.404	3.841	3.406
3	0.4	4.854	4.255	3.788	4.468	3.955	3.548	4.139	3.695	3.337
4	0.6	4.932	4.395	3.964	4.358	3.933	3.584	3.903	3.559	3.271
5	0.8	5.013	4.545	4.157	4.253	3.911	3.621	3.693	3.433	3.207
6	1.0	5.096	4.705	4.370	4.153	3.890	3.658	3.505	3.315	3.146
7	1.2	5.182	4.877	4.607	4.058	3.869	3.696	3.334	3.206	3.087
8	1.4	5.271	5.062	4.870	3.967	3.848	3.736	3.180	3.103	3.030
9	1.6	5.363	5.262	5.165	3.880	3.827	3.775	3.039	3.007	2.975
10	1.7678	5.442	5.442	5.442	3.810	3.810	3.810	2.930	2.930	2.930
11	0.3531	4.837	4.224	3.748	4.495	3.960	3.540	4.198	3.728	3.353

The output data obtained in the designed experiments are analyzed, giving the mean and S/N ratio for each level of the control factor shown in Table 5.3.

Among all the candidate levels for the control factor, the fourth ($A_1 = 0.6$) and the fifth level ($A_1 = 0.8$) present a maximum S/N ratio suggesting the most robust design, whereby the fifth level yields a lower mean. Therefore the best settings for robust design are $A_1 = 0.6$ and $A_1 = 0.8$ based on the experimental results. Both designs are verified with Monte Carlo simulations (sample size: 3000), which reveals the mean value and the standard deviation of the samples are $\overline{u} = 3.9431 \times 10^{-3}$, $\mathrm{s}(u) = 1.8932 \times 10^{-4}$ for the former design and $\overline{u} = 3.9224 \times 10^{-3}$, $\mathrm{s}(u) = 2.1197 \times 10^{-4}$ for the latter. Here and in what follows, the Monte Carlo simulations are always conducted under the assumption of normal distributions of the random input variables.

Table 5.3: Mean values and S/N ratio by Taguchi's robust design method

(The figures in bold denote the maximum mean values and the maximum S/N ratios)

Run	A_1	Mean u ($\times 10^{-3}$)	S/N ratio	Note
1	0	4.061	-12.240	
2	0.2	4.028	-12.158	
3	0.4	4.010	-12.118	
4	0.6	3.989	**-12.079**	Max. S/N ratio
5	0.8	**3.981**	**-12.079**	Min. mean and Max. S/N ratio
6	1.0	3.982	-12.105	
7	1.2	3.991	-12.157	
8	1.4	4.007	-12.234	
9	1.6	4.033	-12.339	
10	1.7678	4.061	-12.448	
11	0.3531	4.009	-12.115	

For comparison, a set of Pareto optima with the present robust design formulation have been obtained using the numerical techniques that will be presented in the following chapters, as shown in Table 5.4. The stochastic analysis results listed in Table 5.4 have been verified by Monte Carlo simulations (MCS, sample size: 3000) and are shown to agree well with the simulation results. The optima for the minimum mean ($A_1 = 1.7678$) and for the minimum standard deviation of the concerned displacement ($A_2 = 0.3531$) are also checked by the Taguchi's procedure for the S/N ratio analysis, with the results listed in Table 5.2 and Table 5.3.

Table 5.4: Optimal solutions by the present robust design formulation

Design var.	$\alpha = 0.0$	$\alpha = 0.05$	$\alpha = 0.1$	$\alpha = 0.2$	$\alpha = 0.4$	$\alpha = 0.6$	$\alpha = 0.8$	$\alpha = 1.0$
A_1	1.7678	1.6659	0.6493	0.4738	0.3974	0.3731	0.3607	0.3531
A_2	0.0000	0.1440	1.5817	1.8300	1.9381	1.9724	1.9900	2.0006
$\mathrm{E}(u)$ ($\times 10^{-3}$)	3.848	3.854	3.937	3.955	3.963	3.966	3.968	3.968
(MCS)	(3.841)	(3.849)	(3.938)	(3.957)	(3.966)	(3.969)	(3.970)	(3.971)
$\sigma(u)$ ($\times 10^{-4}$)	3.810	3.611	1.924	1.798	1.780	1.772	1.772	1.771
(MCS)	(3.971)	(3.750)	(1.939)	(1.810)	(1.787)	(1.785)	(1.784)	(1.784)

As can be seen, in this simple problem the Taguchi's signal-to-noise method presents really sub-optimal designs, whereas a wide set of Pareto optima corresponding to different weighting factors can be obtained with the present formulation of robust design. Moreover, the statistics extracted from the results of the designed experiments fail to predict the actual mean value of the performance, despite the fact that a full factorial design has been employed. Even worse is that, these experimental results can not predict the trend of changes of the performance mean with respect to the design parameter successfully, as seen from Table 5.3 and Table 5.4.

Chapter 6

Robust design of linear structures

In this chapter, the robust design optimization for linear structures is addressed. First, the numerical analysis of response moments sensitivity is presented. The method is developed using direct differentiation in conjunction with the perturbation based stochastic finite element analysis. Then numerical examples are given to demonstrate the proposed method.

6.1 Response moments sensitivity analysis

In the derivation of perturbation equations for response moment analysis, the structural displacements are suitably expressed as a function of the random input variables, as shown in previous chapters. For design problems, however, the design variables also enter the problem. The objective function and the constraints are defined by functions of response moments (mean value and variance/ standard deviations) in the present structural robust design optimization problems. Consequently, the sensitivity expressions of the response moments with respect to these design variables are of great importance for solving the present problem by gradient-based mathematical programming algorithms.

Subsequently, in the framework of the perturbation based stochastic finite element analysis, the computational scheme for structural response moments analysis is developed for use in the structural robust design problem with the direct differentiation method [84][85].

We first consider the sensitivity analysis of the static displacement response moments.

Sensitivity of displacement response moments

Considering the implicit dependence of the terms upon the design variables, differentiation of Eqs. (4.17), (4.18) and (4.19) with respect to the kth design variable d_k leads to the following equations:

$$\bar{\mathbf{K}}\bar{\mathbf{u}}_{,d_k} = \bar{\mathbf{p}}_{,d_k} - \bar{\mathbf{K}}_{,d_k}\bar{\mathbf{u}}\,, \tag{6.1}$$

$$\bar{\mathbf{K}}\bar{\mathbf{u}}_{c_i,d_k} = \bar{\mathbf{p}}_{c_i,d_k} - \bar{\mathbf{K}}_{c_i,d_k}\bar{\mathbf{u}} - \bar{\mathbf{K}}_{c_i}\bar{\mathbf{u}}_{,d_k} - \bar{\mathbf{K}}_{,d_k}\bar{\mathbf{u}}c_i \ \ (i = 1, 2, ..., \hat{q})\,, \tag{6.2}$$

and

$$\begin{aligned}\bar{\mathbf{K}}\bar{\mathbf{u}}_{2,d_k} = & -\bar{\mathbf{K}}_{,d_k}\bar{\mathbf{u}}_2 + \frac{1}{2}\sum_{i=1}^{\hat{q}}(\bar{\mathbf{p}}_{c_ic_i,d_k} - \bar{\mathbf{K}}_{c_ic_i,d_k}\bar{\mathbf{u}} - 2\bar{\mathbf{K}}_{c_i,d_k}\bar{\mathbf{u}}_{c_i} - \bar{\mathbf{K}}_{c_ic_i}\bar{\mathbf{u}}_{,d_k} \\ & -2\bar{\mathbf{K}}_{c_i}\bar{\mathbf{u}}_{c_i,d_k})\mathrm{Var}(c_i) + \frac{1}{2}\sum_{i=1}^{\hat{q}}(\bar{\mathbf{p}}_{c_ic_i} - \bar{\mathbf{K}}_{c_ic_i}\bar{\mathbf{u}} - 2\bar{\mathbf{K}}_{c_i}\bar{\mathbf{u}}_{c_i})\frac{\partial \mathrm{Var}(c_i)}{\partial d_k},\end{aligned} \tag{6.3}$$

where the subscript d_k with a preset comma indicates the derivatives with respect to the kth design variable.

By solving the above equations, the sensitivities of the mean value and the covariance of displacements with respect to d_k can be obtained as:

$$\frac{\partial \mathrm{E}(\mathbf{u})}{\partial d_k} = \bar{\mathbf{u}}_{,d_k} + \bar{\mathbf{u}}_{2,d_k}\,, \tag{6.4}$$

and

$$\frac{\partial \mathrm{Cov}(u^r, u^s)}{\partial d_k} = \sum_{i=1}^{\hat{q}}(\bar{u}^r_{c_i,d_k}\bar{u}^s_{c_i} + \bar{u}^r_{c_i}\bar{u}^s_{c_i,d_k})\mathrm{Var}(c_i) + \sum_{i=1}^{\hat{q}}\bar{u}^r_{c_i}\bar{u}^s_{c_i}\frac{\partial \mathrm{Var}(c_i)}{\partial d_k}. \tag{6.5}$$

Equations (6.3) and (6.5) are obtained by noting the fact that the design variables can affect the covariance of the structural response in two ways, namely, by changing its derivatives with respect to the random parameters and by changing the covariance or variance of the random parameters itself.

Since the system coefficient matrices of Eqs. (6.1)-(6.3) have been decomposed in the previous solution steps, the solutions of Eqs. (6.1), (6.2) and (6.3) involve only forward reductions and backward substitutions. However, the computational costs for sensitivity analysis are still extremely high due to the lengthy calculation of the third-order derivatives on the right hand side of Eq. (6.3). Noting that the second term on the right hand side of Eq. (6.4) consists of only second order variations of basic random variables and thus can be ignored in case of small scatter of input variables, a first-order approximation for the sensitivity of the expected value of the displacement is obtained with

$$\frac{\partial \mathrm{E}(\mathbf{u})}{\partial d_k} \approx \bar{\mathbf{u}}_{,d_k} \, . \tag{6.6}$$

Evaluation of moments and their sensitivities for a generalized performance function

A generalized structural performance function Φ defined as an explicit function of the nodal displacements, the random variables and the design variables can be written as:

$$\Phi = \Phi\left(\mathbf{u}(\mathbf{b}), \mathbf{b}, \mathbf{d}\right) \, . \tag{6.7}$$

Before addressing the sensitivity analysis, we here consider the moments calculations of a generalized structural performance function as defined in Eq. (6.7). Expanding the function Φ in a Taylor series about $\bar{\mathbf{b}}$, the mean value of the random variables, and truncating the series at the linear terms, one obtains the first-order approximate mean value and variance of Φ, as

$$\mathrm{E}(\Phi) = \Phi(\bar{\mathbf{u}}, \bar{\mathbf{b}}, \mathbf{d}) \, , \tag{6.8}$$

$$\mathrm{Var}(\Phi) = \sum_{i,j=1}^{q} \left(\frac{\partial \Phi}{\partial \mathbf{u}}\bigg|_{\bar{\mathbf{b}}} \bar{\mathbf{u}}_{b_i} + \bar{\Phi}_{b_i} \right) \left(\frac{\partial \Phi}{\partial \mathbf{u}}\bigg|_{\bar{\mathbf{b}}} \bar{\mathbf{u}}_{b_j} + \bar{\Phi}_{b_j} \right) \mathrm{Cov}(b_i, b_j)\,. \tag{6.9}$$

Alternatively, in terms of uncorrelated random variables $\mathbf{c}$, Eq. (6.9) approximately reduces to

$$\mathrm{Var}(\Phi) = \sum_{i=1}^{\hat{q}} \left(\frac{\partial \Phi}{\partial \mathbf{u}}\bigg|_{\bar{\mathbf{b}}} \bar{\mathbf{u}}_{c_i} + \bar{\Phi}_{c_i} \right)^2 \mathrm{Var}(c_i). \tag{6.10}$$

By including the second-order terms in the Taylor series, the second-order approximate expected value of Φ can be given by

$$\begin{aligned}
\mathrm{E}(\Phi) &= \bar{\Phi} + \frac{1}{2} \sum_{i,j=1}^{q} \left(\bar{\mathbf{u}}_{b_i}^{\mathrm{t}} \bar{\mathbf{H}}_{\Phi}(\mathbf{u}) \bar{\mathbf{u}}_{b_j} + 2\, \frac{\partial \Phi_{b_i}}{\partial \mathbf{u}}\bigg|_{\bar{\mathbf{b}}} \bar{\mathbf{u}}_{b_j} + \frac{\partial \Phi}{\partial \mathbf{u}}\bigg|_{\bar{\mathbf{b}}} \bar{\mathbf{u}}_{b_i b_j} + \bar{\Phi}_{b_i b_j} \right) \mathrm{Cov}(b_i, b_j) \\
&\approx \bar{\Phi} + \frac{1}{2} \sum_{i=1}^{\hat{q}} \left(\bar{\mathbf{u}}_{c_i}^{\mathrm{t}} \bar{\mathbf{H}}_{\Phi}(\mathbf{u}) \bar{\mathbf{u}}_{c_i} + 2\, \frac{\partial \Phi_{c_i}}{\partial \mathbf{u}}\bigg|_{\bar{\mathbf{b}}} \bar{\mathbf{u}}_{c_i} + \frac{\partial \Phi}{\partial \mathbf{u}}\bigg|_{\bar{\mathbf{b}}} \bar{\mathbf{u}}_{c_i c_i} + \bar{\Phi}_{c_i c_i} \right) \mathrm{Var}(c_i) \\
&= \bar{\Phi} + \frac{\partial \Phi}{\partial \mathbf{u}}\bigg|_{\bar{\mathbf{b}}} \bar{\mathbf{u}}_2 + \frac{1}{2} \sum_{i=1}^{\hat{q}} \left(\bar{\mathbf{u}}_{c_i}^{\mathrm{t}} \bar{\mathbf{H}}_{\Phi}(\mathbf{u}) \bar{\mathbf{u}}_{c_i} + 2\, \frac{\partial \Phi_{c_i}}{\partial \mathbf{u}}\bigg|_{\bar{\mathbf{b}}} \bar{\mathbf{u}}_{c_i} + \bar{\Phi}_{c_i c_i} \right) \mathrm{Var}(c_i),
\end{aligned} \tag{6.11}$$

where $\mathbf{H}_{\Phi}(\mathbf{u})$ is the Hessian matrix of Φ with respect to $\mathbf{u}$. The derivatives of Φ can be easily obtained from the explicit dependence on displacement and random parameters.

Differentiating Eqs. (6.8) and (6.10) with respect to d_k, one obtains the first-order approximate sensitivity of the mean and variance of the performance function Φ:

$$\frac{\partial \mathrm{E}(\Phi)}{\partial d_k} = \frac{\partial \Phi}{\partial \mathbf{u}}\bigg|_{\bar{\mathbf{b}}} \bar{\mathbf{u}}_{,d_k} + \bar{\Phi}_{,d_k}, \tag{6.12}$$

$$\begin{aligned}
\frac{\partial \mathrm{Var}(\Phi)}{\partial d_k} &= \sum_{i=1}^{\hat{q}} 2 \left(\frac{\partial \Phi}{\partial \mathbf{u}}\bigg|_{\bar{\mathbf{b}}} \bar{\mathbf{u}}_{c_i} + \bar{\Phi}_{c_i} \right) \left(\bar{\mathbf{u}}_{,d_k}^{\mathrm{t}} \bar{\mathbf{H}}_{\Phi}(\mathbf{u}) \bar{\mathbf{u}}_{c_i} + \frac{\partial \Phi}{\partial \mathbf{u}}\bigg|_{\bar{\mathbf{b}}} \bar{\mathbf{u}}_{c_i,d_k} + \frac{\partial \Phi_{,d_k}}{\partial \mathbf{u}}\bigg|_{\bar{\mathbf{b}}} \bar{\mathbf{u}}_{c_i} \right. \\
&\quad \left. + \frac{\partial \Phi_{c_i}}{\partial \mathbf{u}}\bigg|_{\bar{\mathbf{b}}} \bar{\mathbf{u}}_{,d_k} + \bar{\Phi}_{c_i,d_k} \right) \mathrm{Var}(c_i) + \sum_{i=1}^{\hat{q}} \left(\frac{\partial \Phi}{\partial \mathbf{u}}\bigg|_{\bar{\mathbf{b}}} \bar{\mathbf{u}}_{c_i} + \bar{\Phi}_{c_i} \right)^2 \frac{\partial \mathrm{Var}(c_i)}{\partial d_k}.
\end{aligned} \tag{6.13}$$

In the case of transient response, the approximate expected value and variance of the generalized structural performance function, and their sensitivity with respect to the design variables can be obtained similarly.

It is worth remarking here, though the adjoint variable method can be used in sensitivity analysis of the deterministic response, it is not recommended for the sensitivity analysis of response moments in this study, since the method can hardly be extended to the purpose of the second-order perturbation based stochastic analysis.

6.2 Numerical examples

Robust compliance minimization problem of a three-bar truss structure

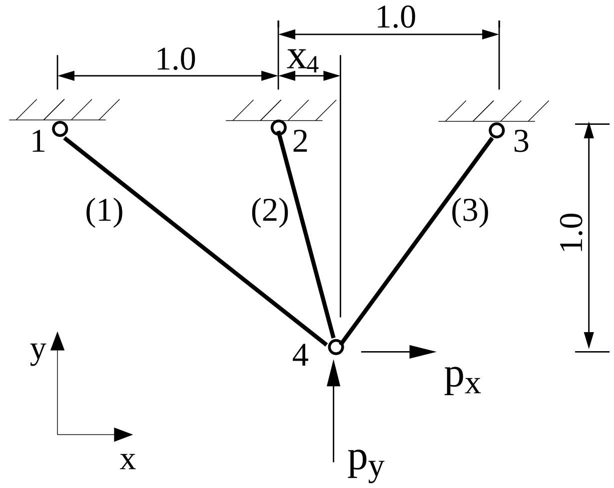

Figure 6.1: The three-bar truss

The three-bar truss structure is shown in Fig. 6.1. The Young's modulus of the i-th bar E_i, the horizontal position of the fourth node X_4 and the cross sectional areas of the bars are random variables and their mean and variances or coefficients of variation (COV) are shown in Table 6.1. All random variables are assumed independent. The cross sectional areas of each bar A_i $(i = 1, 2, 3)$ and the horizontal position of the fourth node are taken as design variables. The loads acting on the structure are $p_x = 1.5$, $p_y = -10.0$. The mass density of the material is $\rho = 1.0$. The constraints considered in this problem include: (a) structural weight constraint

Table 6.1: Random variables for the three-bar truss

Variable	Mean	COV	Standard deviation
$E_1 = E_3$	4.0×10^3	0.1	/
E_2	1.0×10^3	0.1	/
X_4	/	/	0.05
A_1	/	0.1	/
A_2	/	0.1	/
A_3	/	0.15	/

$w \leq 6.0$; (b) nodal displacement constraints $u \leq 0.05$, $v \leq 0.05$; (c) member stress constraints: $(\mathrm{E}(\sigma_i) - 5.0)/\sigma(\sigma_i) \leq -3.0$ $(i = 1, 2, 3)$; (d) bound limits for the design variables: $1.0^{-6} \leq A_i \leq 6.0$ $(i = 1, 2, 3)$, $-0.3 \leq X_4 \leq 0.3$.

Table 6.2: Optimal solutions for the three-bar truss

Des. var.	Init.	Determ.	$\alpha = 0.0$	$\alpha = 0.25$	$\alpha = 0.5$	$\alpha = 0.75$	$\alpha = 1.0$
A_1	2.500	2.835	2.837	2.147	2.048	1.924	1.938
A_2	0.800	0.249	0.249	2.398	2.487	2.742	2.680
A_3	1.500	1.387	1.387	0.530	0.551	0.481	0.510
X_4	0.0	-0.300	-0.300	-0.300	-0.300	-0.300	-0.300
w	6.457	6.000	6.000	6.000	6.000	6.000	6.000
$\mathrm{E}(f) \times 10^{-2}$	1.590	1.408	1.407	1.441	1.450	1.460	1.464
(MCS)	(1.593)	(1.420)	(1.419)	(1.455)	(1.457)	(1.467)	(1.470)
$\sigma(f) \times 10^{-3}$	1.839	1.852	1.851	1.483	1.470	1.461	1.461
(MCS)	(1.881)	(1.899)	(1.896)	(1.492)	(1.481)	(1.476)	(1.477)

The solutions of the optimization are shown in Table 6.2. The results of the Monte Carlo simulation (with 3000 realizations under assumption of normal distribution of the random inputs) corresponding to each design are also listed in the table. It can be seen from the results that in the deterministic formulation resp. mean value minimization the mean value of the structural compliance is notably lowered but its standard deviation is still very high. In contrast, not only the mean value but also the standard deviation of the objective function are reduced in the optimal solutions obtained with robust formulation. Moreover, in the optimum obtained, the standard deviation of the objective function decreases as the weighting factor increases and vice versa.

Structural compliance optimization of a 25-bar space truss structure

The structural compliance, defined as the inner product of the applied load vector and the nodal displacement vector ($\mathbf{p}^t\mathbf{u}$), of a 25-bar truss structure (as depicted in Fig. 6.2) resembling a power transmission tower is to be minimized.

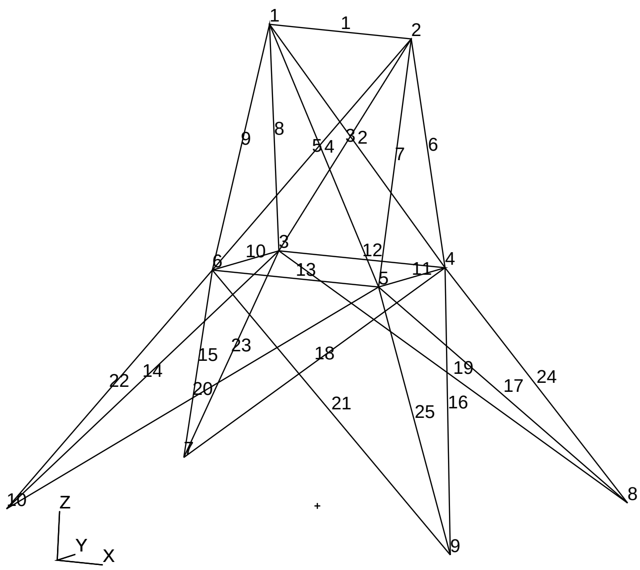

Figure 6.2: The 25-bar space truss

The nodal coordinates of the finite element model are given in Table 6.3. The design variables are bar cross sectional areas. Six independent design variables are selected by linking various member sizes, and the member grouping information is given in Table 6.5. The mass density of the material is $\rho = 0.1$. Four nodal forces with values $p_{1y} = p_{2y} = p_{1z} = p_{2z} = -1.0 \times 10^4$ are imposed at the first and the second nodes and two nodal forces with random values at the third and the sixth nodes. Additionally, forces with random values are applied to the nodes number 3 and 6 along x-direction. The nodal forces applied at the nodes 3 and 6, the Young's moduli and the cross-sectional areas for the grouped bars are considered as random variables with mean values and standard deviations or coefficients of variation (COV) shown in Table 6.4.

Table 6.3: Nodal coordinates of the 25-bar truss

Node	X	Y	Z
1	-37.5	0.0	200.0
2	37.5	0.0	200.0
3	-37.5	37.5	100.0
4	37.5	37.5	100.0
5	37.5	-37.5	100.0
6	-37.5	-37.5	100.0
7	-100.0	100.0	0.0
8	100.0	100.0	0.0
9	100.0	-100.0	0.0
10	-100.0	-100.0	0.0

In this example, the structural weight constraint $\mathrm{E}(w) \leq 750.0$, the member stress constraints $\mathrm{E}(|\sigma_i|) + 3\sigma(\sigma_i) \leq 5000.0 \quad (i = 1, 2, ..., 25)$, the lower and upper bounds of design variables $0.05 \leq A_j \leq 10.0 \quad (j = \mathrm{I,II,...,VI})$ are observed.

Table 6.4: Random variables for the 25-bar truss

No.	Variables	Mean	Standard deviation	COV
1–5	$E_{\mathrm{I}} - E_{\mathrm{V}}$	1.0×10^7	2.0×10^5	
6	E_{VI}	1.0×10^7	1.5×10^6	
7	p_{3x}	5.0×10^2	50.0	
8	p_{6x}	5.0×10^2	50.0	
9–14	$A_{\mathrm{I}} - A_{\mathrm{VI}}$			0.05

The optimal solutions corresponding to different weighting factors are listed in Table 6.6. Compared with the mean value minimization solution ($\alpha = 0$), the standard deviation of the structural compliance is decreased by 14.3 - 22.7% in the robust solutions, which means a considerable improvement of robustness of the design. Moreover, in the obtained optimum, the standard deviation of the objective function decreases and the mean value increases as the weighting factor increases and vice versa (Fig. 6.4). This conflict between the two sub-objectives reveals the essential characteristic of Pareto solutions.

Table 6.5: Group membership for the 25-bar truss

Group number	Members
I	1
II	2,3,4,5
III	6,7,8,9
IV	10,11,12,13
V	14,15,16,17,18,19,20,21
VI	22,23,24,25

The optimal solutions are fairly well verified by the results of Monte Carlo simulations with 3000 realizations given in Table 6.6 (in parentheses). The numerical results of the goal performance are shown to be in good agreement, while the computing time for such a Monte Carlo simulation on a Pentium 4-2.0 GHz computer

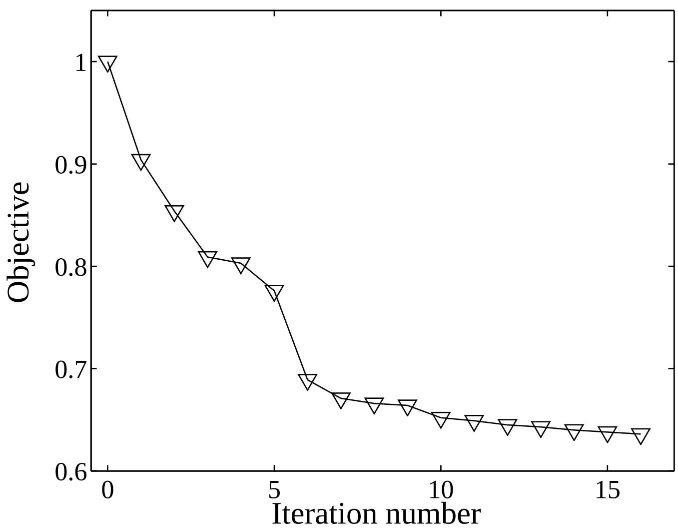

Figure 6.3: Iteration history of the robust design for the 25-bar truss ($\alpha = 0.5$)

is 12.82 seconds, and for a perturbation based analysis only 0.25 second.

Table 6.6: Optimal solutions for the 25-bar truss

Des. var.	Init.	$\alpha = 0$	$\alpha = 0.25$	$\alpha = 0.5$	$\alpha = 0.75$	$\alpha = 1.0$
A_{I}	2.300	0.050	0.050	0.050	0.114	0.147
A_{II}	2.300	0.050	0.075	0.207	0.558	0.672
A_{III}	2.300	5.740	4.882	4.280	3.685	3.465
A_{IV}	2.300	1.718	0.950	0.628	0.575	0.566
A_{V}	2.300	1.054	1.179	1.151	0.925	0.822
A_{VI}	2.300	5.574	6.328	6.940	7.704	8.048
$\text{E}(f)\,(\times 10^3)$	7.768	5.328	5.478	5.775	6.044	6.196
(MCS)	(7.763)	(5.322)	(5.477)	(5.771)	(6.035)	(6.184)
$\sigma(f)\,(\times 10^3)$	0.540	0.357	0.308	0.285	0.277	0.276
(MCS)	(0.557)	(0.377)	(0.323)	(0.297)	(0.289)	(0.287)
$\text{E}(w)\,(\times 10^2)$	7.607	7.500	7.500	7.500	7.500	7.500

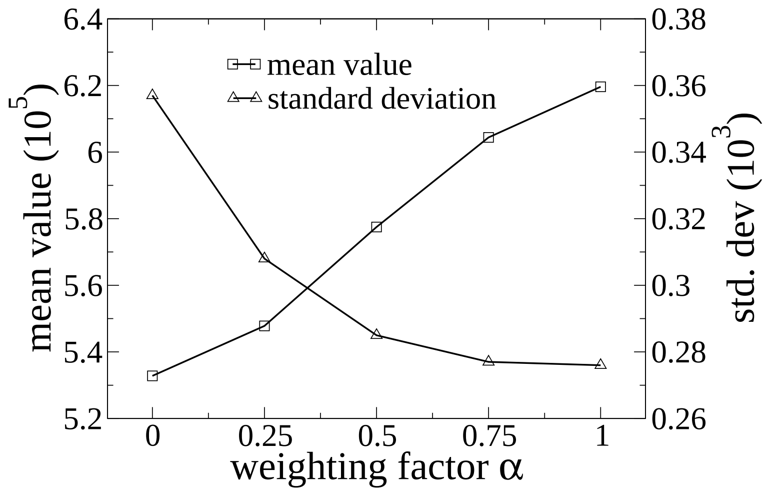

Figure 6.4: The mean and standard deviation of objective function f vs. weighting factor α

Cost minimization problem of a three-bar truss

The cost minimization problem of the three-bar truss structure shown in Fig. 6.1 is considered. The Young's modulus of the first and third bar is $E_{\mathrm{I}} = 4000$ and of the second bar $E_{\mathrm{II}} = 1000$. The loads applied on the structure are $p_x = 20$, $p_y = -40.0$. The mass density of the material is $\rho = 1.0$. The cross sectional areas of each bar A_i $(i = 1, 2, 3)$ are independent random variables. The joint position X_4 and the mean values $\mathrm{E}(A_i)$ as well as standard deviations $\sigma(A_i)$ of bar cross sectional areas are taken as design variables. The cost function as defined in Eq. (6.14) consists of material cost and manufacturing cost

$$c = 10w + \sum_{i=1}^{3}\left(\zeta_i + \frac{\eta_i}{t(A_i)}\right),$$

$$\zeta_i = \begin{cases} 0.05, & i \in \{i|A_i > (A_i)_{\mathrm{L}}\} \\ 0, & i \in \{i|A_i = (A_i)_{\mathrm{L}}\} \end{cases}, \quad \eta_i = \begin{cases} 0.3, & i \in \{i|A_i > (A_i)_{\mathrm{L}}\} \\ 0, & i \in \{i|A_i = (A_i)_{\mathrm{L}}\} \end{cases} \tag{6.14}$$

where w is the structural weight, $t(A_i) \equiv 3\sigma(A_i)$ is the manufacturing tolerance of the ith bar and $(A_i)_\mathrm{L}$ is the lower bound of the ith bar cross sectional area.

The constraints considered in this problem include: (a) nodal displacement constraints $\mathrm{E}(|u|)+3\sigma(|u|) \leq 0.01$, $\mathrm{E}(v)+3\sigma(|v|) \leq 0.01$; (b) member stress constraints: $\mathrm{E}(|\sigma_i|) + 3\sigma(\sigma_i) \leq 45.0 \quad (i = 1, 2, 3)$; (c) bound limits for the mean values and the standard deviations of the cross sectional areas: $1.0^{-6} \leq \mathrm{E}(A_i) \leq 5.0 \ (i = 1, 2, 3)$, $5.0 \times 10^{-3} \leq \sigma(A_i) \leq 0.2 \ (i = 1, 2, 3)$; (d) bound limit for the coordinate design variable $-0.2 \leq X_4 \leq 0.2$.

The solutions of the optimization are shown in Table 6.7. As a comparison, the optimal result obtained with fixed tolerance of member dimensions are also presented in the table. It is shown that the value of the cost function is further reduced by adjusting the tolerance (or standard deviations) of cross sectional areas through optimal design.

Table 6.7: Optimal solutions for the minimum cost optimization of the three-bar truss

Des. var.	Init.	Fixed tolerance	Designed tolerance
X_4	-0.2	-0.2	-0.2
$\mathrm{E}(A_1)$, $\sigma(A_1)$	1.3, 0.15	1.218, (0.15)	1.011, 0.068
$\mathrm{E}(A_2)$, $\sigma(A_2)$	1.3, 0.15	1.821, (0.15)	1.661, 0.066
$\mathrm{E}(A_3)$, $\sigma(A_3)$	1.3, 0.15	10^{-6}, (0.15)	10^{-6}, 0.005
c	52.36	35.60	32.97
$\mathrm{E}(u), \sigma(u)\ (\times 10^{-3})$	$5.42, 0.75$	5.01, 1.66	6.93, 1.02
$\mathrm{E}(v), \sigma(v)\ (\times 10^{-3})$	$7.87, 0.69$	8.19, 0.60	9.06, 0.31
$\mathrm{E}(\sigma_{max})$, $\sigma(\sigma_{max})$	29.76, 3.10	29.75, 3.64	35.62, 2.38

Minimum displacement problem of a ten-bar truss structure subject to impulse loads

The objective of the optimization problem is to minimize the peak value of the vertical displacement response of the fifth node of the planar ten-bar structure shown in Fig. 6.5, which is subject to rectangular impulse excitations acting on the two nodes of the structure. The Young's modulus of the material, the value of the impulses, the Y-coordinate of the fourth node and the cross sectional areas of the bars are considered as independent random variables. The coefficients of variation for the cross sectional areas are 0.1 for bars 5-8 and 0.2 for the other bars. The means and variances or coefficients of variation of other random variables are shown in Table 6.8, where E_{I} denotes the Young's modulus for bars 5-8, E_{II} the Young's modulus for other bars and Y_4 the Y-coordinate of the fourth node. The cross sectional areas of the bars are considered as design variables. They are grouped into four design variables, which are A_1 for bars 1 and 2, A_2 for bars 3 and 4, A_3 for bars 5-8 and A_4 for bars 9 and 10. The mean structural weight constraint $\mathrm{E}(w) \leq 30.0\,\mathrm{kg}$ is to be observed.

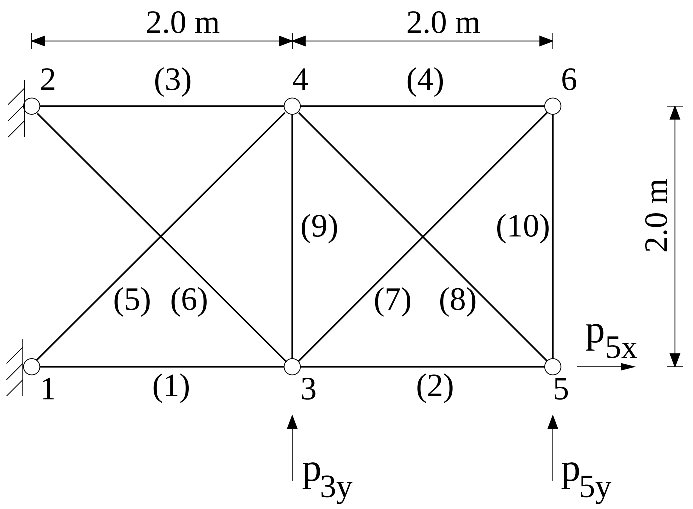

Figure 6.5: The planar ten-bar truss

The optima obtained with different weighting factors α are summarized in Table 6.9. As can be seen from the results, when the weighting factor increases, the optimal solution results in a larger mean value but smaller standard deviation of the objective function.

Robust design optimization of an antenna structure

In this example, the design optimization problem of an antenna structure is considered. The finite element model of the antenna consists of a membrane skin and a complex truss structure, as shown in Fig. 6.6. The structure is subjected to quasi-

Table 6.8: Random variables for the ten-bar truss

Variables	Mean	COV	Variance
E_{I} (N/m^2)	6.9×10^{10}	0.1	/
E_{II} (N/m^2)	2.1×10^{11}	0.2	/
Y_4 (m)	2.00	/	0.01
p_{3y} (N · s)	-500	0.1	/
p_{5x} (N · s)	800	0.1	/
p_{5y} (N · s)	-500	0.1	/

Table 6.9: Optimal solutions for the ten-bar truss

Des. var.	Lower	Upper	Initial	$\alpha = 0.0$	$\alpha = 0.5$	$\alpha = 1.0$
A_1 ($\times 10^{-6}$m^2)	50.00	1500.00	200.00	50.00	193.77	283.57
A_2 ($\times 10^{-6}$m^2)	50.00	1500.00	200.00	257.23	283.93	282.88
A_3 ($\times 10^{-6}$m^2)	50.00	1500.00	250.00	617.23	443.04	352.44
A_4 ($\times 10^{-6}$m^2)	50.00	1500.00	200.00	50.00	50.00	50.00
E(w) (kg)	/	30.00	26.36	30.00	30.00	30.00
E(f) ($\times 10^{-3}$m)	/	/	4.429	2.662	2.974	3.333
$\sigma(f)$ ($\times 10^{-3}$m)	/	/	0.484	0.519	0.390	0.389

static wind loads, which induce deformation and thus causes loss of shape accuracy and pointing accuracy of the reflection of surface. The bars forming the truss structure are divided into five groups according to their positions and directions. The spatial distribution of the skin thickness is modeled with four basic random variables. The Young's moduli of the materials of the skin and the five groups of bars are also assumed to be uncorrelated basic random variables. The design variables considered are the skin thickness t and the cross sectional areas A_1, A_2, A_3, which correspond to the bars supporting the skin along perimetric, radial and skew direction, respectively. The design objective is to minimize the maximum radial displacement at the upper edge of structure under the constraint of mean structural weight $\mathrm{E}(w) \leq 300.0\,\mathrm{kg}$.

The optimum solutions corresponding to the different weighting factors α are listed in Table 6.10. Compared with the initial design, a more robust design is obtained when the weighting factor α is set to be 0.5 or 1.

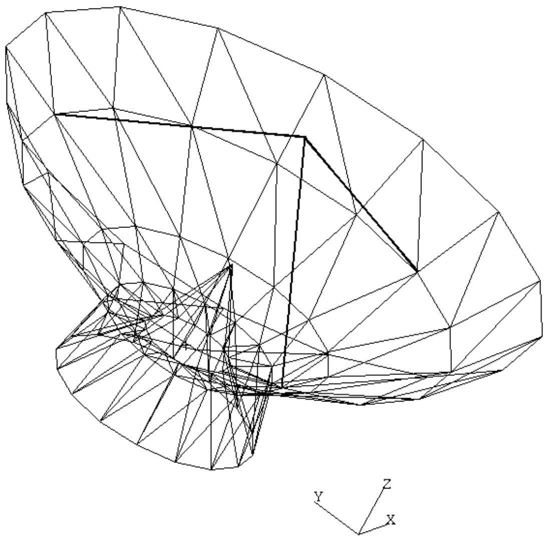

Figure 6.6: The antenna structure

Table 6.10: Optimal solutions for the antenna structure

Des. var.	Lower	Upper	Initial	$\alpha = 0.0$	$\alpha = 0.5$	$\alpha = 1.0$
A_1 ($\times 10^{-6}$m^2)	10.00	25.00	15.00	11.00	19.83	20.14
A_2 ($\times 10^{-6}$m^2)	10.00	25.00	15.00	11.22	19.83	20.15
A_3 ($\times 10^{-6}$m^2)	10.00	25.00	15.00	10.53	19.81	19.23
t ($\times 10^{-3}$m)	2.00	3.50	2.60	2.74	2.50	2.51
E(w) (kg)	/	300.00	291.47	300.00	300.00	300.00
E(f) ($\times 10^{-3}$m)	/	/	8.45	8.28	8.56	8.57
$\sigma(f)$ ($\times 10^{-3}$m)	/	/	0.54	0.49	0.37	0.36

6.3 Remarks

The stochastic structural analysis and sensitivity analysis have been implemented in conjunction with the perturbation based stochastic finite element method, which is efficiently applicable to considerably large scale problems. As a result, the proposed method is capable of covering a wide range of practical applications, where the system variations are relatively small. The feasibility of the proposed method and its adequacy have been demonstrated by numerical applications in some exemplary cases. As shown by the obtained results, in the robust optimum problems where the mean value as well as the variance of the structural performance function are of importance, the optimal design may yield different parameter values or even different structural topology than mean value minimization or deterministic optimization problem. The parameterised Pareto optima obtained in the numerical examples also reveal that the reduction of the variance of the structural performance is frequently achieved at the penalty of worsening its expected value. Bearing this in mind, the solution of the robust optimum design problem provides the engineer with the possibility of selecting a feasible structural design out of the set of Pareto optima obtained with different weighting factors in the compound objective resp. desirability function.

Chapter 7

Robust design of nonlinear structures with path dependence

This chapter deals with the robust design of structures with path-dependent behaviours. First, the perturbation based stochastic finite element analysis is extended to the path-dependent nonlinear problems, where an incremental scheme in consistence with the primary deterministic analysis is proposed. The associated sensitivity analysis is also presented. The method has been illustrated by examples of the robust design problems with material and geometrical nonlinearities.

7.1 Stochastic finite element analysis for nonlinear structures with path dependence

The perturbation based stochastic finite element method has been adapted to the analysis of path-independent nonlinear problems [73][86]. In this section, the perturbation based algorithms are extended to path-dependent nonlinear problems [87], where a rational scheme is proposed for the incremental stochastic analysis.

In vector form, the finite element equations of quasi-static structural problems with random parameters may be expressed as

$$\mathbf{s}(\boldsymbol{\sigma}, \mathbf{x}, \mathbf{b}, t) = \mathbf{p}(\mathbf{b}, t), \tag{7.1}$$

where $\mathbf{s}$ denotes the internal force vector (stress resultants at the nodal points) as a function of the stress state $\boldsymbol{\sigma}$ and geometry $\mathbf{x} =^0 \mathbf{x} + \mathbf{u}(t)$, and $\mathbf{p}$ is the vector of applied loads as a function of time t. The parameters that define the functional dependence of the resultants $\mathbf{s}$ on the stress $\boldsymbol{\sigma}$ like material moduli and member dimensions may exhibit random fluctuations as may do the time varying applied loads. The vector $\mathbf{b} \in \mathrm{R}^{q\times 1}$ collects all the random parameters. For the sake of simplicity, it is assumed here that the load vector $\mathbf{p}$ is independent of the geometry. The extension of the following derivations to deformation-dependent loading conditions is straightforward.

For structures having path-dependent nonlinear behaviour, such as in elastoplasticity, the internal force depends not only on the total displacements, but also on the deformation history. Therefore the equilibrium equation is expressed in an incremental form for the pseudo-time step $(k+1)$

$$^{k+1}\Delta\mathbf{s}(^{k}\mathbf{u}, {}^{k+1}\Delta\mathbf{u}, \mathbf{b}) = {}^{k+1}\Delta\mathbf{p}(\mathbf{b}) \;\; (k = 0, 1, 2, ..., m), \tag{7.2}$$

where

$$^{k+1}\Delta\mathbf{s} = \int_{\Omega} \mathbf{B}^{\mathrm{t}}(^{k}\mathbf{u}, \mathbf{b})\Delta\boldsymbol{\sigma}(^{k+1}\Delta\mathbf{u}, \mathbf{b})\mathrm{d}\Omega, \tag{7.3}$$

and the displacement is advanced by

$$^{k+1}\mathbf{u} = {}^{k}\mathbf{u} + {}^{k+1}\Delta\mathbf{u} \;\; (k = 0, 1, 2, ..., m). \tag{7.4}$$

In the above, $^{k}\mathbf{u}$ is the vector of nodal displacements at time step k, $^{k+1}\Delta\mathbf{u}$, $^{k+1}\Delta\mathbf{s}$ and $^{k+1}\Delta\mathbf{p}$ are the vectors of incremental nodal displacements, incremental internal force and incremental external load at time step $(k+1)$, respectively.

For linear and path-independent nonlinear problems, the governing equations for deterministic analysis are set up based on either the initial configuration (for linear problems) or the current deformation state (for path-independent nonlinear problems) in the updated Lagrange formulation using the total nodal displacements, which means the perturbation equations can be set up by Taylor series expansion of the total displacements, as reported in [73]. By such problems, the perturbation equations need to be solved only once at the last loading step, independent of the number of the increments taken to achieve this final state of deformation process in the deterministic analysis. For problems with path-dependence, however, in order to be consistent with the incremental scheme employed in the deterministic analysis so as to reveal the path-dependent nature of the response, the perturbation based stochastic analysis should also be formulated in an incremental form [88], as proposed in what follows.

To begin with, the incremental internal force vector ${}^{k+1}\Delta\mathbf{s}$ is expanded about the mean value of the random variables via Taylor series:

$$\begin{aligned} {}^{k+1}\Delta\mathbf{s}({}^{k}\mathbf{u},\, {}^{k+1}\Delta\mathbf{u},\mathbf{b}) &= \Delta\bar{\mathbf{s}} + \sum_{r=1}^{q} \frac{\mathrm{d}({}^{k+1}\Delta\mathbf{s})}{\mathrm{d}b_r}\Delta b_r \\ &\quad + \frac{1}{2}\sum_{r,s=1}^{q} \frac{\mathrm{d}^2({}^{k+1}\Delta\mathbf{s})}{\mathrm{d}b_r\mathrm{d}b_s}\Delta b_r\Delta b_s + ..., \end{aligned} \tag{7.5}$$

where $\Delta b_r = b_r - \bar{b}_r$ denotes the deviation of the rth random vector b_r from the mean $\bar{b}_r$ and the upper bar indicates that the corresponding quantity is evaluated at the mean values of the random parameters.

The differentiation of the incremental internal force is further expressed as

$$\frac{\mathrm{d}({}^{k+1}\Delta\mathbf{s})}{\mathrm{d}\mathbf{b}} = \frac{\partial({}^{k+1}\Delta\mathbf{s})}{\partial({}^{k}\mathbf{u})}\frac{\mathrm{d}({}^{k}\mathbf{u})}{\mathrm{d}\mathbf{b}} + {}^{k+1}\mathbf{K}\frac{\mathrm{d}({}^{k+1}\Delta\mathbf{u})}{\mathrm{d}\mathbf{b}} + \frac{\partial({}^{k+1}\Delta\mathbf{s})}{\partial\mathbf{b}}. \tag{7.6}$$

Here, ${}^{k+1}\mathbf{K}$ is the tangential stiffness matrix and is defined as

$${}^{k+1}\mathbf{K}({}^{k}\mathbf{u}, {}^{k+1}\Delta\mathbf{u},\mathbf{b}) = \frac{\partial({}^{k+1}\Delta\mathbf{s})}{\partial({}^{k+1}\Delta\mathbf{u})}. \tag{7.7}$$

The first term on the right-hand side of Eq. (7.6) represents the incremental internal force variation caused by the changing geometry and is much more difficult to calculate than other terms from a computational point of view. Recalling Eq. (7.3), we see that this term is usually of higher order of the incremental nodal displacements. Therefore it is neglected in this study under the assumption that the incremental internal force change related to the fluctuating geometry is relatively small compared with those caused by the variation of the incremental displacements. Consequently, the total differentiation of the incremental internal force takes place at constant displacement ${}^{k}\mathbf{u}$. Thus we have

$$\frac{\mathrm{d}({}^{k+1}\Delta\mathbf{s})}{\mathrm{d}\mathbf{b}} = {}^{k+1}\mathbf{K}\frac{\mathrm{d}({}^{k+1}\Delta\mathbf{u})}{\mathrm{d}\mathbf{b}} + \frac{\partial({}^{k+1}\Delta\mathbf{s})}{\partial\mathbf{b}}. \tag{7.8}$$

By substituting Eq. (7.8) into Eq. (7.5), we have

$$\begin{aligned} {}^{k+1}\Delta\mathbf{s}({}^{k}\mathbf{u}, {}^{k+1}\Delta\mathbf{u}, \mathbf{b}) \;=\; & {}^{k+1}\Delta\overline{\mathbf{s}} + \sum_{r=1}^{q} \left({}^{k+1}\overline{\mathbf{K}}\,{}^{k+1}\Delta\overline{\mathbf{u}}_{b_r} + {}^{k+1}\,\Delta\overline{\mathbf{s}}_{b_r}\right)\Delta b_r \\ & + \frac{1}{2}\sum_{r,s=1}^{q}\left(\left.\frac{\mathrm{d}({}^{k+1}\mathbf{K})}{\mathrm{d}b_r}\right|_{\bar{\mathbf{b}}} {}^{k+1}\Delta\overline{\mathbf{u}}_{b_s} + {}^{k+1}\,\overline{\mathbf{K}}\,{}^{k+1}\Delta\overline{\mathbf{u}}_{b_r b_s} \right. \\ & \left. + \,{}^{k+1}\overline{\mathbf{K}}_{b_r}\,{}^{k+1}\Delta\overline{\mathbf{u}}_{b_s} + {}^{k+1}\,\Delta\overline{\mathbf{s}}_{b_r b_s} \right)\Delta b_r \Delta b_s + ... \end{aligned} \quad (7.9)$$

Here again, the terms with subscripts b_r and $b_r b_s$ denote first-order derivatives with respect to the r-th random variable and the mixed or second-order partial derivatives with respect to the r-th and the s-th random variables, respectively. As the same notation we use in the previous chapters, an upper bar indicates that the corresponding quantities are evaluated at the mean values of the random input variable $\overline{\mathbf{b}}$.

Analogously the expression for ${}^{k+1}\Delta\mathbf{p}$ is

$$ {}^{k+1}\Delta\mathbf{p} = \Delta\overline{\mathbf{p}} + \sum_{r=1}^{q} {}^{k+1}\Delta\overline{\mathbf{p}}_{b_r}\Delta b_r + \frac{1}{2}\sum_{r,s=1}^{q} {}^{k+1}\Delta\overline{\mathbf{p}}_{b_r b_s}\Delta b_r \Delta b_s + ... \quad (7.10)$$

It is noted that the total derivative of the tangential stiffness matrix ${}^{k+1}\mathbf{K}$ is involved in the Taylor expansion of the internal force vector ${}^{k+1}\Delta\mathbf{s}$ since ${}^{k+1}\mathbf{K}({}^{k}\mathbf{u},{}^{k+1}\,\Delta\mathbf{u}, \mathbf{b})$ is determined by both ${}^{k+1}\Delta\mathbf{u}$ and $\mathbf{b}$ in nonlinear problems and this term accounts for the dependence of ${}^{k+1}\mathbf{K}$ on both the change in structural deformation and the other random variables. Neglecting the dependence of the tangential matrix upon the structural deformation as in [73] when deriving the perturbation equations for the nonlinear problems may result in loss of accuracy in geometrical as well as in material nonlinear problems.

Substituting Eqs. (7.9) and (7.10) into Eq. (7.2) and equating the terms with the same orders, one obtains the zeroth-, first- and second-order perturbed equations expressed as:

Zeroth-order equation:

$$^{k+1}\Delta\mathbf{s}(^{k+1}\Delta\overline{\mathbf{u}},\overline{\mathbf{b}}) =^{k+1} \Delta\overline{\mathbf{p}}, \tag{7.11}$$

First-order equations:

$$^{k+1}\overline{\mathbf{K}}\,^{k+1}\Delta\overline{\mathbf{u}}_{b_r} =^{k+1} \Delta\overline{\mathbf{p}}_{b_r} -^{k+1} \Delta\overline{\mathbf{s}}_{b_r} \ \ (r = 1, 2, ..., q), \tag{7.12}$$

Second-order equation:

$$\begin{aligned} ^{k+1}\overline{\mathbf{K}}\,^{k+1}\Delta\overline{\mathbf{u}}_2 &= \frac{1}{2}\sum_{r,s=1}^{q}\left(^{k+1}\Delta\overline{\mathbf{p}}_{b_r b_s} - \left.\frac{\mathrm{d}(^{k+1}\overline{\mathbf{K}})}{\mathrm{d}b_r}\right|_{\overline{\mathbf{b}}}\,^{k+1}\Delta\overline{\mathbf{u}}_{b_s}\right. \\ &\quad - \left.^{k+1}\overline{\mathbf{K}}_{b_r}\,^{k+1}\Delta\overline{\mathbf{u}}_{b_s} -^{k+1} \Delta\overline{\mathbf{s}}_{b_r b_s}\right)\mathrm{Cov}(b_r, b_s). \end{aligned} \tag{7.13}$$

where $^{k+1}\Delta\overline{\mathbf{u}}_2$ is the second order correction to the mean incremental displacement defined by

$$^{k+1}\Delta\overline{\mathbf{u}}_2 \equiv \frac{1}{2}\sum_{r,s=1}^{q}\,^{k+1}\Delta\overline{\mathbf{u}}_{b_r b_s}\mathrm{Cov}(b_r, b_s). \tag{7.14}$$

In Eqs. (7.12)–(7.13), the partial derivatives of $^{k+1}\Delta\mathbf{p}$, $^{k+1}\mathbf{K}$ and $^{k+1}\Delta\mathbf{s}$ with respect to the random vector $\mathbf{b}$ can be determined analytically or by finite differences on the element level. The total derivatives of the tangential stiffness matrix with respect to the random variables are evaluated with the finite difference approximation, where a sensitivity-based first-order estimation of the perturbed displacement vector is involved:

$$\begin{aligned} \left.\frac{\mathrm{d}(^{k+1}\overline{\mathbf{K}})}{\mathrm{d}b_r}\right|_{\overline{\mathbf{b}}} &\approx \frac{\mathbf{K}\left(^{k+1}\Delta\mathbf{u}(\overline{\mathbf{b}}+\delta b_r\mathbf{e}_r), \overline{\mathbf{b}}+\delta b_r\mathbf{e}_r\right) - \mathbf{K}\left(^{k+1}\Delta\overline{\mathbf{u}},\overline{\mathbf{b}}\right)}{\delta b_r} \\ &\approx \frac{\mathbf{K}(^{k+1}\Delta\overline{\mathbf{u}} + \,^{(k+1)}\Delta\overline{\mathbf{u}}_{b_r}\delta b_r, \overline{\mathbf{b}}+\delta b_r\mathbf{e}_r) - \mathbf{K}(^{k+1}\Delta\overline{\mathbf{u}},\overline{\mathbf{b}})}{\delta b_r}(r = 1, 2, ..., q), \end{aligned} \tag{7.15}$$

where δb_r is a small perturbation of the rth random variable and $\mathbf{e}_r = \{0...1...0\}$ denotes the incidence vector with the rth component being 1 and the other components zero.

Once Eqs. (7.11)-(7.13) are solved, one obtains the first-order and the second-order approximate mean values of the incremental displacements, as shown in Eqs. (7.16) and (7.17), respectively:

$$\mathrm{E}_1(^{k+1}\Delta\mathbf{u}) =^{k+1} \Delta\overline{\mathbf{u}}, \tag{7.16}$$

$$\mathrm{E}_2(^{k+1}\Delta\mathbf{u}) =^{k+1} \Delta\overline{\mathbf{u}} +^{k+1} \Delta\overline{\mathbf{u}}_2. \tag{7.17}$$

The mean value of the total displacements at time step $(k+1)$ reads:

$$\mathrm{E}(^{k+1}\mathbf{u}) = \mathrm{E}(^{k}\mathbf{u}) + \mathrm{E}(^{k+1}\Delta\mathbf{u}). \tag{7.18}$$

The first-order approximation for the covariance/ variance of the nodal displacements can also be obtained using the solutions of the perturbation equations. Particularly, the first-order approximate variance of the ith total displacements at time step $k+1$ is

$$\mathrm{Var}(^{k+1}u^i) = \mathrm{Var}(^{k}u^i) + \sum_{r,s=1}^{q} (^{k+1}\Delta\overline{u}^i{}_{b_r}\, {}^{k+1}\Delta\overline{u}^i{}_{b_s} + 2^k\overline{u}^i_{b_r}\, {}^{k+1}\Delta\overline{u}^i{}_{b_s})\mathrm{Cov}(b_r, b_s). \tag{7.19}$$

Using the above expressions as in Eqs. (7.18) and (7.19), the mean value and the variance of the total nodal displacements $\mathbf{u}$ at any stage can be evaluated in a step-wise procedure.

In order to reduce the computational efforts caused by the double summations in evaluating the terms on the right hand side of the second-order equation, the original random variables $\mathbf{b}$ can be transformed into a set of uncorrelated random variables $\mathbf{c}$ through the principal component transformation, as addressed in the case of linear structures.

As shown above, for a path-dependent nonlinear system, the response moments must be determined by an incremental procedure in consistency with the path-following strategy employed in the deterministic finite element analysis. However, no extra computational efforts are involved in additionally decomposing the stiffness matrix for the solution of the perturbation equations in each loading step. Additionally, the perturbation equations are solved after the deterministic response analysis for each loading step has converged and therefore do not require any convergence iterations. In this sense, the perturbation based stochastic finite element analysis retains its advantage to Monte Carlo simulation techniques in terms of computational efficiency.

7.2 Response moment sensitivity analysis

Sensitivity of displacement response moments

To begin with, the sensitivity analysis of the mean and the variance/ covariance of nodal displacements with respect to design variables is first considered.

Taking the lth design variable d_l as the independent variable and differentiating the left-hand side of Eq. (7.11) with respect to d_l yields

$$\frac{\partial({}^{k+1}\Delta\overline{\mathbf{s}})}{\partial d_l} = {}^{k+1}\,\overline{\mathbf{K}}\frac{\partial({}^{k+1}\Delta\overline{\mathbf{u}})}{\partial d_l} + \left.\frac{\partial({}^{k+1}\Delta\overline{\mathbf{s}})}{\partial d_l}\right|_{{}^{k+1}\Delta\overline{\mathbf{u}}=\mathrm{const}}, \tag{7.20}$$

and

$${}^{k+1}\overline{\mathbf{K}}\,{}^{k+1}\Delta\overline{\mathbf{u}}_{,d_l} = {}^{k+1}\Delta\overline{\mathbf{p}}_{,d_l} - {}^{k+1}\Delta\overline{\mathbf{s}}_{,d_l}, \qquad (l = 1, 2, ..., n). \tag{7.21}$$

Analogously from Eq. (7.12),

$$\begin{aligned} {}^{k+1}\overline{\mathbf{K}}\,{}^{k+1}\Delta\overline{\mathbf{u}}_{b_r,d_l} \;=\;& {}^{k+1}\Delta\overline{\mathbf{p}}_{b_r,d_l} - {}^{k+1}\,\Delta\overline{\mathbf{s}}_{b_r,d_l} - {}^{k+1}\,\overline{\mathbf{K}}_{b_r}\,{}^{k+1}\Delta\overline{\mathbf{u}}_{,d_l} \\ & - \frac{\mathrm{d}({}^{k+1}\overline{\mathbf{K}})}{\mathrm{d}d_l}{}^{k+1}\Delta\overline{\mathbf{u}}_{b_r} \qquad (r = 1, 2, ..., q;\; l = 1, 2, ..., n). \end{aligned} \tag{7.22}$$

The subscript following by a comma denotes partial differentiation with respect to the design variable as in

$${}^{k+1}\Delta\overline{\mathbf{u}}_{,d_l} \equiv \frac{\partial({}^{k+1}\Delta\overline{\mathbf{u}})}{\partial d_l}. \tag{7.23}$$

Similarly as in Eq. (7.15), the total derivative in Eq. (7.22) can be calculated by finite differences based on the first-order approximation of nodal displacements.

The first-order approximate sensitivities of the mean value and the variance of total displacements are then expressed as

$$\frac{\partial \mathrm{E}({}^{k+1}\mathbf{u})}{\partial d_l} = {}^k\,\overline{\mathbf{u}}_{,d_l} + {}^{k+1}\,\Delta\overline{\mathbf{u}}_{,d_l}\,, \tag{7.24}$$

and

$$\begin{aligned}\frac{\partial \mathrm{Var}({}^{k+1}u^i)}{\partial d_l} = & \frac{\partial \mathrm{Var}({}^{k}u^i)}{\partial d_l} + 2\sum_{r,s=1}^{q}\big({}^{k+1}\Delta\overline{u}^i_{b_r,d_l}\,{}^{k+1}\Delta\overline{u}^i_{b_s} \\ & + {}^{k}\overline{u}^i_{b_r,d_l}\,{}^{k+1}\Delta\overline{u}^i_{b_s} + {}^{k}\,\overline{u}^i_{b_r}\,{}^{k+1}\Delta\overline{u}^i_{b_s,d_l}\big)\,\mathrm{Cov}(b_r,b_s) \\ & + \sum_{r,s=1}^{q}\big({}^{k+1}\Delta\overline{u}^i_{b_r}\Delta\overline{u}^i_{b_s} + 2{}^{k}\overline{u}^i_{b_r}\,{}^{k+1}\Delta\overline{u}^i_{b_s}\big)\,\frac{\partial \mathrm{Cov}(b_r,b_s)}{\partial d_l}\,,\end{aligned} \tag{7.25}$$

where the last term in Eq. (7.25) results from the dependence of the parameter variability upon the design variable.

Evaluation of moments and their sensitivities for a generalized performance function

Consider a structural performance functional f defined as an explicit function of the nodal displacements $\mathbf{u}$, random variables $\mathbf{b}$ and the design variables $\mathbf{d}$:

$$f = f(\mathbf{u}, \mathbf{b}, \mathbf{d})\,. \tag{7.26}$$

Expanding the functional f in a Taylor series about $\bar{\mathbf{b}}$, the mean value of the random variables, and truncating the series at the linear terms, one obtains the first-order approximate mean and variance of f, as

$$\mathrm{E}(f) \approx f(\overline{\mathbf{u}}, \overline{\mathbf{b}}, \mathbf{d})\,, \tag{7.27}$$

$$\mathrm{Var}(f) = \sum_{r,s=1}^{q} \left(\left.\frac{\partial f}{\partial \mathbf{u}}\right|_{\bar{\mathbf{b}}} \bar{\mathbf{u}}_{b_r} + \bar{f}_{b_r} \right) \left(\left.\frac{\partial f}{\partial \mathbf{u}}\right|_{\bar{\mathbf{b}}} \bar{\mathbf{u}}_{b_s} + \bar{f}_{b_s} \right) \mathrm{Cov}(b_r, b_s)\,. \tag{7.28}$$

By including the second-order terms in the Taylor series, the second-order approximate mean of f can be given by the expectation

$$\mathrm{E}(f) \;=\; \overline{f} + \left.\frac{\partial f}{\partial \mathbf{u}}\right|_{\bar{\mathbf{b}}} \overline{\mathbf{u}}_2 + \frac{1}{2}\sum_{r,s=1}^{q} \left(\overline{\mathbf{u}}^{\mathrm{t}}_{b_r} \overline{\mathbf{H}}_f(\mathbf{u}) \overline{\mathbf{u}}_{b_s} + 2 \left.\frac{\partial f_{b_r}}{\partial \mathbf{u}}\right|_{\bar{\mathbf{b}}} \overline{\mathbf{u}}_{b_s} + \overline{f}_{b_r b_s} \right) \mathrm{Cov}(b_r, b_s), \tag{7.29}$$

where the vector $\overline{\mathbf{u}}_2$ comprises the sum over the incremental steps of the second order corrections to the mean incremental displacements, $\mathbf{H}_f(\mathbf{u})$ is the Hessian matrix of f with respect to $\mathbf{u}$. The derivatives of f can be easily obtained since f is an explicit function of displacement and random parameters.

Differentiating Eqs. (7.27) and (7.28) with respect to the design variable d_l, one obtains the first-order approximate sensitivity of the mean and variance of the performance function f, respectively

$$\frac{\partial \mathrm{E}(f)}{\partial d_l} \approx \left.\frac{\partial f}{\partial \mathbf{u}}\right|_{\bar{\mathbf{b}}} \bar{\mathbf{u}}_{,d_l} + \bar{f}_{,d_l}, \tag{7.30}$$

and

$$\begin{aligned}\frac{\partial \mathrm{Var}(f)}{\partial d_l} \;\approx\; & \sum_{r,s=1}^{q} 2 \left(\left.\frac{\partial f}{\partial \mathbf{u}}\right|_{\bar{\mathbf{b}}} \overline{\mathbf{u}}_{b_r} + \overline{f}_{b_r} \right) \left(\overline{\mathbf{u}}^{\mathrm{t}}_{,d_l} \overline{\mathbf{H}}_f(\mathbf{u}) \overline{\mathbf{u}}_{b_s} + \left.\frac{\partial f_{,d_l}}{\partial \mathbf{u}}\right|_{\bar{\mathbf{b}}} \overline{\mathbf{u}}_{b_s} \right. \\ & \left. + \left.\frac{\partial f}{\partial \mathbf{u}}\right|_{\bar{\mathbf{b}}} \overline{\mathbf{u}}_{b_s,d_l} + \left.\frac{\partial f_{b_s}}{\partial \mathbf{u}}\right|_{\bar{\mathbf{b}}} \overline{\mathbf{u}}_{,d_l} + \bar{f}_{b_s,d_l} \right) \mathrm{Cov}(b_r, b_s) \\ & + \sum_{r,s=1}^{q} \left(\left.\frac{\partial f}{\partial \mathbf{u}}\right|_{\bar{\mathbf{b}}} \overline{\mathbf{u}}_{b_r} + \bar{f}_{b_r} \right) \left(\left.\frac{\partial f}{\partial \mathbf{u}}\right|_{\bar{\mathbf{b}}} \overline{\mathbf{u}}_{b_s} + \bar{f}_{b_s} \right) \frac{\partial \mathrm{Cov}(b_r, b_s)}{\partial d_l}. \end{aligned} \tag{7.31}$$

Similarly as in the case of response moment analysis, the computational efforts involved in sensitivity analysis of response moment can be also reduced notably by using transformed uncorrelated variables.

7.3 Numerical examples

Stochastic analysis and robust optimum design of a planar ten-bar truss structure with material and geometrical nonlinearity

The method has been tested on the exemplary case of a well-known planar ten-bar cantilever truss structure shown in Fig. 7.1. Two steadily increasing forces of magnitude p applied vertically at nodes number 3 and number 5 induce large displacements in the truss. The material is assumed to be elastic–plastic with the yield stress being 250.0 and the stress–strain relationship in the linear elastic and the plastic hardening range reading

$$\mathrm{d}\sigma = \begin{cases} 1.0 \times 10^4 \mathrm{d}\varepsilon & (|\varepsilon| \leq 0.025) \\ (250.0/\varepsilon)\mathrm{d}\varepsilon & (|\varepsilon| > 0.025). \end{cases}$$

The mass density of the material is $\rho = 1.0$.

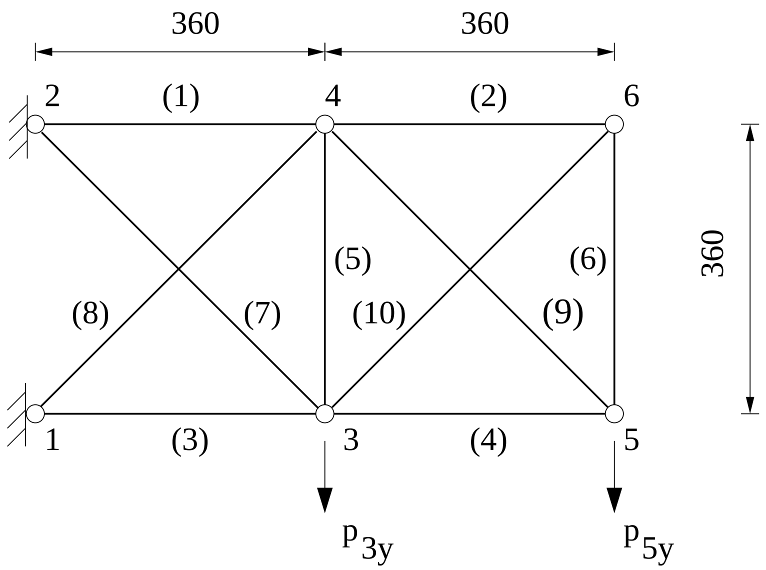

Figure 7.1: The planar ten-bar truss

The horizontal position of node number 4, denoted by x_4, the elastic moduli E_{I} (for bars 1,2), E_{II} (for bars 3,4), E_{III} (for bars 5,6), E_{IV} (for bars 7,8,9,10) and the cross-section areas of the bar members are considered as random variables with the following mean values, standard deviation or coefficient of variation (COV): $\mathrm{E}(x_4) = 360.0$, $\sigma(x_4) = 20.0$, $\mathrm{E}(E_{\mathrm{I}}) = \mathrm{E}(E_{\mathrm{II}}) = \mathrm{E}(E_{\mathrm{III}}) = \mathrm{E}(E_{\mathrm{IV}}) = 1.0 \times 10^4$, $\sigma(E_{\mathrm{I}}) = \sigma(E_{\mathrm{II}}) = \sigma(E_{\mathrm{III}}) = 3.0 \times 10^2$, $\sigma(E_{\mathrm{IV}}) = 1.0 \times 10^3$, $\mathrm{E}(A_i) = 5.0$ ($i = 1, 2, ...10$), $\mathrm{COV}(A_i) = 0.05$, ($i = 1, 2, ..., 6$), $\mathrm{COV}(A_i) = 0.1$ ($i = 7, 8, ..., 10$).

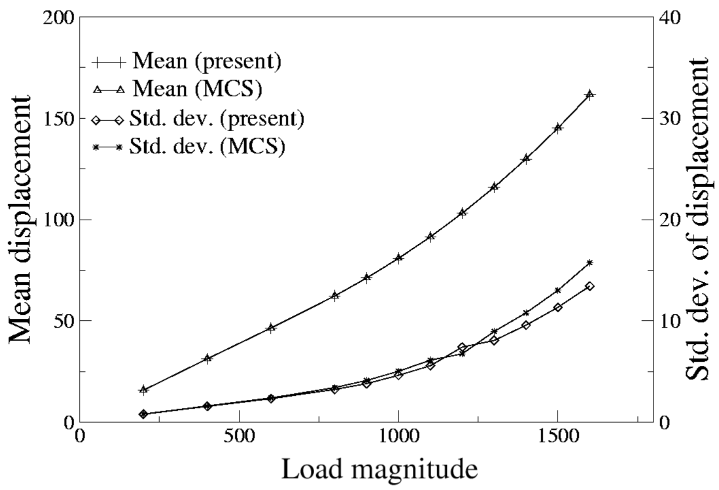

Figure 7.2: The mean and the standard deviation of the nodal displacement v_5

To examine the accuracy of the stochastic analysis method set forth, the results for the second-order means and first-order standard deviations of the vertical nodal displacement v_5 and maximum member stress for various values of p are shown in Fig. 7.2 and Fig. 7.3, where 10 equidistant incremental loading steps are considered. For comparison, results from synthetic Monte-Carlo sampling with 3000 realizations are also presented. It is seen from the figures that the numerical results obtained with the present method are in good agreement with those of the Monte-Carlo simulations. The deviations in the variance may arise because the present approach neglects the accumulated scatter in the geometry.

The results for the sensitivity of mean value and standard deviation of the quantity v_5 with respect to the cross-section area of bar number 5 are shown in Fig. 7.4. For comparison, the results obtained with finite difference approximations, where Monte-Carlo sampling with 3000 realizations is used for stochastic analysis, are also

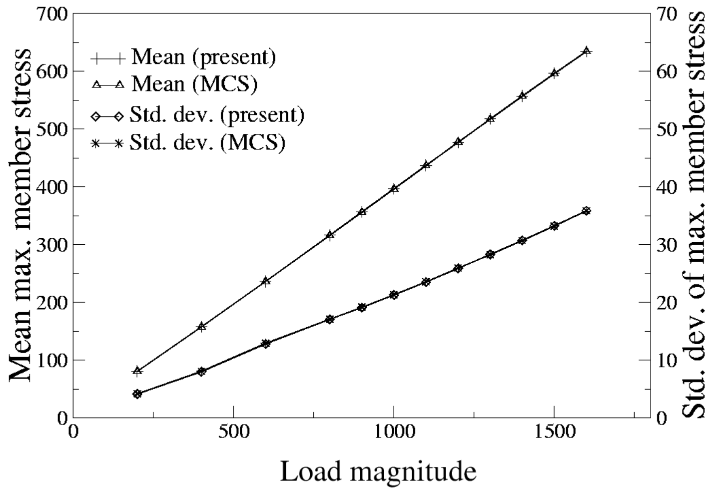

Figure 7.3: The mean and the standard deviation of the maximum member stress

shown in Fig. 7.4. As seen from Fig. 7.4, though the disparity of displacement sensitivity results between the present method and Monte-Carlo simulations increases to some extent as higher external loads are applied and much stronger nonlinearities are induced, the results still agree well with those obtained with Monte-Carlo simulations. This indicates that the proposed method works better when moderate, respectively structural nonlinearities are present.

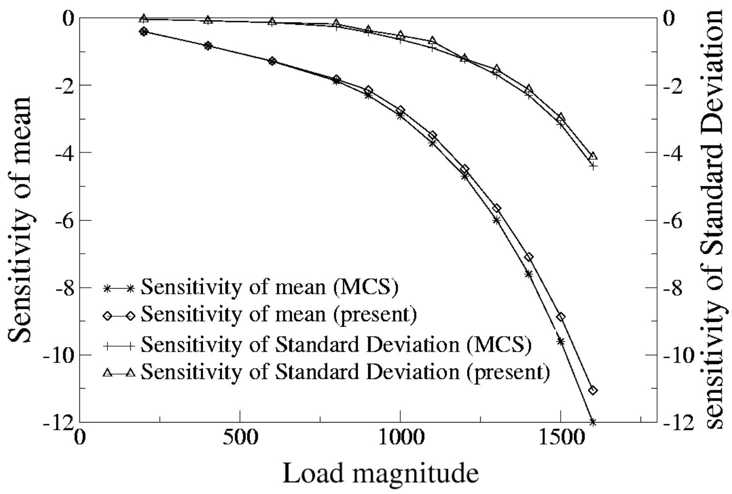

Figure 7.4: Sensitivity of mean and standard deviation of displacement v_5

The design objective in this example problem is to minimize the vertical displacement v_5 at node number 5, under the loading condition $p = 1000.0$. A structural weight constraint $\mathrm{E}(w) \leq 1.8 \times 10^4$ and member stress constraints $(\mathrm{E}(|\sigma_i|) - 400)/\sigma(\sigma_i) \leq -3$ $(i = 1, 2, ..., 10)$ are imposed in this problem. The design variables are the mean cross-section areas of the bars with lower and upper bound limits $0.05 \leq A_i \leq 10.0$ $(i = 1, 2, ..., 10)$.

Table 7.1: Optimal solutions for the ten-bar truss

Des. var.	Init.	(Determ.)	$\alpha = 0$	$\alpha = .25$	$\alpha = .5$	$\alpha = .75$	$\alpha = 1.0$
A_1	4.00	(9.14)	9.54	8.34	7.15	6.73	6.19
A_2	4.00	(0.05)	0.05	0.05	0.58	0.60	0.81
A_3	4.00	(8.83)	8.02	7.83	7.98	7.89	7.76
A_4	4.00	(6.05)	4.92	4.82	4.21	3.61	3.13
A_5	5.00	(0.05)	0.31	0.27	0.05	0.05	0.05
A_6	5.00	(0.05)	0.05	0.05	0.54	0.61	0.78
A_7	4.00	(4.07)	4.80	4.93	5.54	5.65	5.75
A_8	4.00	(7.61)	6.90	7.30	6.85	7.26	7.21
A_9	4.00	(6.54)	7.42	7.96	7.46	7.51	7.45
A_{10}	4.00	(0.05)	0.05	0.06	1.01	1.15	1.70
$\mathrm{E}(f)$	92.35	(56.30)	59.30	59.62	61.68	62.66	64.51
$\sigma(f)$	6.13	(3.53)	3.76	3.55	3.38	3.30	3.27
$\mathrm{E}(w)$ $\times 10^4$	2.16	(1.80)	1.80	1.80	1.80	1.80	1.80

The optimal solution obtained with different weighting factors α in the design desirability function are shown in Table 7.1, where $\alpha = 0$ corresponds to the stochastic *mean value minimization* and $\alpha = 1.0$ to the purely *variance minimization* problem. For the sake of comparison, the deterministic optimum (nominal values, no randomness) is also presented, but it results in a violation of the stress constraints (for instance, the mean and standard deviation of the member stress for the 7th bar are 375.3 and 40.0, respectively, such that (375.3-400)/40.0 > -3). The stochastic mean value minimization design exhibits a standard deviation of the objective function $\sigma(f) = 3.76$, which is reduced to $\sigma(f) = 3.27$ for the most robust design ($\alpha = 1$). At the same time, the mean value increases from $\mathrm{E}(f) = 59.30$ to $\mathrm{E}(f) = 64.51$, respectively. By setting different values of the weighting factor α in the desirability function, Pareto optima with a trade-off between the two conflicting sub-objectives are obtained. The results show that robust design ($\alpha > 0$) indeed diminishes the variability of the demanded structural performance. It is worth noting that the optimal solution obtained in the robust design may suggest a different topology of the truss than the optimum for mean response ($\alpha = 0$) if the bars assuming minor values of cross-section area are removed. This underlines the fact that additional members help improve the structural robustness.

Robust optimum design of an elastoplastic 25-bar space truss structure under non-monotonic loading

The nodal displacement minimization problem of a elastoplastic 25-bar truss, as shown in Fig. 6.2 is considered here. The design variables are bar cross-section areas. Using the design variable linking technique, six design variables are defined. The nodal coordinates and the member grouping information are given in Tables 6.3 and 6.5, respectively. The material in the bars is assumed to be elastoplastic and isotropic hardening, with the stress–strain relationship for the elastic and hardening deformation as represented in Fig. 7.5. Following the loading path depicted in Fig. 7.6, four nodal forces with magnitude $p_{1x} = p_{2x} = 750$, $p_{1y} = p_{2y} = 3000$ are ultimately imposed at nodes number 1 and number 2. Additionally, forces with random values are applied to the nodes number 3 and 6 along the x-direction in the same manner.

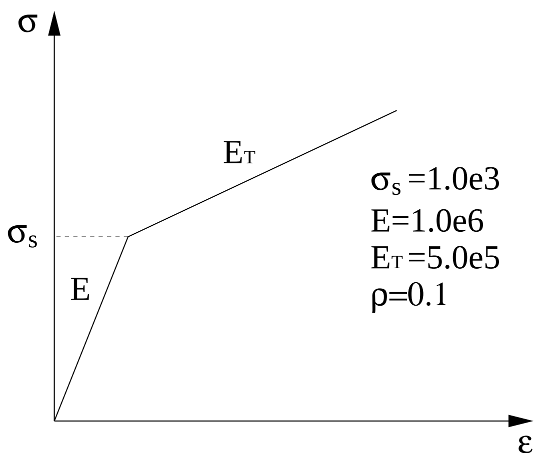

Figure 7.5: The elastoplastic material property

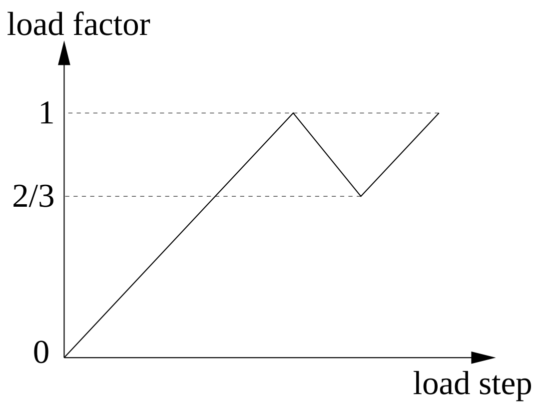

Figure 7.6: The loading history

Table 7.2: Random variables for the 25-bar truss

No.	Variable	Mean	Standard deviation	COV
1-5	$E_{\mathrm{I}}, E_{\mathrm{II}}, E_{\mathrm{IV}}, E_{\mathrm{V}}$	1.0×10^6	2.0×10^4	
6	$E_{\mathrm{III}}, E_{\mathrm{VI}}$	1.0×10^6	1.5×10^5	
7	p_{3x}	750	75	
8	p_{6x}	750	75	
9-14	$A_{\mathrm{I}} \sim A_{\mathrm{VI}}$			0.05

In this example, the nodal forces applied at the nodes number 3 and 6, the elastic moduli and the cross-section areas for the grouped bars are considered as random variables with mean values and standard deviations resp. coefficients of variation as shown in Table 7.2. In the design problem, the nodal displacement of the first node along $x-$direction u_1 is to be minimized and the structural weight constraint $\mathrm{E}(w) \leq 850$, the nodal displacement constraints on the second node $\mathrm{E}(u_2) \leq 0.4$ and $\mathrm{E}(v_2) \leq 0.4$, the lower and upper bounds of design variables $0.05 \leq A_j \leq 10.0\,(j =$ I,II,...,VI) are to be observed.

The deterministic optimum and the optimal solutions for different values of the weighting factor α are listed in Table 7.3. The mean values and the standard deviations of the objective function for the Pareto optima obtained are depicted in Fig. 7.7. Compared with the mean value minimization solution ($\alpha = 0$), the standard deviation of the structural compliance is notably decreased in the robust solutions ($\alpha > 0$), which means a remarkable improvement in robustness of the design.

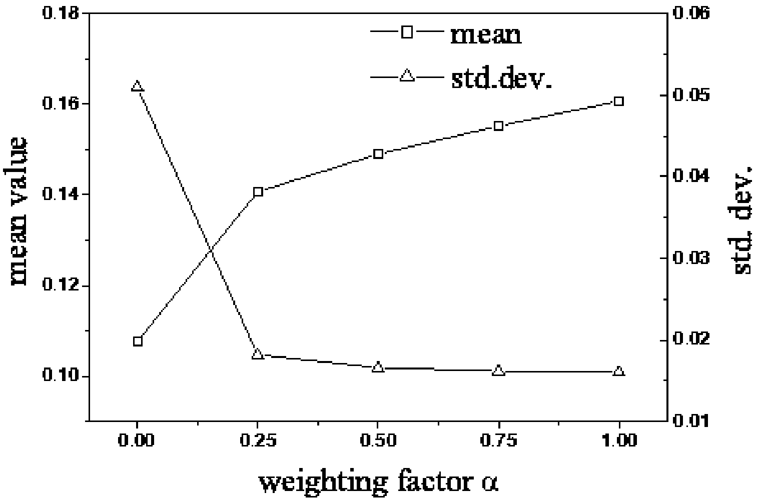

Figure 7.7: Objective function values of the Pareto optima for the 25-bar truss

Table 7.3: Optimal solutions for the 25-bar truss

Des. var.	Init.	(Determ.)	$\alpha = 0$	$\alpha = .25$	$\alpha = .5$	$\alpha = .75$	$\alpha = 1$
A_{I}	2.000	(0.050)	0.050	0.539	0.915	1.050	1.108
A_{II}	2.000	(4.706)	4.650	4.168	4.042	3.841	3.648
A_{III}	2.000	(4.090)	4.161	3.691	3.708	3.608	3.558
A_{IV}	2.000	(0.050)	0.050	0.058	0.091	0.177	0.141
A_{V}	3.000	(1.435)	1.437	1.506	1.524	1.610	1.694
A_{VI}	3.000	(4.109)	4.108	4.698	4.687	4.697	4.674
$\mathrm{E}(f)\,(\times 10^{-1})$	4.254	(1.076)	1.076	1.407	1.490	1.552	1.607
$\sigma(f)\,(\times 10^{-1})$	0.403	(0.509)	0.510	0.182	0.166	0.162	0.161

Robust optimum design of an antenna space structure with large deformation

The algorithm is applied to the design optimization problem of the antenna structure as shown in Fig. 6.6 where geometrical nonlinearity resulting from large deformation is encountered. The structure is subjected to quasi-static wind loads inducing large nodal displacements, which cause the loss of shape accuracy as well as pointing accuracy of the reflection surface. The finite element model of the antenna consists of a complex truss structure extending in three-dimensional space, which is covered by a membrane skin, as depicted in Fig. 6.6. The uncertain parameters having major effects are considered as uncorrelated random variables, among which are five random variables for the elastic moduli of the grouped bar members, one for the elastic modulus of the skin material, and four for the spatial distribution of the skin thickness. The mean values of the elastic moduli are 7.1×10^{10} N/m^2 and the coefficients of variation are 0.1 for all the random quantities. The design variables considered are the skin thickness t and the cross-section areas A_1, A_2, A_3, which correspond to the bars supporting the skin along perimetric, radial and skew direction, respectively. The design objective is to minimize the maximum displacement in the radial direction at the upper edge of the antenna structure under the constraint of total structural weight $\mathrm{E}(w) \leq 350.0$ kg. The optimum solutions corresponding to different values of the weighting factor α are listed in Table 7.4. Compared with the initial design and the mean value minimization design ($\alpha = 0$), a more robust design is obtained when the weighting factor α is given the value of 0.5 or 1.0, where the standard variation of the concerned displacement is remarkably reduced.

Table 7.4: Optimal solutions for the antenna structure

Des. var.	Lower	Upper	Init.	$\alpha = 0.0$	$\alpha = 0.5$	$\alpha = 1.0$
A_1 ($\times 10^{-6}$m^2)	10.00	25.00	15.00	13.30	25.00	25.00
A_2 ($\times 10^{-6}$m^2)	10.00	25.00	15.00	13.62	18.47	19.15
A_3 ($\times 10^{-6}$m^2)	10.00	25.00	15.00	12.53	18.63	18.08
t ($\times 10^{-3}$m)	2.00	3.50	2.80	3.02	2.68	2.65
$\mathrm{E}(w)$(kg)	/	350.0	331.5	350.0	350.0	350.0
$\mathrm{E}(f)$ ($\times 10^{-3}$m)	/	/	102.7	87.28	90.56	91.27
$\sigma(f)$ ($\times 10^{-3}$m)	/	/	7.4	6.9	5.9	5.8

7.4 Discussions and remarks

It can be expected that the structural performance variability may become more significant for structures exhibiting nonlinear properties. Therefore, it might be of particular importance to take the design robustness into consideration in the optimization of nonlinear structures. In this chapter, the basic idea of the robust design method presented in the previous chapter is extended to the path-dependent nonlinear problems.

The nature of path-dependent response implies incrementation of the loading process. The proposed procedure for stochastic finite element analysis and sensitivity analysis is consistent with the incremental path-following strategy employed in the deterministic analysis. The incremental scheme, however, raises the issue of stability and accuracy. The method employed here makes use of explicit integration, which is particularly sensitive to the step size. Implicit integration, known to be less sensitive, must be employed in association with iterative solution techniques that complicate the computational algorithm and the theoretical exposition [89]. It should be of interest to extend step size considerations familiar from deterministic response analysis to the solution of mean and variance, which has not been the objective of the present study, however.

Incrementation enters the algorithms also at a different point, since the derivatives of the tangent stiffness matrix with respect to the random variables are computed by a finite difference approximation where analytical computing schemes are not available. In order to ensure accuracy in the computational examples, the quality of the approximation has bee studied for a varying increment size of the random variables. In this connection, the step sizes adopted in the finite difference approximations appeared not to have significant influence on both the response and the sensitivity analysis for a reasonable range of values. This statement refers to the range from 0.1% to 1% of the design variable intervals resp. the standard deviations of random parameters.

Chapter 8

Robust design of inelastic deformation processes

Concurrent engineering characterized by an integration between design and manufacturing raises the need for studying process robust design. In this chapter, the perturbation-based stochastic finite element analysis and the robust design optimization of deformation processes of inelastic solids are developed. The proposed method is applied to the design of an extrusion die for robustness with respect to friction variability, and to a workpiece preform design problem.

8.1 Introduction

In a number of industrial forming processes, particularly in bulk metal forming operations such as hot extrusion and forging, elasticity has not an appreciable effect on the deformation. Under this aspect an elastic material constituent can be neglected, and the deformation process is modeled as inelastic in the numerical simulation based on the viscous, viscoplastic or plastic constitutive approach to the material behaviour. Elasticity may nevertheless be of importance in determining the stress state in the solid [90].

Deformation processes often involve random uncertainties in several parameters, such as loading conditions, material properties, boundary conditions, and geometrical dimensions. For instance, friction is one significant source of uncertainty in the modeling of metal forming processes. The actual friction coefficient frequently exhibits large scatter about the nominal value due to variation of the actual manufacturing conditions such as the surface roughness and the lubricant condition. The deformation process in concern may reflect the variability of the parameters to an extent inducing undesirable effects on the product quality. The concept of process robust design, aims at reducing such a variability without eliminating the source of uncertainties by seeking a design that is less sensitive to the scatter of the system parameters.

Perturbation based stochastic finite element analysis has been extended recently to the variability analysis of forming processes. Sluzalec [91], and Grzywinski and Sluzalec [92] presented stochastic finite element analysis of rigid-viscoplastic and rigid-thermo-viscoplastic deformation. The authors adopt the second-order perturbation technique for the incorporation of system uncertainties into the finite element equations. However, the perturbation equations are derived based on linearized matrix expressions in which the implicit dependence of the system matrix upon the velocity field is neglected. Doltsinis [89] presented a theoretical formulation of perturbation based stochastic analysis for deformation processes of viscous solids. Thereby, both the geometry and other random variables at the current instant are considered as random input, which enables the formalism to account consistently for random variables evolving during the course of the deformation.

In engineering practice, a variety of requirements may be imposed on the design of deformation processes of solids. For example, an important issue in the design of an extrusion die is the pressure distribution in the workpiece material. In a different task, the preform design, the initial shape of the workpiece material is to be determined in such a way that a final product with the desired material state and geometry is achieved. Conventional process design techniques usually employ trial-and-error procedures or approaches based on the Design of Experiments (DOE), such as Taguchi's robust design methodology. The developed state of computer process simulation and of engineering optimization, enables cost effective conception of industrial forming processes by computer aided design.

In the literature, much work is reported on the optimal design of forming processes, but rarely addressing non-deterministic optimization. Studies on process design in metal forming under deterministic assumptions can be found in the papers by Byon and Hwang [93], Badrinarayanan and Zabaras [94], Antonio et al. [95], Doltsinis and Rodic [30]. Non-deterministic design optimization has been employed by Kok and Stander [96] for the optimal design of a sheet metal forming process.

In the present study, the perturbation equations for the first-order approximate mean and variance of the process state variables (velocity and geometry) are presented on full account of the non-linearity of the problem, for both steady-state and non-stationary conditions [97]. In the latter problems, an iteration scheme based on the secant operator is given for the solution of the perturbation equations. The robust design of the forming process is stated as a multi-criteria optimal design problem and is solved using optimization techniques in conjunction with the stochastic moment analysis. To illustrate the applicability of the proposed technique, two numerical examples of robust design in industrial forming processes are given, one regarding the die design in steady-state extrusion, and the other referring to a preform design problem.

8.2 Quasi-static deformation of inelastic solids

8.2.1 Constitutive law

For an isotropic inelastic material the constitutive equation relating the deviatoric stress $\sigma_{ij}^{'}$ and deformation rate e_{ij}' is

$$\sigma_{ij}' = 2\mu e_{ij}', \tag{8.1}$$

where $\mu(\bar{e})$, the viscosity coefficient, is stated as a function of the equivalent deformation rate

$$\bar{e} = \left(\frac{2}{3} e_{ij}' e_{ij}'\right)^{\frac{1}{2}}. \tag{8.2}$$

Equation (8.1) formally covers rigid-plastic solids as well in which elastic effects are discarded. In such a case the coefficient μ is obtained as

$$\mu = \frac{\sigma_{\mathrm{f}}(\bar{\varepsilon})}{3\bar{e}}. \tag{8.3}$$

In the above, σ_{f} denotes the flow stress of the material as a function of the accumulated equivalent strain

$$\bar{\varepsilon} = \int_0^t \bar{e} \mathrm{d}t. \tag{8.4}$$

For rigid-viscoplastic materials the flow stress in Eq. (8.3) obeys a relationship of the form $\sigma_{\mathrm{f}}(\bar{\varepsilon}, \bar{e})$ that accounts for deformation rate effects in addition to strain hardening [98].

The complete stress reads

$$\sigma_{ij} = \sigma'_{ij} + \sigma_{\mathrm{H}}\delta_{ij}, \tag{8.5}$$

where σ_{H}, the mean normal stress, defines the hydrostatic part and δ_{ij} is the Kronecker delta.

The deformation rate

$$e_{ij} = e'_{ij} + e_{\mathrm{V}}\delta_{ij}, \tag{8.6}$$

is assumed isochoric, such that the volumetric part

$$3e_{\mathrm{V}} = e_{ii} \tag{8.7}$$

strictly vanishes. Here the Einstein convention of summing over the repeated indices is used.

In a penalty approach to incompressibility the volumetric deformation rate supplies the hydrostatic stress as

$$\sigma_{\mathrm{H}} = 3(\lambda_{\mathrm{V}}\,\mu)e_{\mathrm{V}}, \tag{8.8}$$

the pseudo constitutive parameter λ_{V} being a penalty factor, which relaxes the strict isochoric condition. It has to be chosen from the numerical point of view in compliance with the physics of the problem.

On the body surface, it is assumed that the boundary conditions can be described by prescribed normal stress, prescribed velocity or by contact conditions in conjunction with Coulomb friction. According to the Coulomb's friction law, the friction shear stress is expressed by a relation of the form

$$\tau_{\mathrm{c}} = -C\,|\sigma_{\mathrm{n}}|\,\frac{\Delta v_{\mathrm{t}}}{|\Delta v_{\mathrm{t}}|}, \tag{8.9}$$

where C denotes the friction coefficient, σ_{n} is the normal stress, and Δv_{t} the sliding velocity (tangential velocity difference) at the contact point.

The contact conditions are treated using a suitable penalty method extending over a kinematic approach to friction [99], which is effective on the system matrix for enforcing the non-penetration constraints and eventually sticking.

The following addresses problems where material parameters, friction coefficients, and boundary conditions may exhibit scatter.

8.2.2 The equilibrium equations and computational aspects

After spatial discretization of the solid by finite elements, the equilibrium condition during the course of an inelastic deformation process with random uncertainties can be presented as the vector equation

$$\mathbf{r}(\mathbf{v},\mathbf{x},\mathbf{b}) = \mathbf{s}(\mathbf{v},\mathbf{x},\mathbf{b}) - \mathbf{p}(t,\mathbf{x},\mathbf{b}) = \mathbf{0}, \tag{8.10}$$

which refers to nodal point quantities. The vector $\mathbf{x}$ denotes the geometry, $\mathbf{v}$ the velocity, $\mathbf{r}$, $\mathbf{s}$, $\mathbf{p}$ are the residual vector function, the internal force vector and the vector of the applied loads, respectively. The vector $\mathbf{b}$ collects the discretized random variables describing stochastic input such as material properties, friction coefficients and load parameters. It is assumed independent of the solution of the evoluting deformation problem. In view of the material constitutive law, the internal force (stress) vector can be presented as

$$\mathbf{s} = \mathbf{D}(\mathbf{x},\mathbf{v},\mathbf{b})\mathbf{v}. \tag{8.11}$$

where $\mathbf{D}$ is the material viscosity matrix comprising the effect of contact as by the penalty approach. In the following elucidation of the background, or primary algorithm employed for the numerical process simulation the random variables in the vector $\mathbf{b}$ are considered frozen, resp. they represent a single realization of the input.

Steady-state problems

For steady-state problems, Eqs. (8.10) and (8.11) assume the form:

$$\mathbf{r}(\mathbf{v},\mathbf{b}) = \mathbf{s}(\mathbf{v},\mathbf{b}) - \mathbf{p}(\mathbf{b}) = \mathbf{0}, \tag{8.12}$$

and

$$\mathbf{s} = \mathbf{D}(\mathbf{v}, \mathbf{b})\mathbf{v}. \tag{8.13}$$

Equation (8.12) that governs the velocity can be solved iteratively by the modified Newton-Raphson method based on the secant operator $\mathbf{D}$ from Eq. (8.13):

$$\mathbf{D}^{(k)}\Delta\mathbf{v}^{(k+1)} = \mathbf{r}^{(k+1)}, \tag{8.14}$$

and

$$\mathbf{v}^{(k+1)} = \mathbf{v}^{(k)} + \Delta\mathbf{v}^{(k+1)}. \tag{8.15}$$

Alternatively, Eq. (8.12) can be solved by the Newton-Raphson method with the tangential operator $\mathbf{D}_{\mathrm{T}}$ of the system, which is given by the derivative of the internal force vector $\mathbf{s}$ with respect to the velocity vector $\mathbf{v}$:

$$\mathbf{D}_{\mathrm{T}} = \frac{\partial \mathbf{r}}{\partial \mathbf{v}} = \frac{\partial \mathbf{s}}{\partial \mathbf{v}}. \tag{8.16}$$

Non-stationary problems

In the numerical simulation of the non-stationary process, the equilibrium condition, Eq. (8.10) is considered at distinct instants as

$$\mathbf{r}({}^c\mathbf{v}, {}^c\mathbf{x}, \mathbf{b}) = \mathbf{s}({}^c\mathbf{v}, {}^c\mathbf{x}, \mathbf{b}) - \mathbf{p}({}^ct, {}^c\mathbf{x}, \mathbf{b}) = \mathbf{0}, \tag{8.17}$$

and the deforming geometry ${}^c\mathbf{x}$ is advanced incrementally according to the time integration scheme

$${}^c\mathbf{x}(\mathbf{b}) = {}^a\mathbf{x}(\mathbf{b}) + (1-\zeta)\tau\, {}^a\mathbf{v}(\mathbf{b}) + \zeta\tau\, {}^c\mathbf{v}(\mathbf{b}), \qquad 0 \le \zeta \le 1. \tag{8.18}$$

The superscript c marks the quantities at the current instant ${}^ct$ and the superscript a stands for those at the previous instant ${}^at$, the beginning of the incremental time step, τ is the time increment and ζ is the collocation parameter specifying the time integration. For the implicit time integration scheme, we have $\zeta > 0$.

Equation (8.17) can be solved for the velocity by the modified Newton-Raphson method similar to Eq. (8.12) using the decomposition of the viscosity matrix $\mathbf{D}({}^c\mathbf{x}, {}^c\mathbf{v}, \mathbf{b})$ appertaining to the current solution state. Alternatively, the method can be applied in the original form, in which the correction to the velocity at the $(k+1)$th iteration step is computed with the tangential operator derived for the deforming system

$$\begin{aligned} \widetilde{\mathbf{D}}_{\mathrm{T}} &= \frac{\partial({}^c\mathbf{r})}{\partial({}^c\mathbf{v})} + \frac{\partial({}^c\mathbf{r})}{\partial({}^c\mathbf{x})} \frac{\mathrm{d}({}^c\mathbf{x})}{\mathrm{d}({}^c\mathbf{v})} \\ &= \mathbf{D}_{\mathrm{T}} + \zeta\tau\,\mathbf{K}_{\mathrm{G}}, \end{aligned} \tag{8.19}$$

where $\mathbf{K}_{\mathrm{G}}$, accounts for changes of the internal force induced by geometry variations at constant velocity [100]:

$$\mathbf{K}_{\mathrm{G}} = \left. \frac{\partial({}^c\mathbf{s})}{\partial({}^c\mathbf{x})} \right|_{{}^c\mathbf{v}} . \tag{8.20}$$

It differs therefore from the geometric stiffness matrix of elastic structures, which is taken at constant stress. In Eq. (8.19) additional contributions arise if the applied load is actually geometry dependent and are covered by the so-called load correction matrix.

In both the modified Newton method and the original Newton Raphson method, the contact forces are updated from the previous iteration during the solution process and added to the internal forces $\mathbf{s}$. The iteration process is continued until the convergence criterion measured by the mean quadratic norms for the residual forces or for the velocity corrections for the current instant is achieved.

8.3 Stochastic finite element analysis of inelastic deformation processes

8.3.1 Steady-state problems

It is observed that the equation governing the steady-state viscous problem resembles that for the static finite element analysis of structures with nonlinear elasticity, except that the unknowns are the velocities but not the displacements. Therefore, with reference to the actually random input vector $\mathbf{b}$ the perturbation technique used in the stochastic analysis of nonlinear elastic structures can be applied also to the steady-state problems of viscous solids. In what follows, the perturbation equations for the first order approximate mean value and variance are derived with similar procedures as in the formulation of the stochastic finite element analysis of structures [85].

The nodal velocity $\mathbf{v}$, the internal force $\mathbf{s}$ and the external force $\mathbf{p}$ are expanded via first-order Taylor series about the mean value of the q random variables in the vector $\overline{\mathbf{b}} = \mathrm{E}(\mathbf{b})$:

$$\mathbf{v}(\mathbf{b}) = \overline{\mathbf{v}} + \left.\frac{\mathrm{d}\mathbf{v}}{\mathrm{d}\mathbf{b}}\right|_{\overline{\mathbf{b}}} \Delta\mathbf{b} + ..., \tag{8.21}$$

$$\mathbf{s}(\mathbf{v},\mathbf{b}) = \overline{\mathbf{s}} + \left(\overline{\mathbf{D}}_{\mathrm{T}} \left.\frac{\mathrm{d}\mathbf{v}}{\mathrm{d}\mathbf{b}}\right|_{\overline{\mathbf{b}}} + \left.\frac{\partial\mathbf{s}}{\partial\mathbf{b}}\right|_{\overline{\mathbf{b}}}\right) \Delta\mathbf{b} + ..., \tag{8.22}$$

and

$$\mathbf{p}(\mathbf{b}) = \overline{\mathbf{p}} + \left.\frac{\mathrm{d}\mathbf{p}}{\mathrm{d}\mathbf{b}}\right|_{\overline{\mathbf{b}}} \Delta\mathbf{b} + ..., \tag{8.23}$$

where an over-bar denotes that the corresponding quantities are evaluated at $\overline{\mathbf{b}}$, for instance the internal force

$$\overline{\mathbf{s}} = \mathbf{s}\left(\mathbf{v}(\overline{\mathbf{b}}), \overline{\mathbf{b}}\right) = \mathbf{D}\left(\mathbf{v}(\overline{\mathbf{b}}), \overline{\mathbf{b}}\right)\overline{\mathbf{v}} = \overline{\mathbf{D}}\,\overline{\mathbf{v}}. \tag{8.24}$$

Substituting Eqs. (8.22) and (8.23) into Eq. (8.12), collecting the terms of the same order, and with Eq. (8.24) we obtain the following zeroth-order and first-order perturbation equations :

Zeroth-order equation:

$$\mathbf{s}\left(\mathbf{v}(\overline{\mathbf{b}}), \overline{\mathbf{b}}\right) = \overline{\mathbf{D}}\,\overline{\mathbf{v}} = \overline{\mathbf{p}}\,, \tag{8.25}$$

First-order equation:

$$\overline{\mathbf{D}}_{\mathrm{T}} \left.\frac{\mathrm{d}\mathbf{v}}{\mathrm{d}\mathbf{b}}\right|_{\overline{\mathbf{b}}} = \left.\frac{\mathrm{d}\mathbf{p}}{\mathrm{d}\mathbf{b}}\right|_{\overline{\mathbf{b}}} - \left.\frac{\partial \mathbf{s}}{\partial \mathbf{b}}\right|_{\overline{\mathbf{b}}} . \tag{8.26}$$

Equation (8.25) is solved for the velocity vector $\overline{\mathbf{v}} = \mathbf{v}(\overline{\mathbf{b}})$ as usually, Eq. (8.26) for the q columns $\partial\mathbf{v}/\partial b_r|_{\overline{\mathbf{b}}}$ of the derivative matrix $\mathrm{d}\mathbf{v}/\mathrm{d}\mathbf{b}|_{\overline{\mathbf{b}}}$. It is observed that in the first-order equation the tangential operator of the velocity problem appears, which suggests to base the zeroth-order solution on the original Newton–Raphson iteration. If the solution algorithm for the primary analysis employs the secant matrix $\mathbf{D}$, however, the first-order equation should also be based on the secant operator and requires then an iterative technique as outlined subsequently for the non-stationary case.

By definition, the mean value and the covariance of the nodal velocity $\mathbf{v}$ are expressed as

$$\mathrm{E}(\mathbf{v}) = \int_{-\infty}^{\infty} \mathbf{v}\, f_{\mathrm{PDF}}(\mathbf{b})\mathrm{d}\mathbf{b}, \tag{8.27}$$

and

$$\mathrm{Cov}(v^i, v^j) = \int_{-\infty}^{\infty} (\, v^i - \overline{v}^i)(\, v^j - \overline{v}^j)\, f_{\mathrm{PDF}}(\mathbf{b})\mathrm{d}\mathbf{b}, \tag{8.28}$$

where $f_{\mathrm{PDF}}(\mathbf{b})$ is the joint probability density function of the random vector $\mathbf{b}$, v^i is the ith degree of freedom of $\mathbf{v}$.

Substituting Eq. (8.21) into Eqs. (8.27) and (8.28), the first order approximate mean value and the covariance matrix of the nodal velocities are expressed using the solutions of the perturbation equations as:

$$\mathrm{E}(\mathbf{v}) \approx \overline{\mathbf{v}}, \tag{8.29}$$

and

$$\mathbf{\Sigma}_{\mathbf{v}} \approx \left.\frac{\mathrm{d}\mathbf{v}}{\mathrm{d}\mathbf{b}}\right|_{\overline{\mathbf{b}}} \mathbf{\Sigma}_{\mathbf{b}} \left.\frac{\mathrm{d}\mathbf{v}}{\mathrm{d}\mathbf{b}}\right|_{\overline{\mathbf{b}}}^{\mathrm{t}} . \tag{8.30}$$

8.3.2 Non-stationary problems

For the stochastic finite element analysis of non-stationary viscous deformation processes, the situation becomes more complicated due to the evolutionary geometry during the deformation process. In order to reveal the history-dependence of the non-stationary deformation process, perturbation based stochastic finite element analysis must be formulated in consistency with the time integration procedure of the background, or primary process simulation.

Therefore, the geometry is considered as an implicit variable depending on the random input rather than an independent random variable. The process variations caused by the geometry variations are accounted for by tracing the dependence of the velocity field upon the updated geometry and the derivatives of the accumulated deformation with respect to the random variables.

The state of the solid at instant ${}^{c}t$ is governed by Eq. (8.17) along with Eq. (8.18) for the incremental transition. It is assumed that the random input variables $\mathbf{b}$ do not evolve in the course of the deformation process.

The first-order Taylor series expansion of the internal force vector $\mathbf{s}$ and the external load vector $\mathbf{p}$ about the mean $\overline{\mathbf{b}}$ yields

$$\mathbf{s}({}^{c}\mathbf{v}, {}^{c}\mathbf{x}, \mathbf{b}) \quad = \quad {}^{c}\overline{\mathbf{s}} + \left(\overline{\mathbf{D}}_{\mathrm{T}} \left.\frac{\mathrm{d}({}^{c}\mathbf{v})}{\mathrm{d}\mathbf{b}}\right|_{\overline{\mathbf{b}}} + \overline{\mathbf{K}}_{\mathrm{G}} \left.\frac{\mathrm{d}({}^{c}\mathbf{x})}{\mathrm{d}\mathbf{b}}\right|_{\overline{\mathbf{b}}} + \left.\frac{\partial({}^{c}\mathbf{s})}{\partial\mathbf{b}}\right|_{\overline{\mathbf{b}}} \right) \Delta\mathbf{b} + ..., \tag{8.31}$$

and

$$\mathbf{p}(\mathbf{b}) \quad = \quad {}^{c}\overline{\mathbf{p}} + \left.\frac{\mathrm{d}({}^{c}\mathbf{p})}{\mathrm{d}\mathbf{b}}\right|_{\overline{\mathbf{b}}} \Delta\mathbf{b} + ... \tag{8.32}$$

To not complicate the formal presentation, the applied loads are assumed to not depend on the deforming geometry.

The first-order Taylor series expansion of the velocity ${}^{c}\mathbf{v}$ about the mean value of the random variable $\overline{\mathbf{b}}$ reads

$${}^{c}\mathbf{v}(\mathbf{b}) = {}^{c}\overline{\mathbf{v}} + \left.\frac{\mathrm{d}({}^{c}\mathbf{v})}{\mathrm{d}\mathbf{b}}\right|_{\overline{\mathbf{b}}} \Delta\mathbf{b} + ..., \tag{8.33}$$

and analogously for geometry

$$ {}^{c}\mathbf{x}(\mathbf{b}) = {}^{c}\overline{\mathbf{x}} + \left.\frac{\mathrm{d}({}^{c}\mathbf{x})}{\mathrm{d}\mathbf{b}}\right|_{\overline{\mathbf{b}}} \Delta\mathbf{b} + ... \tag{8.34} $$

Differentiating Eq. (8.18) for the incremental transition with respect to $\mathbf{b}$, the derivative of the current geometry ${}^{c}\mathbf{x}$ with respect to the random input vector becomes

$$ \left.\frac{\mathrm{d}({}^{c}\mathbf{x})}{\mathrm{d}\mathbf{b}}\right|_{\overline{\mathbf{b}}} = \left.\frac{\mathrm{d}({}^{a}\mathbf{x})}{\mathrm{d}\mathbf{b}}\right|_{\overline{\mathbf{b}}} + (1-\zeta)\tau \left.\frac{\mathrm{d}({}^{a}\mathbf{v})}{\mathrm{d}\mathbf{b}}\right|_{\overline{\mathbf{b}}} + \zeta\tau \left.\frac{\mathrm{d}({}^{c}\mathbf{v})}{\mathrm{d}\mathbf{b}}\right|_{\overline{\mathbf{b}}} . \tag{8.35} $$

Utilization in Eq. (8.31) furnishes

$$ \begin{aligned} \mathbf{s}({}^{c}\mathbf{v}, {}^{c}\mathbf{x}, \mathbf{b}) \;=\; & {}^{c}\overline{\mathbf{s}} + \Bigg((\overline{\mathbf{D}}_{\mathrm{T}} + \zeta\tau\overline{\mathbf{K}}_{\mathrm{G}}) \left.\frac{\mathrm{d}({}^{c}\mathbf{v})}{\mathrm{d}\mathbf{b}}\right|_{\overline{\mathbf{b}}} + \overline{\mathbf{K}}_{\mathrm{G}} \left.\frac{\mathrm{d}({}^{a}\mathbf{x})}{\mathrm{d}\mathbf{b}}\right|_{\overline{\mathbf{b}}} \\ & + (1-\zeta)\tau\overline{\mathbf{K}}_{\mathrm{G}} \left.\frac{\mathrm{d}({}^{a}\mathbf{v})}{\mathrm{d}\mathbf{b}}\right|_{\overline{\mathbf{b}}} + \left.\frac{\partial({}^{c}\mathbf{s})}{\partial\mathbf{b}}\right|_{\overline{\mathbf{b}}} \Bigg) \Delta\mathbf{b} + ... \end{aligned} \tag{8.36} $$

Substituting Eqs. (8.32) and (8.36) into Eq. (8.17) and equating terms of the same order, the zeroth-order and the first-order perturbation equations are obtained as follows.

Zeroth-order equation:

$$ \mathbf{s}({}^{c}\overline{\mathbf{v}}, {}^{c}\overline{\mathbf{x}}, \overline{\mathbf{b}}) = \overline{\mathbf{D}}\,{}^{c}\overline{\mathbf{v}} = {}^{c}\overline{\mathbf{p}}, \tag{8.37} $$

First-order equation:

$$ \begin{aligned} (\overline{\mathbf{D}}_{\mathrm{T}} + \zeta\tau\overline{\mathbf{K}}_{\mathrm{G}}) \left.\frac{\mathrm{d}({}^{c}\mathbf{v})}{\mathrm{d}\mathbf{b}}\right|_{\overline{\mathbf{b}}} \;=\; & -\overline{\mathbf{K}}_{\mathrm{G}} \left.\frac{\mathrm{d}({}^{a}\mathbf{x})}{\mathrm{d}\mathbf{b}}\right|_{\overline{\mathbf{b}}} - (1-\zeta)\tau\overline{\mathbf{K}}_{\mathrm{G}} \left.\frac{\mathrm{d}({}^{a}\mathbf{v})}{\mathrm{d}\mathbf{b}}\right|_{\overline{\mathbf{b}}} - \left.\frac{\partial({}^{c}\mathbf{s})}{\partial\mathbf{b}}\right|_{\overline{\mathbf{b}}} \\ & + \left.\frac{\mathrm{d}({}^{c}\mathbf{p})}{\mathrm{d}\mathbf{b}}\right|_{\overline{\mathbf{b}}} . \end{aligned} \tag{8.38} $$

Equation (8.37) for the velocity is conveniently solved using the secant matrix $\overline{\mathbf{D}}$ in the iteration. In contrast, the solution of Eq. (8.38) requires the geometric stiffness matrix $\overline{\mathbf{K}}_{\mathrm{G}}$ as well as the system tangential matrix $\overline{\mathbf{D}}_{\mathrm{T}}$. Therefore, an alternative first-order equation is derived with reference to the secant form of the internal force: $\mathbf{s} = \mathbf{D}(\mathbf{x}, \mathbf{v}, \mathbf{b})\mathbf{v}$. The expansion about the mean random input can then be symbolized as

$$\mathbf{s}({}^c\mathbf{v}, {}^c\mathbf{s}, \mathbf{b}) \;=\; \overline{\mathbf{D}}\,{}^c\overline{\mathbf{v}} + \left(\overline{\mathbf{D}}\frac{\mathrm{d}(\,{}^c\mathbf{v})}{\mathrm{d}\mathbf{b}}\bigg|_{\overline{\mathbf{b}}} + \left(\frac{\mathrm{d}(\mathbf{D}\,{}^c\mathbf{v})}{\mathrm{d}\mathbf{b}}\bigg|_{\mathbf{v}} \right)_{\overline{\mathbf{b}}} \right) \Delta\mathbf{b} + ..., \tag{8.39}$$

where the notation $|_{\mathbf{v}}$ indicates that the explicit dependence of the internal force $\mathbf{s}$ on the velocity $\mathbf{v}$ is discarded and thus the differentiation applies to the implicit appearances of the velocity in $\mathbf{D}(\mathbf{x}, \mathbf{v}, \mathbf{b})$ due to non-linearity in the constitutive law.

While the above leaves the zeroth-order equation unchanged, the appertaining first-order form is

$$\overline{\mathbf{D}}\,\frac{\mathrm{d}(\,{}^c\mathbf{v})}{\mathrm{d}\mathbf{b}}\bigg|_{\overline{\mathbf{b}}} = -\left(\frac{\mathrm{d}(\,{}^c\mathbf{s})}{\mathrm{d}\mathbf{b}}\bigg|_{\mathbf{v}} \right)_{\overline{\mathbf{b}}} + \frac{\mathrm{d}(\,{}^c\mathbf{p})}{\mathrm{d}\mathbf{b}}\bigg|_{\overline{\mathbf{b}}}. \tag{8.40}$$

Solving Eq. (8.40) rather than Eq. (8.38) is preferable from the computational perspective of the primary simulation algorithm. In this context, $\mathrm{d}^c\mathbf{v}/\mathrm{d}\mathbf{b}|_{\overline{\mathbf{b}}}$ can be determined using the following iteration strategy:

$$\overline{\mathbf{D}}\,\frac{\mathrm{d}(\,{}^c\mathbf{v})}{\mathrm{d}\mathbf{b}}\bigg|_{\overline{\mathbf{b}}}^{(k+1)} = -\left(\frac{\mathrm{d}(\,{}^c\mathbf{s})}{\mathrm{d}\mathbf{b}}\bigg|_{\mathbf{v}} \right)_{\overline{\mathbf{b}}}^{(k)} + \frac{\mathrm{d}(\,{}^c\mathbf{p})}{\mathrm{d}\mathbf{b}}\bigg|_{\overline{\mathbf{b}}}. \tag{8.41}$$

In Eq. (8.41), the first term on the right-hand side is approximated using a finite difference scheme. To be specific

$$\begin{aligned}\left(\frac{\mathrm{d}(\,{}^c\mathbf{s})}{\mathrm{d}b_r}\bigg|_{\mathbf{v}} \right)_{\overline{\mathbf{b}}}^{(k)} \;=\; & \left(\frac{\mathrm{d}(\mathbf{D}\,{}^c\mathbf{v})}{\mathrm{d}b_r}\bigg|_{\mathbf{v}} \right)_{\overline{\mathbf{b}}}^{(k)} \approx \frac{\partial(\,{}^c\mathbf{s})}{\partial b_r}\bigg|_{\overline{\mathbf{b}}} \\ & + \frac{\mathbf{D}\left({}^c\overline{\mathbf{x}} + (\delta^c\overline{\mathbf{x}})^{(k)}, {}^c\overline{\mathbf{v}} + (\delta^c\overline{\mathbf{v}})^{(k)}, \overline{\mathbf{b}}\right){}^c\overline{\mathbf{v}} - \mathbf{D}\left({}^c\overline{\mathbf{x}}, {}^c\overline{\mathbf{v}}, \overline{\mathbf{b}}\right){}^c\overline{\mathbf{v}}}{\delta b_r},\end{aligned} \tag{8.42}$$

where δb_r is the small difference imposed on the rth random variable b_r, $(\delta^c\overline{\mathbf{x}})^{(k)}$ and $(\delta^c\overline{\mathbf{v}})^{(k)}$ represent the associated geometry change and the velocity change calculated with the velocity derivative obtained from the last iteration, respectively, as expressed by

$$(\delta^c \overline{\mathbf{x}})^{(k)} = \sum_{r=1}^{q} \left(\left. \frac{\mathrm{d}(\,^a\mathbf{x})}{\mathrm{d}b_r} \right|_{\overline{\mathbf{b}}} + (1-\zeta)\tau \left. \frac{\mathrm{d}(\,^a\mathbf{v})}{\mathrm{d}b_r} \right|_{\overline{\mathbf{b}}} + \zeta\tau \left. \frac{\mathrm{d}(\,^c\mathbf{v})}{\mathrm{d}b_r} \right|_{\overline{\mathbf{b}}}^{(k)} \right) \delta b_r, \tag{8.43}$$

and

$$(\delta^c \overline{\mathbf{v}})^{(k)} = \sum_{r=1}^{q} \left. \frac{\mathrm{d}(\,^c\mathbf{v})}{\mathrm{d}b_r} \right|_{\overline{\mathbf{b}}}^{(k)} \delta b_r. \tag{8.44}$$

It should be noticed at this place, that the operations with the system matrix in Eqs. (8.39) and (8.42) stand merely for a transparent symbolic, but the computations actually take place on the element level.

Since the coefficient matrix has been decomposed in the primary analysis, the solution of Eq. (8.41) requires only back- and forth substitutions. It is worth noticing that the computation converges if $\zeta\tau$ is sufficiently small. As shown by numerical investigations, solutions which are accurate enough for practical applications can be obtained after a few iterations in most cases. At this point we recall that the original form, Eq. (8.38) offers a direct solution for the first-order terms, and is favoured if the zeroth-order solution by the primary analysis algorithm bases on the tangent operator for the velocity system given in Eq. (8.19).

After solving the perturbation equations, one gets the first order approximations for the mean velocity and the mean geometry

$$\mathrm{E}(^c\mathbf{v}) \approx {}^c\overline{\mathbf{v}}, \tag{8.45}$$

and

$$\mathrm{E}(^c\mathbf{x}) \approx {}^c\overline{\mathbf{x}}. \tag{8.46}$$

The first order covariance matrix of the velocity, and of the geometry are obtained as

$${}^c\mathbf{\Sigma}_{\mathbf{v}} \approx \left. \frac{\mathrm{d}(\,^c\mathbf{v})}{\mathrm{d}\mathbf{b}} \right|_{\overline{\mathbf{b}}} \mathbf{\Sigma}_{\mathbf{b}} \left. \frac{\mathrm{d}(\,^c\mathbf{v})}{\mathrm{d}\mathbf{b}} \right|_{\overline{\mathbf{b}}}^{\mathrm{t}}, \tag{8.47}$$

and

$$ {}^{c}\boldsymbol{\Sigma}_{\mathbf{x}} \approx \left.\frac{\mathrm{d}({}^{c}\mathbf{x})}{\mathrm{d}\mathbf{b}}\right|_{\bar{\mathbf{b}}} \boldsymbol{\Sigma}_{\mathbf{b}} \left.\frac{\mathrm{d}({}^{c}\mathbf{x})}{\mathrm{d}\mathbf{b}}\right|_{\bar{\mathbf{b}}}^{\mathrm{t}} . \tag{8.48} $$

The approximate covariance matrix of the geometry is completely determined by Eq. (8.48). In order to show the involvement of historical terms in the incremental transition, however, use of Eq. (8.35) gives

$$ \begin{aligned} {}^{c}\boldsymbol{\Sigma}_{\mathbf{x}} \approx\ & {}^{a}\boldsymbol{\Sigma}_{\mathbf{x}} + (1-\zeta)^2\tau^2\, {}^{a}\boldsymbol{\Sigma}_{\mathbf{v}} + \zeta^2\tau^2\, {}^{c}\boldsymbol{\Sigma}_{\mathbf{v}} + 2(1-\zeta\tau) \left.\frac{\mathrm{d}({}^{a}\mathbf{x})}{\mathrm{d}\mathbf{b}}\right|_{\bar{\mathbf{b}}} \boldsymbol{\Sigma}_{\mathbf{b}} \left.\frac{\mathrm{d}({}^{a}\mathbf{v})}{\mathrm{d}\mathbf{b}}\right|_{\bar{\mathbf{b}}}^{\mathrm{t}} \\ & + 2(1-\zeta)\zeta\tau^2 \left.\frac{\mathrm{d}({}^{a}\mathbf{v})}{\mathrm{d}\mathbf{b}}\right|_{\bar{\mathbf{b}}} \boldsymbol{\Sigma}_{\mathbf{b}} \left.\frac{\mathrm{d}({}^{c}\mathbf{v})}{\mathrm{d}\mathbf{b}}\right|_{\bar{\mathbf{b}}}^{\mathrm{t}} + 2\zeta\tau \left.\frac{\mathrm{d}({}^{a}\mathbf{x})}{\mathrm{d}\mathbf{b}}\right|_{\bar{\mathbf{b}}} \boldsymbol{\Sigma}_{\mathbf{b}} \left.\frac{\mathrm{d}({}^{c}\mathbf{v})}{\mathrm{d}\mathbf{b}}\right|_{\bar{\mathbf{b}}}^{\mathrm{t}} . \end{aligned} \tag{8.49} $$

Equation (8.49) indicates the evolution of the geometry covariance matrix.

8.4 Robust design of deformation processes

8.4.1 Optimization for process robust design

The process robust design is cast into an optimization problem:

$$ \begin{aligned} &\text{find} && \mathbf{d}, \\ &\text{minimizing} && \tilde{f} = (1-\alpha) f_1\left(\mathrm{E}(\mathbf{u}), \mathrm{E}(\mathbf{v}), \mathbf{d}\right)/\eta_1 + \alpha f_2\left(\sigma(\mathbf{u}), \sigma(\mathbf{v}), \mathbf{d}\right)/\eta_2, \\ &\text{subject to} && g_i\left(\mathrm{E}(\mathbf{u}), \mathrm{E}(\mathbf{v}), \sigma(\mathbf{u}), \sigma(\mathbf{v}), \mathbf{d}\right) \le 0 \qquad (i = 1, 2, ..., k)\,, \\ & && \mathbf{d}_{\mathrm{L}} \le \mathbf{d} \le \mathbf{d}_{\mathrm{U}}, \end{aligned} \tag{8.50} $$

where $\mathbf{d}$ is the vector of design variables, $\mathbf{d}_{\mathrm{L}}$ and $\mathbf{d}_{\mathrm{U}}$ denote the lower and upper bound limits of the design variables, f_1 and f_2 represent the objective functions related to the mean and the standard deviation of the system state variables (deformation and velocity field), respectively, g_i $(i = 1, 2, ..., k)$ are the constraint functions regarding the mean and the variability of the performance. The desirability function $\tilde{f}$ is defined as a weighted sum of the two objective functions, with $0 \le \alpha \le 1$ being the weighting factor. The two quantities η_1 and η_2 are prescribed normalization factors.

Compared with the conventional, deterministic formulation, the variability of the system response is involved in the design objective of the robust design. The optimization problem stated in Eq. (8.50) is solved with the optimization package-FSQP, where the sensitivity of the objective function and the constraints with respect to the design variables are evaluated with the finite difference method implemented in the package.

8.4.2 Numerical examples

Die design for steady-state extrusion

As a numerical example, the die profile design for the extrusion process described in Fig. 8.1 is considered. The extrusion speed is $v = 10\,\text{mm/sec}$. The die profile is represented as a B–spline curve, specified by four control points (P1–P4) on it. Since the hydrostatic pressure is known to be one of the most important factors regarding the defects of the final product, the vertical positions of the four control points are to be determined, such that the maximum level of the hydrostatic pressure in the material is minimized. Assuming symmetry, one half of the problem domain is discretized with quadrilateral plane strain elements in the interior and line elements along the contact boundaries, as shown in Fig. 8.1.

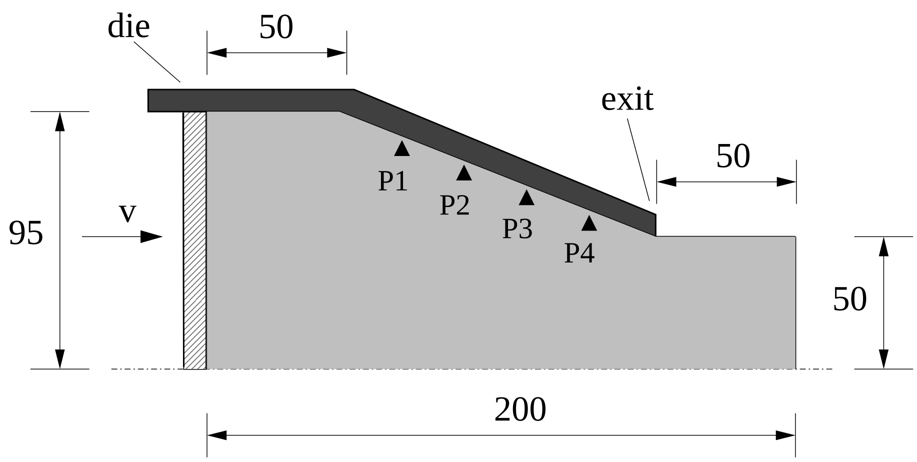

Figure 8.1: Design of extrusion die (Dimensions in mm)

Table 8.1: Random variables for the extrusion die design problem

Random variables	Mean value	Standard deviation
μ [Mpa s]	120.0	12.0
C	0.3	0.03

The material is assumed linear viscous. The random variables for the present problem are the material viscosity μ and the coefficient of Coulomb friction C between the die and the workpiece material. Their mean values and standard deviations are collected in Table 8.1.

In the initial design, where the shape of the die profile is a straight line segment, the mean value of the maximum hydrostatic pressure is $\mathrm{E}(p_{\max}) = 108.72$ Mpa and its standard deviation amounts to $\sigma(p_{\max}) = 15.81$ MPa. The distribution of the mean hydrostatic pressure is shown in Fig. 8.2. This result has been verified by a Monte Carlo simulation with 300 realizations, by which the mean value and the standard deviation of hydrostatic pressure at the same location are predicted to be $\bar{p}_{\max} = 105.5$ Mpa and $\mathrm{s}(p_{\max}) = 15.82$ MPa. The computational time is 12.7 seconds for the present method and 3059.4 seconds for the Monte Carlo simulation, respectively.

As a reference design, the optimum corresponding to the conventional deterministic optimization statement is first obtained (see Table 8.2), where the design objective is to minimize the value of the maximum hydrostatic pressure based on nominal input values. An optimal solution obtained by the developed robust design algorithm is also listed in the table. The distribution of the mean hydrostatic pressure for the two designs is given in Fig. 8.3 and Fig 8.4.

Table 8.2: Objective function values for the optima of the extrusion die design

Objective function	Initial	Determ.	Robust
$\mathrm{E}(p_{\max})$ [MPa]	108.72	86.65	87.71
$\sigma(p_{\max})$ [MPa]	15.81	12.83	9.33

The results show that the variability of the maximum hydrostatic pressure has been reduced using the robust design methodology. At the same time the mean value increases only slightly in conjunction with the employed objective function $\tilde{f} = (1-\alpha)\mathrm{E}(p_{\max})/\eta_1 + \alpha\sigma(p_{\max})/\eta_2$, where $\eta_1 = 108.72$, $\eta_2 = 15.81$ and $\alpha = 0.9$.

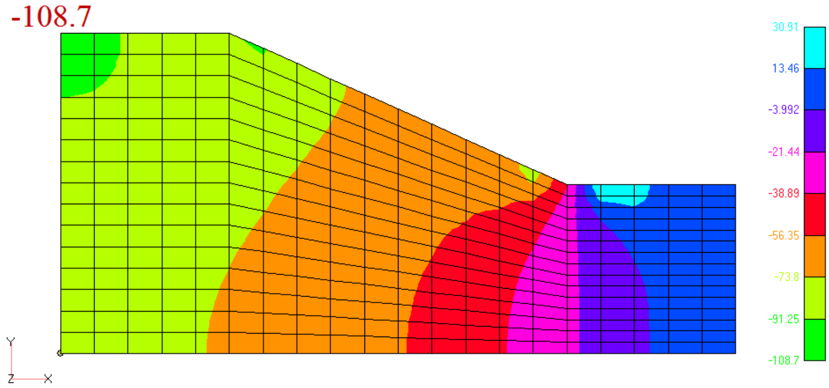

Figure 8.2: Hydrostatic pressure distribution for the initial design

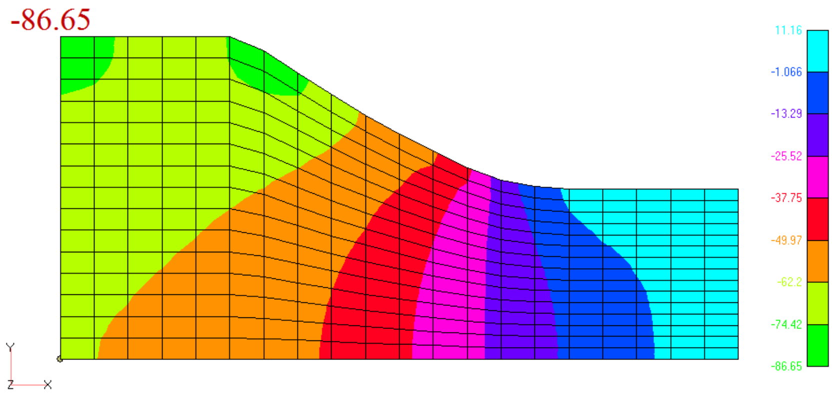

Figure 8.3: Hydrostatic pressure distribution for the design with nominal values

Axisymmetric metal preform design problem

In the metal preform design, it is of practical interest to find an appropriate workpiece shape that will produce the required profile of the final product after forging (Fig. 8.5).

In this example, the optimal shape of the workpiece material is to be determined such that the shape requirements on the final product will be satisfied as in Fig. 8.6. The height of the initial workpiece is 600 mm. A constant die speed of 100

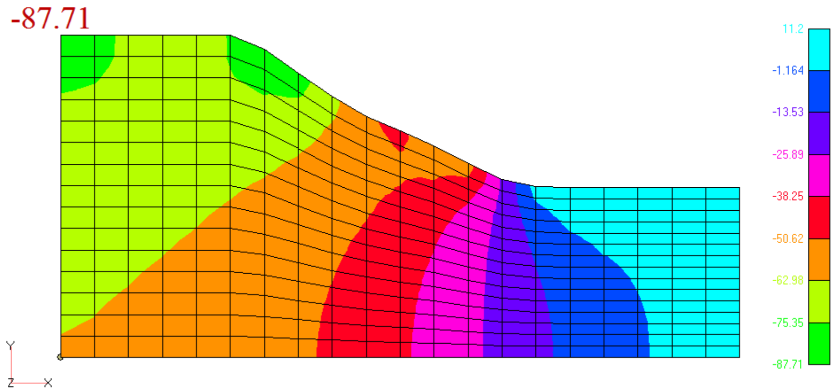

Figure 8.4: Hydrostatic pressure distribution for the robust design

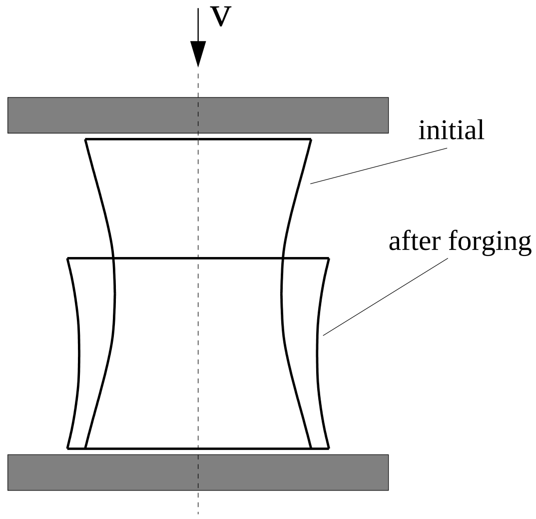

Figure 8.5: The geometry before and after forging

mm/sec is imposed for a 50% reduction. The shape of the final product is required to be a cylinder with 300 mm in height and 100 mm in radius. Stating the problem symmetric with respect to midlength the upper half of the workpiece is modeled with 10×10 quadrilateral axisymmetric elements. The 11 boundary nodes (P1–P11) of the initial mesh are the control points determining the workpiece profile and their horizontal positions are considered as the design variables.

The material of the workpiece is AISI 8260 steel. The rate-dependence of the material properties is considered by the flow stress which at the temperature of about 1100 ^{o}C is given by

$$\sigma_{\mathrm{f}} = 75.92\,\bar{e}^{0.134}\,(1.275 - 2.5 \times 10^{-4}T)\ \mathrm{MPa},$$

where T is the temperature of the workpiece.

The coefficient of friction between the workpiece and the tool C and the operation temperature T are assumed to be random variables, with mean values and standard deviations as given in Table 8.3.

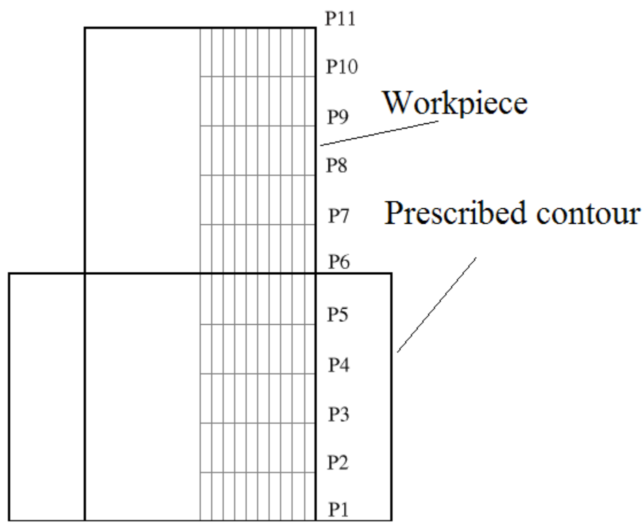

Figure 8.6: The workpiece and the prescribed contour of the final product (upper half)

The shape error of the final product is measured by the distances between the actual radial positions of the control points and the prescribed value, as expressed by

$$\Delta r_i = r_i - r^* \qquad (i = 1, 2, ..., 11),$$

Table 8.3: Random variables for the preform design problem

Random variables	Mean value	Standard deviation
T [^{o}C]	1100.0	110.0
C	0.2	0.02

where $r_i = {}^0r_i + u_i \ \ (i = 1, 2, ..., 11)$ are the final positions of the control points and r^* the prescribed radius of the final product.

As an initial design, a cylindrical workpiece geometry is considered with a radius of 70 mm. For this design the numerical simulation of the process with 10 time incremental steps predicts that the upper edge of the workpiece has both, the maximum shape error and the maximum variability in the deformed geometry. The mean value and the standard deviation of the final displacement at this point are $\mathrm{E}(u) = 8.93\,\mathrm{mm}$ and $\sigma(u) = 1.528\,\mathrm{mm}$, associated with $\max[|\mathrm{E}(\Delta r_i)|] = 21.07\,\mathrm{mm}$ and $\max[\sigma(\Delta r_i)] = 1.528\,\mathrm{mm}$. The initial shape of the workpiece and the final product are shown in Fig. 8.7 . The perturbation results are verified by a Monte Carlo simulation with 300 realizations. The Monte Carlo simulation furnishes a mean value $\bar{u} = 9.11\,\mathrm{mm}$ and the standard deviation $\mathrm{s}(u) = 1.552\,\mathrm{mm}$ for the nodal displacement of the upper edge. As regards the computation, the average time for the Monte Carlo simulation amounts to 237.5 seconds, whereas perturbation based analysis is performed within 8.2 seconds.

For the nominal design, which is based on mean input values an optimal solution is obtained by seeking the set of initial control point positions that minimize the maximum absolute shape error $\max(|\Delta r_i|)$. The appertaining objective function is

$$\tilde{f} = \max[|\mathrm{E}(\Delta r_i)|].$$

Such a design is shown in Fig. 8.8. With the maximum mean shape error $\max[|\mathrm{E}(\Delta r_i)|] = 0.202\,\mathrm{mm}$, this design yields almost exactly the final shape as prescribed, but it exhibits a maximum standard deviation $\max[\sigma(u_i)] = 0.601\mathrm{mm}$, however.

In order to seek a more robust design of the initial geometry of the workpiece, which will reduce the shape variability of the final product with respect to the actually

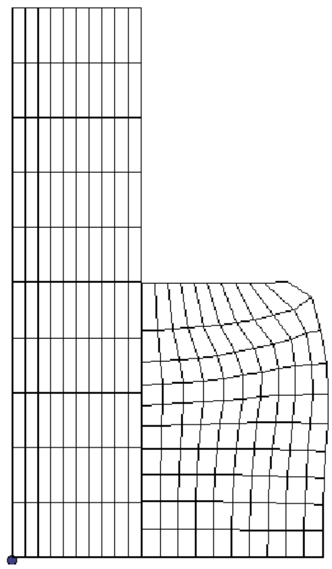

Figure 8.7: Workpiece and final product for the initial design

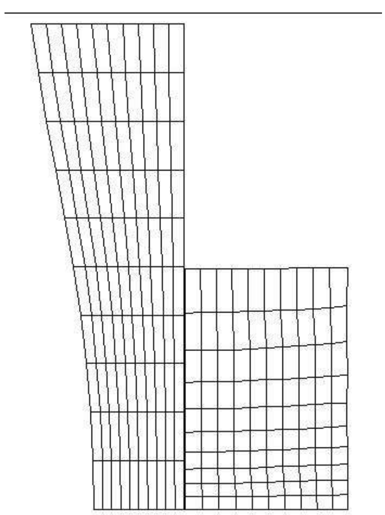

Figure 8.8: Workpiece and final product for the design with nominal values

random input, a term relating to the boundary shape variations is introduced into the objective function. Thus the objective function is defined as

$$\tilde{f} = (1-\alpha)\max[|\mathrm{E}(\Delta r_i)|]/\eta_1 + \alpha \max[\sigma(\Delta r_i)]/\eta_2,$$

where $\eta_1 = 21.07$, $\eta_2 = 1.528$.

The Aggregate Function method [101] is employed to improve the convergence of the optimization. To this end, an exponential penalty function is used to approximate the Min-max objective function, regarding the mean, for instance,

$$\max[|\mathrm{E}(\Delta r_i)|] = \frac{1}{p}\ln\left(\sum_{i=1}^{11} \mathrm{e}^{p\,|\mathrm{E}(\Delta r_i)|}\right),$$

where p is a given large number.

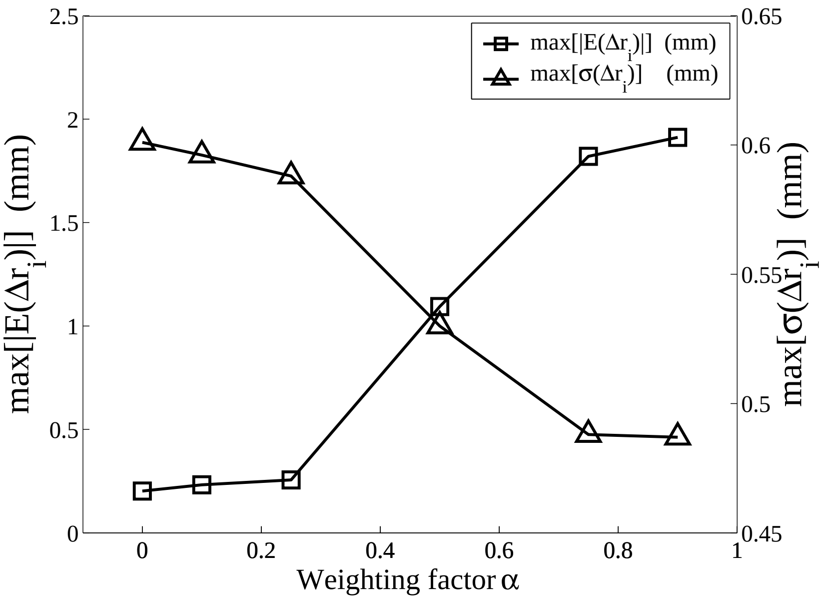

Figure 8.9: Maximum absolute value of mean and maximum standard deviation of the distance $\Delta r_i\,(i = 1, 2, ..., 11)$ versus the weighting factor α

Table 8.4: Objective function values for the optima of the preform design

Objective function	Initial	$\alpha = 0$	$\alpha = 0.1$	$\alpha = 0.25$	$\alpha = 0.5$	$\alpha = 0.75$	$\alpha = 0.9$
$\max[\lvert E(\Delta r_i)\rvert]$ [mm]	21.07	0.202	0.232	0.256	1.094	1.864	1.912
(MCS)	(20.89)	(0.152)	(0.241)	(0.282)	(1.121)	(1.820)	(1.869)
$\max[\sigma(\Delta r_i)]$ [mm]	1.528	0.601	0.596	0.588	0.530	0.488	0.487
(MCS)	(1.552)	(0.664)	(0.654)	(0.653)	(0.579)	(0.538)	(0.531)

A set of robust designs is obtained by solving the modified optimization problem with different weighting factors. The values of the objective function for these designs are listed in Table 8.4. The results of Monte Carlo simulations (MCS) are also given for comparison. In the table, the case of $\alpha = 0$ corresponds to the aforementioned nominal design. In the robust design optima ($\alpha > 0$), the shape accuracy of the final product is still satisfactory, but the maximum standard deviation of the deformation of the controls points has been reduced. One of these robust designs obtained with $\alpha = 0.5$ is shown in Fig. 8.10.

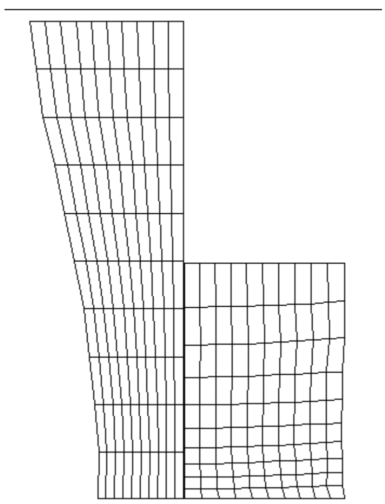

Figure 8.10: Workpiece and final product for the robust design with $\alpha = 0.5$

In this specific problem, the robust design results reveal that the shape variability of the product can not be significantly diminished beyond the optimal design that uses nominal input parameters. While the nominal design does not care about the variability, it has improved also the robustness. For this reason the shape variability of the final product can not be notably reduced by adjusting the initial shape of the workpiece. This is an explorative result of the employed design methodology.

8.5 Discussions and remarks

The chapter describes the extension of the stochastic perturbation technique to the optimum design of robust deformation processes of inelastic solids. To this end, the perturbation method for the finite element analysis of the evolving process is developed and enters the optimization procedure for robust design. The latter compromises the requirements on mean value and variance resp. standard deviation of the objective function that measures the performance of the deformation process. Accordingly, the optimum of the expected outcome and its variability depends on the functional relationship between these two quantities. The proposed methodology has been demonstrated by two applications from metal forming: one referring to the steady-state of an extrusion operation, the other to the deformation process as it evolutes in upsetting.

The methodology developed for the stochastic analysis of the deformation process adapts the perturbation technique to the simulation algorithm available in the Finite Element Programming System (FEPS) [90][82][83]. The simulation algorithm employs the secant operator resp. the viscosity matrix of the system in solving the momentary velocity problem in conjunction with an incremental scheme for the advancement of the deformation process with progressing time. On this background, since tangent operators are not provided by the system, the mean of the stochastic response is not approximated but to the first order. The numerical results obtained show, however, a fairly good agreement with the outcome of alternative Monte Carlo simulations. For the same reason, the computational tools available for the primary process simulation, the procedure employed for the optimum robust design utilizes the finite difference options offerred in the optimization package FSQP [81] for the computation of the sensitivity of the objective function. An optimization that makes use of analytical sensitivity expressions, instead, should improve the computational efficiency, and is planned as an extension of the present work.

In the formulation of the stochastic analysis for deformation processes, the current geometry at each instant can also be treated as random input, as proposed in [89]. Such a formulation is capable of treating random variables evolving during the course of the deformation but requires the computation of the derivatives of the nodal velocities with respect to the geometry, which may become awkward and inefficient for practical applications. The present method considers random input variables that are invariant with time. The random variation of the geometry, however, is traced using the derivatives the accumulated deformation with respect to the random input variables at each time increment.

In the simulation algorithm, the contact conditions are treated with the penalty method, so is the constraint of incompressibility. Thus the problem arises of a trade-off between the model accuracy and the numerical stability in the solution especially for the first-order perturbation equations. Though larger penalty factors will impose more accurate incompressibility and contact conditions, they may cause numerical difficulties depending on the computer arithmetics. Particularly, in case of a too large penalty factor for the contact conditions, the loss of computational accuracy will occur in the evaluation of some derivative terms when the finite difference method is used. Moreover, the first order perturbation equations are seen to be more sensitive to an ill-conditioned system matrix as compared with the original, zeroth order, finite element equations. Therefore, particular care is required in selecting the penalty factors in order to avoid possible numerical difficulties. In the present study, a penalty factor of $10^2 - 10^3$ for the incompressibility constraint is recommended in conjunction with the computer accuracy of 16 digits. The choice of the penalty factor for the contact conditions relies on the norm of the viscosity matrix. The numerical investigations indicate that a value of $10^6 - 10^8$ is appropriate for the situations considered.

Chapter 9

Summary and outlook

9.1 Summary

Structural optimization has experienced a significant progress in the past twenty years and is now commonly used in engineering design. The conventional deterministic design optimization may lead to a design which perform well under specified conditions. However, the stochastic nature of the structural parameters raises the need of accounting for the system variations in the optimal design problem. In particular, robust design has become a recent subject in the structural optimization research.

In the present treatise, the current state of research on structural optimization considering uncertainty is first reviewed and conceptual differences between the structural robust design and other non-deterministic structural optimization approaches are revealed. In reliability based design optimization problems, assumptions on the probability distribution must be made if data for the statistics of the random parameters are insufficient. It has been reported that this may yield large errors in computations of the probability of failure, which diminishes the validity of this approach. To overcome this drawback when information about the uncertainties is not available or not sufficient to permit a reliability analysis, alternative approaches have been developed within the context of convex modeling, interval set and fuzzy set. As another formulation of the design optimization problem with uncertainty, robust design is conceptually different from the well developed probabilistic approaches (e.g. reliability based design optimization) and possibility approaches (e.g. Fuzzy set method) since it puts more emphasis on reducing performance variability.

The structural robust design problem is formulated as a multi-criteria optimization problem, in which not only the mean structural performance function but also its standard deviation is to be minimized. An alternative statement is also presented, where a merit function accounting for the costs associated with the variability (such as the tolerance) of the design parameter is introduced. The robustness of the constraints are accounted for by introducing the standard deviation of the original constraint function and a so-called feasibility index into the constraint conditions. The larger the feasibility index is set, the more robust the feasibility of the corresponding constraint condition is required to be. The present formulation requires no priori assumptions on the distribution types of the random uncertainties, and makes use of only the first two statistical moments, which are much easier to obtain.

For scalarization of the proposed multi-criteria optimization for structural robust design, a weighted convex sum of the two design criteria is used to form the objective or desirability function. In this way, the two-criteria optimization problem is converted into a scalar minimization problem, whose optimal solution corresponds to a Pareto solution of the original optimization problem. The weighting factor of the desirability function defines the relative importance of each sub-criterion. By changing the weighting factor, one obtains a set of trade-off solutions - the Pareto solution set so as to allow the decision-making task easier for the designer.

The stochastic structural analysis techniques including the Monte Carlo simulation and the second-order perturbation based stochastic finite element analysis are discussed. The latter is used for evaluating the mean value and the variance of the structural response in the robust design problem. The perturbation based approach is also extended to the stochastic analysis of path-dependent structures, in accordance with the incremental scheme used for the corresponding deterministic analysis. Furthermore, the moments sensitivity analysis for structural performance functions are developed based on the perturbation based stochastic finite element analysis. This sensitivity information is used in the gradient based optimization algorithms for solving the robust design optimization problem.

The feasibility of the presented method has been demonstrated by numerical examples, involving both static and transient, linear and path-dependent nonlinear structural behaviours. As shown by the obtained results, in the robust optimization problems where the mean value as well as the variance of the structural performance functions are accounted for, the optimal design may yield different design parameter or even different structural topology as in the case of a deterministic optimization formulation. The Pareto optima of the numerical examples also revealed that the decrease of the variance of the structural performance is often obtained at the penalty of worsening its expected value. However, the solution of the robust design optimization problem provides the possibility for the designers to choose a feasible structural design from the set of Pareto solutions obtained with different weighting factors in the objective function.

In the last part of the treatise, the method for the robust design of processes is developed. The perturbation technique is used for the stochastic analysis of the inelastic deformation process, where an iterative algorithm based on the secant operator is employed for solving the perturbation equations. Numerical examples regarding two typical industrial forming processes are specifically addressed. The obtained results show the potential applicability of the proposed method for the robust design of industrial forming.

Though the robustness of the design needs to be strengthened in structural optimization problems, the importance of conventional design optimization techniques should not be underestimated in practice. As a matter of fact, our case studies reveal that the conventional deterministic optimization does improve to some extent the robustness of the design as well in most problems. In this sense, the investigations actually support the conventional optimality and the proposed robust design method can in some cases be regarded as a procedure to examine the relevance, which provides the designer a deeper insight into the optimal solutions of the design problem. For the same reason, the technique of robust structural optimization was developed with the intention to extend the applicability of the techniques used in conventional deterministic optimization by incorporating system uncertainties.

9.2 Outlook

In the present stage of the work, we have gained more understanding of the structural optimization problems considering system uncertainty. The importance of accounting for design robustness in such problems is highlighted through the present study. It is also shown that the conventional optimization techniques, in conjunction with the stochastic structural analysis methods, can be extended to the robust design problems. Within the present framework of structural robust design, the stochastic analysis techniques and the optimization techniques developed in this research provide a foundation for future studies. The following remarks are made with regard to continuation of extent of this research.

- The present study focuses on local optima of the structural robust design problems. The global optimal design for such problems is an interesting and challenging target as well. Using the perturbation based approaches described in the literature or developed in this work as an analysis tool, the global optimization techniques such as Genetic Algorithm and Simulated Annealing can be employed for this purpose.

- The robust design of deformation processes of solids as encountered in metal forming or in the safety task of crashworthiness, requires considerable computational effort. It might be of interest to combine the use of midrange or global approximate model such as response surface model with the developed optimization techniques in order to obtain cost effective optimal designs.

Bibliography

[1] H. Adeli and N. Cheng. Concurrent genetic algorithms for optimization of large structures. *Journal of Aerospace Engineering, ASCE*, 7:276–296, 1994.

[2] Y.X. Gu and Zhan Kang. Optimum design of composite space structures under static and dynamics constraints. In *Proc. 4th USNCCM*, pages 484–490, 1997.

[3] Y.X. Gu and Zhan Kang. Sensitivity analysis of structural frequency responses and dynamic optimization of space structures. In *Proc. 2nd World Congress of Structural and Multidisciplinary Optimization (WCSMO-2)*, pages 211–216, 1997.

[4] Y.X. Gu, Zhan Kang, Z.Q. Guan, and Z.W. Jia. Dynamic sensitivity analysis and optimum design of aerospace structures. *Int. J. Struct. Eng. Mech.*, 6:31–40, 1998.

[5] G. Taguchi. *Taguchi on Robust Technology Development: Bringing Quality Engineering Upstream.* ASME Press, New York, 1993.

[6] Y.X. Gu and G.D. Cheng. Structural shape optimization integrated with CAD environment. *Structural Optimization*, 2:23–28, 1990.

[7] M.P. Bendsoe and C.A. Mota Soares (Eds). *Topology Design of Structures.* Kluwer Academic Publishers, Dordrecht, the Netherlands, 1993.

[8] T. Buhl, C.B.W. Pedersen, and O. Sigmund. Stiffness design of geometrically nonlinear structures using topoloty optimization. *Structural and Multidisciplinary Optimization*, 19:93–104, 2000.

[9] J.S. Arora. Computational design optimization: A review and future directions. *Structural Safety*, 7:131–148, 1990.

[10] G.I.N. Rozvany. *Structural Design via Optimality Criteria.* Kluwer, Dordrecht, 1989.

[11] M. Zhou and R. T. Haftka. A comparison of optimality criteria methods for stress and displacement constraints. *Computer Methods in Applied Mechanics and Engineering*, 124:253–271, 1995.

[12] M. Papadrakakis, N. Lagaros, and Y. Tsompanakis. Structural optimization using evolution strategies and neural networks. *Computer Methods in Applied Mechanics and Engineering*, 156:303–333, 1998.

[13] K. Deb. *Multi-objective Optimization Using Evolutionary Algorithms*. John wiley & Sons, LTD, Chichester, England, 2001.

[14] W. Stadler. Multicriteria optimization in mechanics (a survey). *Appl. Mech. Rev.*, 37:277–286, 1984.

[15] R.B. Statnikov and J.B. Matusov. *Multicriteria Optimization and Engineering*. Chapman & Hall, New York, 1995.

[16] G.E.P. Box and K.B Wilson. On the experimental attainment of optimum conditions. *Journal of the Royal Statistical Society B*, 13:1–45, 1951.

[17] U. Kirsch. *Design-Oriented Analysis of Structures- A Unified Approach*. Kluwer Academic Publishers, Dordrecht, 2003.

[18] A.M. Abu Kassim and B.H.V. Topping. Static reanalysis: a review. *Journal of Structural Engineering*, 113:1029–1045, 1987.

[19] C. Broudiscou, M. Masmoudi, and P.H. Guillaume. *Application of Automatic Differentiation to optimal shape design*, pages 413–446. Advances in Structural Optimization. Kluwer Academic Publishers, Netherlands, herskovitz, j. edition, 1995.

[20] F. Keulen, R. Haftka, and X. Qu. Review of options for structural sensitivity calculation. In *41st AIAA/ASME/ASCE/AHS/ASC Structures, Structural Dynamics, and Materials Conference*, Atlanta, GA, 2000.

[21] R. T. Haftka and H.M. Adelman. Recent developments in structural sensitivity analysis. *Structural Optimization*, 1:1137–1151, 1989.

[22] M. Kleiber, H. Antunez, T.D. Hien, and P. Kowalczyk. *Parameter Sensitivity in Nonlinear Mechanics: Theory and Finite Element Computations*. Wiley & sons, Chichester, 1997.

[23] G.D. Cheng, Y.X. Gu, and Y. Zhou. Accuracy of semi-analytical sensitivity analysis. *Finite Elements in Analysis and Design*, 6:113–128, 1989.

[24] P. Pedersen, G.D. Cheng, and J. Rasmussen. On accuracy problems for semi-analytical sensitivity analysis. *Mechanics of Structures and Machines*, 17(4):373–384, 1989.

[25] X. Chen, T. Hisada, Kleiber M., and H. Noguchi. Comparison of different sensitivity analysis algorithms for large deformation elastic-plastic problems. In M. Kleiber and T. Hisada, editors, *Design-sensitivity Analysis*, pages 209–229. Atlanta Technology Publications, 1993.

[26] T. H. Lee and J. S. Arora. A computational method for design sensitivity analysis of elastoplastic structures. *Computer Methods in Applied Mechanics and Engineering*, 122:27–50, 1995.

[27] S. Schwarz. *Sensitivitätsanalyse und Optimierung bei nichtlinearem Strukturverhalten, ISBN 3-00-007419-8.* PhD dissertation, Universitity of Stuttgart, 2001.

[28] N. H. Kim, K. K. Choi, and J. S. Chen. Shape design sensitivity analysis and optimization of elasto-plasticity with frictional contact. *AIAA Journal*, 38(9):1742–1753, 2000.

[29] N. Zabaras and A. Srikanth. An updated Lagrangian finite element sensitivity analysis of large deformation using quadrilateral elements. *International Journal for Numerical methods in Engineering*, 52:1131–1163, 2001.

[30] I. Doltsinis and T. Rodic. Process design and sensitivity analysis in metal forming. *International Journal for Numerical Methods in Engineering*, 45:661–692, 1999.

[31] I. Doltsinis (Ed.). *Stochastic Analysis of Multivariate Systems in Computational Mechanics and Engineering.* CIMNE, Barcelona, Spain, 1999.

[32] G.I. Schueller. Computational stochastic mechanics - recent advances. *Computers and Structures*, 79:2225–2234, 2001.

[33] W.H. Press, S.A. Teukolsky, W.T. Vetterling, and B.P. Flannery. *Numerical Recipes in C- the Art of Scientific Computing.* Cambridge University Press, Cambridge, 1988.

[34] Z. Qiu and I. Elishakoff. Antioptimization of structures with large uncertain-but-non-random parameters via interval analysis. *Computer Methods in Applied Mechanics and Engineering*, 152:361–72, 1998.

[35] S.S. Rao and L. Berke. Analysis of uncertain structural systems using interval analysis. *AIAA Journal*, 35(4):727–735, 1997.

[36] N. Yoshikawa, I. Elishakoff, and S. Nakagiri. Worst case estimation of homology design by convex analysis. *Computers and Structures*, 67:191–196, 1998.

[37] Y. Ben-Haim and I. Elishakoff. *Convex Models of Uncertainty in Applied Mechanics*. Elsevier Science Publishers, Amsterdam, 1990.

[38] C.P. Pantelides and S. Ganzerli. Design of trusses under uncertain loads using convex models. *Journal of Structural Engineering*, 124(3):318–329, 1998.

[39] M. Sakawa. *Fuzzy Sets and Interactive Multi-objective Optimization*. Plenum Press, 1993.

[40] S. Rao. Optimum design of structures in a fuzzy environment. *AIAA Journal*, 25:1633–1636, 1987.

[41] K.L. Tsui. An overview of Taguchi method and newly developed statistical methods for robust design. *IIE Transactions*, 24:44–57, 1992.

[42] F. Tonon and A. Bernardini. A random set approach to the optimization of uncertain structures. *Computers and Structures*, 68:583–600, 1998.

[43] N. Kuschel and R. Rackwitz. Optimal design under time-variant reliability constraints. *Structural Safety*, 22:113–127, 2000.

[44] R. Rackwitz, G. Augusti, and A. Borii (Eds). *Reliability and Optimization of Structural Systems, Proc. IFIP WG 7.5 Working Conference*. Chapman & Hall, Assisi, Italy, 1995.

[45] I. Enevoldsen and J.D. Sorensen. Reliability-based optimization on structural engineering. *Structural Safety*, 15(3):169–196, 1994.

[46] R. Rackwitz. Reliability analysis - a review and some perspectives. *Structural Safety*, 23:365–395, 2001.

[47] R.V. Grandhi and L.P. Wang. Reliability-based structural optimization using improved two-point adaptive nonlinear approximations. *Finite Elements in Analysis and Design*, 29(1):35–48, 1998.

[48] I. Kaymaz, C. McMahon, and X. Meng. Reliability based structural optimizaiton using the response surface method and Monte Carlo simulation. In *Proc. 8th International Machine Design and Production Conference*, Ankara Turkey, September 1998.

[49] M. Kleiber, A. Siemaszko, and R. Stocki. Interactive stability-oriented reliability-based design optimization. *Computer Methods in Applied Mechanics and Engineering*, 168:243–253, 1999.

[50] Y.K. Wen. Minimum lifecycle cost design under multiple hazards. *Reliability Engineering and Syetem Safety*, 73:223–231, 2001.

[51] S. McWilliam. Anti-optimisation of uncertain structures using interval analysis. *Computers and Structures*, 79:421–430, 2000.

[52] I. Elishakoff, R.T. Haftka, and J. Fang. Structural design under bounded uncertainty-optimization with anti-optimization. *Computers and Structures*, 53:1401–1405, 1994.

[53] M. Lombardi and R.T. Haftka. Anti-optimization technique for structural design under load uncertainties. *Computer Methods in Applied Mechanics and Engineering*, 57:19–31, 1998.

[54] G. Venter and R.T. Haftka. Using response surface approximations in fuzzy set based design optimization. *Structural Optimization*, 18:218–227, 1999.

[55] S. Rao. Multi-objective optimization of fuzzy structural systems. *International Journal for Numerical Methods in Engineering*, 24:1157–1171, 1987.

[56] V. Gerhard and R.T. Haftka. Using response surface methodology in fuzzy set based design optimization. Technical report, AIAA-98-1776, 1998.

[57] T. A. Zang, M. J. Hemsch, M. W. Hilburger, S. P. Kenny, J. M. Luckring, P. Maghami, S. L. padula, and W. J. Stroud. Needs and opportunities for uncertainty-based multidisciplinary design methods for aerospace vehicles. *NASA/ TM-2002-211462, Langley Research Center, Hampton, Virginia, http://techreports.larc.nasa.gov/ltrs*, 2002.

[58] S. Schmidt and R.A. Launsby. *Understanding Industrial Designed Experiments, 3rd Edition.* Air Academy Press,Colorado Springs, CO., 1991.

[59] J.M. Lucas. How to achieve a robust process using response surface methodology. *Journal of Quality Technology*, 26:248–260, 1994.

[60] Makkapati Satheesh. *Robust Design Optimization with Applications to Composite-material Structures.* Ph.D dissertation, West Virginia University, 1997.

[61] W. Chen, W. Fu, S.B. Biggers, and R.A. Latour. An affordable approach for robust design of thick laminated composite structure. *Optimization and Engineering*, 1:305–322, 2000.

[62] U. Lautenschlager and H.A. Eschenauer. Design-of-experiments methods and their application to robust multi-criteria optimization problems. *Zeitschrift für Angewandte Mathematik und Mechanik*, 79 (S1):71–74, 1999.

[63] H.W. Chi and C.L. Bloebaum. Mixed variable optimization using taguchi's orthogonal arrays. *Structural Optimization*, 12:147–152, 1996.

[64] K.H. Lee, I.S. Eom, G.J. Park, and W.I. Lee. Robust design for unconstrained optimization problems using the taguchi method. *AIAA Journal*, 34:1059–1063, 1996.

[65] J. Latalski. Structural optimization of trusses with members' tolerances. In *Proc. the Fourth World Congress of Structural and Multidisciplinary Optimization*, Dalian, China, June 4-8, 2001.

[66] D. K. Anthony and S. J. Elliott. Robustness of optimal design solutions to reduce vibration transmission in a lightweight 2–D structure, Part I: geometric design. *Journal of Sound and Vibration*, 229(3):505–528, 2000.

[67] K.H. Lee and G.J. Park. Robust optimization considering tolerances of design variables. *Computers and Structures*, 79:77–86, 2001.

[68] E. Sandgren and T.M. Cameron. Robust design optimization of structures through consideration of variation. *Computers and Structures*, 80:1605–1613, 2002.

[69] C.R. Gumbert, G.J.W. Hou, and P.A. Newman. Reliability assessment of a robust design under uncertainty for a 3-d flexible wing. In *Proc. 16th AIAA Computational Fluid Dynamics Conference, AIAA 2003-4094*, page p. 11, Orlando, Florida, 2003. Academic Press.

[70] M. Shinozuka and E. Lenoe. A probabilistic model for spatial distribution of material properties. *Engineering Fracture Mechanics*, 8:217–227, 1976.

[71] I. Doltsinis and Zhan Kang. What the engineer should know of stochastic methods. In *Proc. of 3rd European Stochastic Experts Forum (ESEF 2002)*, Baden-Baden, 2002. Alzenau, EASI Engineering.

[72] D.N. Mavris and O. Bandte. A probabilistic approach to multivariate constrained robust design simulation. In *SAE/AIAA 1997 World Aviation Congress (AIAA-97-5508)*, Anaheim, CA, 1997.

[73] W.K. Liu, T. Belytschko, and A. Mani. Random field finite element. *International Journal for Numerical Methods in Engineering*, 23:1831–1845, 1986.

[74] G. Adomian and K. Malakian. Inversion of stochastic partial differential operators – the linear case. *Journal of Mathematical Analysis and Applications*, 77(2):505–512, 1980.

[75] F. Yamazaki and M. Shinozuka. Neumann expansion for stochastic finite element analysis. *ASCE Journal of Engineering Mechanics*, 114(8):1335–1354, 1988.

[76] S. Rahman and B.N. Rao. A perturbation method for stochastic meshless analysis in elastostatics. *International Journal for Numerical Methods in Engineering*, 50:1969–1991, 2001.

[77] E.H. Vanmarcke and M. Grigoriu. Stochastic finite element analysis of simple beams. *ASCE Journal of Engineering Mechanics*, 109(5):1203–1214, 1983.

[78] P.D. Spanos and R.G. Ghanem. Stochastic finite element expansion for random media. *ASCE Journal of Mechanics*, 115(5):1035–1053, 1989.

[79] W.K. Liu, G. Besterfield, and T. Belytschko. Transient probabilistic systems. *Computer Methods in Applied Mechanics and Engineering*, 67:27–54, 1988.

[80] A. Messac and C.A. Mattson. Generating well-distributed sets of Pareto points for engineering design using physical programming. *Optimization and Engineering*, 3:431–450, 2002.

[81] C. Lawrence, J.L. Zhou, and A.L. Tits. User's guide for CFSQP version 2.5. *Available from <http://www.aemdesign.com>*.

[82] H. Wüstenberg. *FEPS 3.3 Finite Element Programming System – User's Guide*. Institute für Computer Anwendungen, Universität Stuttgart, 1986.

[83] H. Wüstenberg. *FEPS 3.3 Finite Element Programming System – Element Library*. Institute für Computer Anwendungen, Universität Stuttgart, 1986.

[84] I. Doltsinis and Zhan Kang. Robust design optimization of structures with stochastic parameters. In H.A. Mang, F.G. Rammerstorfer, and J. Eberhardsteiner, editors, *Proc. Fifth World Congress on Computational Mechanics*

(WCCM V), ISBN 3-9501554-0-6, Vienna, Austria, 2002. Vienna University of Technology.

[85] I. Doltsinis and Zhan Kang. Robust design of structures using optimization methods. *Computer Methods in Applied Mechanics and Engineering*, 193:2221–2237, 2004.

[86] M. Kleiber and T.D. Hien. *The Stochastic Finite Element Method: Basic Perturbation Technique and Computer Implementation.* John Wiley & Sons ltd., Chichester, England,, 1992.

[87] I. Doltsinis, Zhan Kang, and G.D. Cheng. Robust design of nonlinear structures using optimization methods. *Computer Methods in Applied Mechanics and Engineering*, 194:1779–1795, 2005.

[88] I. Doltsinis, Zhan Kang, and G.D. Cheng. Robust design of structures using optimization algorithms - path-dependent nonlinear problems. In P. Neittaanmaki, T. Rossi, S. Korotov, E. Onate, J. Periaux, and Knorzer D., editors, *European Congress on Computational Methods in Applied Science and Engineering (ECCOMAS) 2004*, Jyväskyvä, 24-28 July 2004.

[89] I. Doltsinis. Inelastic deformation processes with random parameters– methods of analysis and design. *Computer Methods in Applied Mechanics and Engineering*, 192:2405–2424, 2003.

[90] I. Doltsinis. *Large Deformation Processes of Solids.* WIT Press, Southampton, 2003.

[91] A. Sluzalec. Simulation of stochastic metal-forming process for rigid-viscoplastic material. *International Journal of Mechanical Science*, 42:1935–1946, 2000.

[92] M. Grzywinski and A. Sluzalec. Stochastic equations of rigid-thermo-viscoplasticity in metal forming process. *International Journal of Engineering Science*, 40:367–383, 2002.

[93] S.M. Byon and S.M. Hwang. Process optimization design in non-isothermal, steady-state metal forming by the finite element method. *International Journal for Numerical Methods in Engineering*, 46:1075–1100, 1999.

[94] S. Badrinarayanan and N. Zabaras. A sensitivity analysis for the optimal design of metal forming processes. *Computer Methods in Applied Mechanics and Engineering*, 129:319–348, 1996.

[95] C.C. Antonio and M.N. Dourado. Metal-forming process optimisation by inverse evolutionary search. *Journal of Material Processing Technology*, 121:403–413, 2002.

[96] S. Kok and N. Stander. Optimization of a sheet metal forming process using successive multipoint approximation. *Structural Optimization*, 18:277–295, 1999.

[97] I. Doltsinis and Zhan Kang. Perturbation-based stochastic FE analysis and robust design of inelastic deformation process. *Computer Methods in Applied Mechanics and Engineering (accepted).*

[98] I. Doltsinis. *Elements of Plasticity.* WIT Press, 2000.

[99] I. Doltsinis, J. Luginsland, and S. Nölting. Some developments in the numerical simulation of metal forming processes. *Engineering Computations*, 4:266–280, 1987.

[100] J. Argyris and I. Doltsinis. A primer on superplasticity in natural formulation. *Computer Methods in Applied Mechanics and Engineering*, 46:83–131, 1984.

[101] X.S. Li. An aggregate function method for nonlinear programming. *Science in China (A)*, 34:1467–1473, 1991.

Curriculum vitae

Personal Details

Name	Zhan Kang
Date and place of birth	July 27, 1970 in Liaoning, China
Family status	Married since March 1998

Education

1977-1982	Beigangqiao Elementary School, Dalian, China
1982-1988	Dalian No.1 Middle School, Dalian, China
1988-1992	Department of Engineering Mechanics, Shanghai Jiaotong University Bachelor of Science in June, 1992
1992-1995	Department of Engineering Mechanics, Dalian University of Technology Majoring in Computational Mechanics MSc. in April, 1995
2000-2002 and 2003-2004	Institute of Statics and Dynamics of Aerospace Structures (ISD) Faculty of Aerospace Engineering and Geodesy, University of Stuttgart

Professional Experience

1995-1997	State Key Laboratory of Structural Analysis for Industrial Equipment Dalian University of Technology Assistant
1997-	State Key Laboratory of Structural Analysis for Industrial Equipment Dalian University of Technology University Lecturer